Leveraging Client Processing for Location Privacy in Mobile Local Search

Wisam Mohamed Eltarjaman
University of Denver

Leveraging Client Processing for Location Privacy in Mobile Local Search

---

A Dissertation

Presented to

the Faculty of the Daniel Felix Ritchie School of Engineering and Computer Science

University of Denver

In Partial Fulfillment

of the Requirements for the Degree

Doctor of Philosophy

---

by

Wisam M. Eltarjaman

November 2016

Advisor: Prof. Ramakrishna Thurimella

Co Advisor: Dr. Rinku Dewri

Author: Wisam M. Eltarjaman
Title: Leveraging Client Processing for Location Privacy in Mobile Local Search
Advisor: Prof. Ramakrishna Thurimella
Co Advisor: Dr. Rinku Dewri
Degree Date: November 2016

Abstract

Usage of mobile services is growing rapidly. Most Internet-based services targeted for PC based browsers now have mobile counterparts. These mobile counterparts often are enhanced when they use user's location as one of the inputs. Even some PC-based services such as point of interest Search, Mapping, Airline tickets, and software download mirrors now use user's location in order to enhance their services. Location-based services are exactly these, that take the user's location as an input and enhance the experience based on that. With increased use of these services comes the increased risk to location privacy. The location is considered an attribute that user's hold as important to their privacy. Compromise of one's location, in other words, loss of location privacy can have several detrimental effects on the user ranging from trivial annoyance to unreasonable persecution.

More and more companies in the Internet economy rely exclusively on the huge data sets they collect about users. The more detailed and accurate the data a company has about its users, the more valuable the company is considered. No wonder that these companies are often the same companies that offer these services for free. This gives them an opportunity to collect more accurate location information. Research community in the location privacy protection area had to reciprocate by modeling an adversary that could be the service provider itself. To further drive this point, we show that a well-equipped service provider can infer user's location even if the location information is not directly available by using other information he collects about the user.

There is no dearth of proposals of several protocols and algorithms that protect location privacy. A lot of these earlier proposals require a trusted third party to play as an intermediary between the service provider and the user. These protocols use anonymization and/or obfuscation techniques to protect user's identity and/or location. This requirement of trusted third parties comes with its own complications and risks and makes these proposals impractical in real life scenarios. Thus it is preferable that protocols do not require a trusted third party.

We look at existing proposals in the area of private information retrieval. We present a brief survey of several proposals in the literature and implement two representative algorithms. We run experiments using different sizes of databases to ascertain their practicability and performance features. We show that private information retrieval based protocols still have long ways to go before they become practical enough for local search applications.

We propose location privacy preserving mechanisms that take advantage of the processing power of modern mobile devices and provide configurable levels of location privacy. We propose these techniques both in the single query scenario and multiple query scenario. In single query scenario, the user issues a query to the server and obtains the answer. In the multiple query scenario, the user keeps sending queries as she moves about in the area of interest. We show that the multiple query scenario increases the accuracy of adversary's determination of user's location, and hence improvements are needed to cope with this situation. So, we propose an extension of the single query scenario that addresses this riskier multiple query scenario, still maintaining the practicability and acceptable performance when implemented on a modern mobile device. Later we propose a technique based on differential privacy that is inspired by differential privacy in statistical databases. All three mechanisms proposed by us are implemented in realistic hardware or simulators, run against simulated but real life data and their characteristics ascertained to show that they are practical and ready for adaptation.

This dissertation study the privacy issues for location-based services in mobile environment and proposes a set of new techniques that eliminate the need for a trusted third party by implementing efficient algorithms on modern mobile hardware.

Acknowledgments

My whole gratitude goes first to Allah Almighty.

I thank my advisors Dr. Ramki Thurimella and Dr. Rinku Dewri, for their guidance, patience and more importantly their wholehearted support. No dissertation can come to fruition without the advisor's guidance and mine is no different. But mine would not have happened without their support that was immensely needed and useful during these eventful several years of my research. I want to thank my committee members Dr. Matthew Rutherford and Dr. Nathan Sturtevant, whose constructive criticism made me think, and greatly improved the final product. My thanks go to fellow student Prasad Annadata, who did draft reviews and served as a sounding board for my ideas. My sincere thanks go to Mr. Andre Roudik, who often bent over backward to cleverly fulfill always urgent and big requests, always with a smile. He has become a true friend. Lastly, my thanks to Ms. Susan Bolton, often working in the background and making sure things run smoothly and often keep us in check, always available and took on whatever we threw at her.

The study years for me at the University of Denver, have been eventful, to say the least. My family and I went through several events any of which would have easily broken my resolve to keep going. This would not have happened without His blessings. The blessings came in the form of my family that went through the roller coaster of the last few years with me, supporting me wholeheartedly, believing in me and more importantly motivating me to get this done. My deepest gratitude goes to my wife and kids.

Contents

List of Figures

Nomenclature

A_I	Interest Area
A_R	Retrieval Area
A_Z	Obfuscation Area
cPIR	computational PIR
FHE	Fully Homomorphic Encryption
GIS	Geographic Information System
GPS	Global Positioning System
itPIR	information-theoretic PIR
LBS	Location Based Service
LoP	Level of Privacy
LPPM	Location Privacy Preserving Mechanism
LSP	Location Based Service Provider
P2P	Peer-to-Peer
PIR	Private Information Retrieval
POI	Point Of Interest
QI	Quasi Identifiers
QoS	Quality of Service
TTP	Trusted Third Party

Chapter 1

Introduction

Privacy or the right to be left alone in the realm of computer science can be understood as a personal preference of how much of information an individual wants others to have access to. In general, there is no direct quantitative measurement for privacy and it can be different from one person to another and varies based on many factors such as culture, circumstance, financial gain, services being consumed or the entity trying to access the information.

Recent evolution in mobile phones and communication technologies has lead to a significant increase in the number of subscribers to mobile networks. It is estimated that there will be 6.1 billion smartphone users across the world by 2020, which represents 70% of the global population at that time [24]. Further, the development of mobile data technologies allow many mobile users to access the Internet via their mobile devices and leads to very attractive and useful applications. Examples of these applications include mobile entertainment, locating nearby points of interest, updating friends and family of one's location, tourist guidance, language translation etc. Improvements both in the quantity and quality of publicly available data lead to significant improvements to the capabilities of these mobile applications. For example, a user can not only search for nearby restaurants but put additional criteria such as availability of specific food (e.g. gluten free) or having a higher than threshold user review rating. While there are multiple categories of mobile applications available, the category of applications that is most interesting to the privacy research community falls under Location Based Services (LBS).

An LBS is a service provided to a mobile user, typically using a mobile application, that has at least two entities involved, a server and a client. It works like any other client/server architecture where the client initiates the transaction by placing a service request, and the server responds to that request. What differentiates LBS from other mobile services is the fact that the location of the user is one of the inputs to the service request. While some service providers and devices support the concept of “push” services that allow the server to push relevant service messages to the mobile phone, they can be considered a special case of the client/server transaction, as one could consider the installation and registration of the application with the service provider represents the initial service request by the client.

In LBSs the transactions between the user terminal and the service provider are usually carried over mobile networks. For the service provider to provide a useful service to the user, the location of the user needs to be known by the server. It can be obtained either by using the Global Positioning System (GPS) which is supported today by most of the smartphones and tablets. Other approaches such as WiFi/cell tower triangulation are possible. A set of different location sensing techniques has been explored by Hightower and Borriello in [84]. If the service provider was not able to manipulate all the location data that is required to accomplish the service, then the service provider will obtain that data from the Geographic Information System (GIS). A GIS database is a separate entity that is designed to store and process geographic data.

LBSs are used in a wide variety of applications that includes locating an object such as grocery store or locating people such as finding a friend on a social network. It may also include some business applications such as advertising coupons or deals to clients, or billing them for a service dynamically based on their current location. A new application of LBSs is mobile location based gaming such as a *Geocaching*[1] hunting game, where the player tries to locate a hidden container in an interesting location based on the GPS coordinates.

[1]www.geocaching.com

Location-based services are very useful and so are consumed by many mobile users. One of the query parameters, namely, the user's current location, is of immense importance to the privacy research community. The current or the past location of the user is considered private information. Moreover, it is generally thought that the more accurate the location of a user traced by an unauthorized entity, the bigger breach it is of user's privacy. On the other hand, the more accurate the user location supplied to the service provider, the more useful response the service provider can give. A considerable amount of research, including the current dissertation, deals with the fine balancing required between these two conflicting aspects.

People consider their geographic location to be private information. They do not want unauthorized entities to know where they are or where they have been. Breach of location privacy could present several serious problems to the user. Moreover, precise location information of consumers has proven to be a profitable asset in this day of personalized marketing. This has caused several breaches, escalations of privileges and very service provider leaning privacy policies such as longer retention intervals of user's location data. Because of the financial gains, there is added motivation on the part of service providers to be able to obtain and use precise user location information. On the other hand, the users, equipped with their smartphone, want and sometimes need, to consume location-based services. So, techniques are needed to preserve the location privacy of the user even when the attacker happens to be the service provider itself while allowing the user to still consume location-based services without considerable degradation of quality.

1.1 Mobile Local Search

One area of interest for the privacy research community within the LBS space is *mobile local search*. While in several LBSs like navigation systems, friend finders, social networking apps etc., the mobile local search is arguably the most widely used system where the semi-trusted service provider can gain considerable knowledge based on both the location and query string used as part of the query. A typical search transaction starts with a user

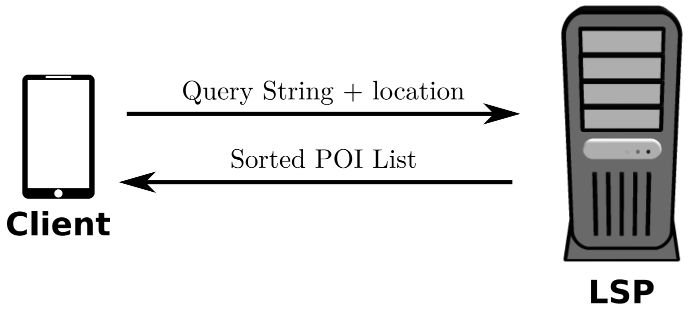

Figure 1.1: Typical mobile local search architecture.

looking for a certain object (often called Point Of Interest or POI). The user sends a query to the service provider with a keyword that defines the type of required POIs in addition to the location information that refers to her current geographical position. With proper permissions, the location data can be directly obtained by the application from an on-board positioning device. The LBS provider receives this query and the geographic position of the user and returns a list of POIs that match the query, sorted based on some criteria. If the service provider already maintains a database of the requested type of POIs, then it can answer the query immediately; otherwise, the server must request this information from GIS.

The most common architecture for mobile local search prevalent today is depicted in Figure 1.1. It is a simple client/server architecture where the client is a mobile application that directly communicates with the server. When it comes to location privacy of the user in this architecture, it is totally based on the privacy policy as published by the Location Based Service Provider (LSP). In other words, the LSP is trusted completely: the LSP will only use the location information in accordance with published privacy policy. Of course, there are many issues even if the LSP is trusted, as the privacy policies themselves can be long and complicated that few users really understand them. A detailed discussion of policy-based privacy mechanism is presented later in Chapter 2.

When the service provider is completely trusted, then the location privacy problem with respect to mobile local search becomes a privacy policy research issue. Assuming that mechanisms from information security research area are already implemented that

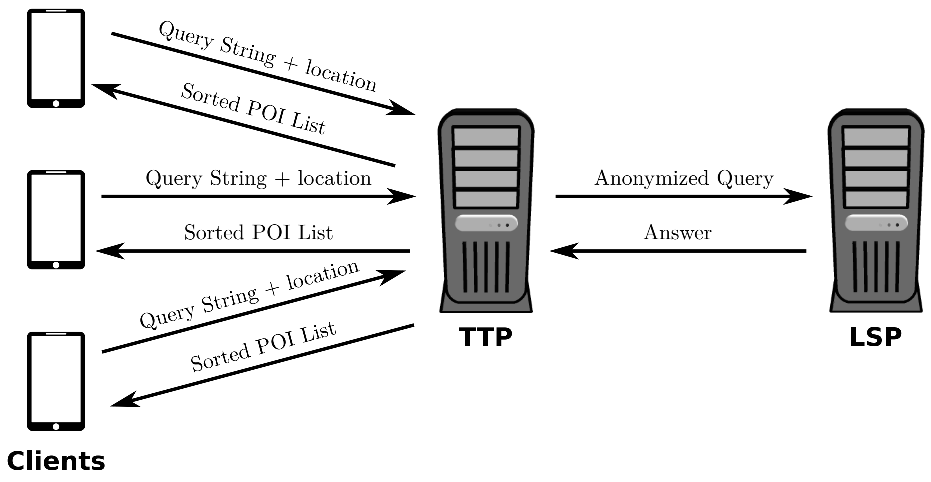

Figure 1.2: A TTP-based location privacy architecture.

encrypt the communications between the client and the server and prevent attackers from eavesdropping, the problem becomes trivial. But, what would be the case if the LSP is semi-trusted instead of completely trusted? The challenge is to come up with a solution that provides the user all the advantages of mobile local search, without compromising her location privacy even in the case of a semi-trusted LSP.

An often proposed solution in the literature for this problem is to find a Trusted Third Party (TTP) that could act as a mediator between the user and the LSP. As shown in Figure 1.2, the TTP runs some anonymization algorithm that prevents the LSP from learning the exact location information of the user. Instead of direct communication with the LSP, the user now will send her query to the TTP which anonymizes this query (usually with other queries from different users) and sends it to the LSP, which searches its database and replies back the found answer. The LSP can answer the anonymized query but should not learn any information about the user who issued the query. Normally, this answer includes additional mixed data, and it is the TTP's job to split out this data and return the correct answer to each user. Numerous problems come with this solution will be discussed in Section 2.3.

1.2 Impacts of Location Privacy Breaches

Violation of location privacy are considered serious in many privacy conscious societies. Research shows several potential impacts of location privacy breach, especially on the user's front. Some of these impacts are listed and described below.

A feeling of being violated. One could imagine that a feeling of being violated is the primary impact of a location privacy breach. But this impact happens only on the user discovering that her location privacy is breached. This feeling is common among all privacy breaches. A discovery of location privacy breach or even the perception by the user of an LBS can have further secondary impacts such as loss of trust, reduced usage of location-based services, implementation of privacy enhancing mechanisms, retaliation, and legal actions.

Personal safety. With a lot of vulnerable persons such as activists, victims of various social crimes, potential victims and children using Internet increasingly, their personal safety could be in jeopardy if their location privacy is breached and their location is revealed to powerful attackers. One could imagine that this risk increases if the fact about the location breach is unknown to the user.

Escalation to further privacy breaches. A powerful attacker may have even worse goals (e.g. personal physical attack, burglary, arrest etc.) and figuring out the location of the victim could be the first step in such an attack. In other words, a breach of location privacy can be escalated by a motivated attacker to facilitate further more serious attacks.

Unreasonable prosecution. With the Internet and mobile technologies being used in various social causes by the activists, particularly in restrictive societies, a breach of location privacy of these activists could lead to their identification (or worse could implicate an innocent person) and could subject to greater scrutiny or even prosecution.

Uninvited marketing. Intrusive solicitations and uninvited marketing arguably is the most prevalent impact of location privacy breaches. The intentional or unintentional revelation of location leads to more targeted marketing by various entities. In most practical scenarios, the marketing entities or marketing facilitators are themselves providers of LBSs making this risk very prevalent.

Breach of privacy of others. This is particularly true in the case where the attackers are antagonistic administrations whose intention is to identify and locate the entire group of activists. A breach of location privacy of one victim could reveal the locations of close associates, co-workers, and friends even if those third parties are non-users of LBS.

Loss of trust. When the users discover or perceive the breach of location privacy, even unintentional (e.g. the service provider itself being victim of a hacking attack), it results in loss of trust on service providers causing reduced utilization of useful services and increase in overall costs, as the victims usually overcome this by implementing various privacy preserving mechanisms.

Loss of revenue. Loss of trust in service providers generally results in reduced utilization that could result in major losses in revenue to service providers. The mere perception of loss of privacy by users, not a full knowledge of a breach, is enough to cause loss of trust and loss of revenue. It results in service providers spending resources to portray a perception of trust. One example is the amount of time and money spent by major LBS providers on public relationship campaigns.

Changes in behavior. Privacy of a person includes behavioral aspects, especially sensitive ones such as religious practices and political activities. The privacy breach of the user's location can be escalated to the breach of privacy of these aspects; the breach of privacy can lead to changes in behavior. The changes could range from towing the party line, implementation of privacy preserving techniques, reduced use of LBSs or even disloyalty.

Societal impact. Breach of privacy and loss of trust indirectly affects the ability for individuals to communicate and share sensitive information with each other without any concerns of being monitored by other people or organizations. In the long run, this can have major impacts on the society as a whole and could cause regressive societies.

Technical Impacts. Loss of trust for LBSs not only have financial costs. It also impacts the efficiency of the systems. For example, Parris and Henderson [131] run a simulation of two real-world datasets and show that users' privacy concerns can significantly downgrade routing performance in the opportunistic networks. Their results show that message delivery ratio can be reduced to zero. From the users' perspective, implementation of additional measures to preserve privacy often result in loss of Quality of Service (QoS), which results from an increase in bandwidth costs and processing resources.

1.3 Location Privacy Attacks

LBSs are very useful and are being used by more and more mobile users today [28]. Along with their adoption and increased utilization comes increased risk to location privacy. In the previous section, several possible impacts of location privacy breach are discussed that ranged from benign risks such as intrusive marketing to serious ones such as unreasonable prosecution or bodily harm. Privacy protection techniques can be appreciated and their efficacy can be judged better if one has an understanding of different attack techniques that a capable and smart attacker could use. In this section, the broad categories of location privacy attacks in the literature are discussed. The corresponding preservation techniques proposed will be discussed in Chapter 2.

1.3.1 Identity inference

Perhaps the most obvious location privacy protection technique is to replace the actual identifier of the user with an alias identifier or *pseudonym*. Since certain locations such as the office or home can be strongly related to the user, an attacker could easily identify the user by linking the pseudonym to these locations. This kind of attack was demonstrated by Beresford and Stajano [15] and the results show that all users in the tested database can be identified correctly. The algorithm is run in two steps: (1) given a pseudonym, observe where that pseudonym spends most of the time and (2) given a location, see which pseudonym spends more time than any other in that location.

In many situations where the attacker is a third party that can observe the communications happening between clients of LBS and the server, it is often possible for the attacker to determine the location of the query origination and sometimes even the contents of the query. In an identity inference attack, the attacker, who is assumed to have access to the location the query originated from, tries to infer the identity of the user that originated the query. The attacker who is also assumed to have access to publicly available databases and some background information, like the work location of the victim, could try to combine this information with observations of the communications between the user and LSP to guess the identity of the user. Once a user is identified, more powerful attacks are possible as the attacker now can associate any observed pseudonym or a quasi-identifier such as a phone ID or electronic serial number to the actual identity of the user during future observations. *Quasi-identifiers* are attributes of a database record that are non-identifying by themselves, but can be used to uniquely identify individuals when used in combination. The attacker could exploit quasi-identifiers to escalate the attacks or to identify other users of the system; for example, by simply ruling out already identified users. Re-identification of the Massachusetts Governor, William Weld's health records was done based on gender, postal code and date of birth [73, 149]. Later research showed that individuals can be identified using different pseudo-identifiers such as web search history [13], social network structure [119], movie rating content or even familial structures [74].

A more powerful attack is presented by Gruteser and Hoh in [76] that uses Reid's algorithm of multiple-tracking hypothesis [132]. They demonstrated their attack by tracking three anonymous users over extended periods of time using sample GPS location data. The sampled locations can be linked to the identity of each individual by building separate path for each user. A simplified version of Reid's algorithm is used to repeatedly generates hypotheses for the new locations of the users and adjust this information with new location samples. The results show that the algorithm may be confused between users temporarily, especially if the paths are crossing, but eventually for a long run it can recover and correctly sample the users. Krumm [97] runs an experiment over a sample of 172 volunteers. The author shows that given GPS locations, the home for each user is identified with a median error of about 60 meters. About 5% of users could be identified by name using free Web-based services. While using a commercial reverse geocoder, the accuracy raises to 13%. De Montjoye et al. [40] shows that 95% of individuals can be uniquely identified using just four spatiotemporal points. This is done by analyzing data collected for fifteen months from a half million mobile users. By analyzing more than 30 billion call records, Zang and Bolot [166] tried to find the top N records of users. They set up an experiment that determined the user's location at different granularity level such as sector, city, county, whole state, etc. They concluded that 50% of users can be identified by using their top 3 locations determined by analyzing their call records to the granularity of a sector. Using the same top 3 locations, 10% and up to 50% of users' locations can be determined to the city level and 1% and up to 5% to the county level.

1.3.2 Predicting user's location of interest

To identify user's places of interest, Marmasse and Schmandt [111] propose the "comMotion" software which uses GPS to determine the user's location and track her movement. This software links the movement traces to the important places for the user by gradually learning the locations visited by her on a regular basis. The place is identified by circular region around a point within which the GPS appears and disappears. A similar work by Ashbrook and Starner [9] cluster the location data collected from GPS and use a Markov model to learn useful information from this data, such as prediction of the next place the user is going to visit and the presence of other people at the same location as the user.

Kang et al. [91] used a time-based clustering algorithm for coordinate traces of the user to recognize the important places for her, while Hariharan and Toyama [79] consider both time and location to build a hierarchy from the location data histories. The hierarchy is represented as “stays” and “destinations”. The destination is a cluster of stays while the stay is defined as the place where the user had spent some time. Instead of mapping GPS location coordinates, “BeaconPrint” algorithm by Hightower et al. [85] identifies important places for the user by collecting WiFi and GSM base stations visited frequently by the user.

Montoliu and Gatica-Perez [117] developed a smartphone application to obtain the user’s location by integrating different sensors of the phone. Similar to Hariharan and Toyama [79], the authors use time and location-based clustering to identify significant places. “CrowdSense@Place” algorithm by Chon et al. [30] monitors everyday user’s places by opportunistically collecting images and audio clips from a smartphone. The collected image and audio data is classified in the processing stage and linked to location marks obtained by the GPS/WiFi sensors. Several approaches recently are proposed by researchers for predicting the next destination of the user (e.g. [31, 39, 99, 138, 151]), making not just the current location vulnerable to the attacks, but the future locations of the user as a target for several attacks.

Sometimes quasi-identifiers can be used to infer the location data. Dewri et al. [14, 43] implemented an attack that shows how driving habits data such as speed and time collected by auto-insurance companies to assess accident risk can be manipulated to infer the destination of the trip. We discuss this attack in more detail later in Chapter 3 as an example of how a semi-trusted service provider can use other data to predict the user’s location.

1.4 Contribution

In this dissertation, we begin by arguing why the requirement of a TTP is not a practical solution and how it can be eliminated by taking advantage of the power of modern smart devices. We propose a TTP free two-round trip generic architecture upon which

Location Privacy Preserving Mechanisms (LPPM) can be implemented. Proceeding from that architecture we, therefore:

- present a kd-tree efficient POI ranking process that considers both location and prominence[2] information of the POIs in contrast to existing LPPMs which use only the location,
- explore the practicability of implementing cryptography-based methods, namely PIR techniques, as an LPPM and show that none of the available techniques are practical enough,
- present a novel LPPM for single queries that enable location and prominence based ranking of POIs, and implement it entirely on a mobile device to demonstrate feasibility,
- show how there is a higher risk of privacy loss in the multiple query scenario, and propose an improved LPPM to handle this scenario,
- present and implement an alternative LPPM that uses differential privacy whose privacy guarantees can be mathematically ascertained.

The proposed LPPMs in this dissertation are implemented to show that they are all practical to be run entirely on a mobile device without compromising too much of the QoS. We analyze our results and, where appropriate, compare them with some representative algorithms to show that our contribution makes significant improvements to location privacy in the context of mobile local search with minimal communication and computation costs.

1.5 Dissertation Outline

This dissertation addresses the privacy issues encountered by the users of LBS during POI searches. As explained above, location privacy is important and loss of privacy has real consequences to the users. There is a lot of progress in terms of protecting privacy

[2]More discussion about POI ranking process and the prominence value in Section 4.1

against third parties. But during these days where richer user profiles are monetized, the service providers themselves have an incentive to both track and store location data of the users as accurately as possible. So there is a need for techniques that not only avoid third parties but also protect user's privacy against semi-trusted service providers. This dissertation investigates existing techniques, studies their practicability after implementation and proposes a few practical techniques.

In the next chapter, we survey the existing research in LBS privacy and present a view of the progression of these techniques. In Chapter 3, we show that protecting location privacy does not stop at protecting just the location coordinates. We show that a clever semi-trusted provider can use quasi-identifiers to infer the location of the user pretty closely. In Chapter 4, we propose an architecture for third party free protocols. We present nomenclature that will be used in rest of the dissertation as other techniques are explained. In Chapter 5, we delve into Private Information Retrieval , a set of cryptography-based techniques and investigate them as a potential solution for our third party free architecture. Chapters 6 through 8, present heuristics-based techniques. In chapter 6, we propose a third party free technique that can be implemented on a smart mobile device that achieves user desired privacy level in the single query scenario. We extend this technique in Chapter 7 to address the same issue in the multiple query scenario where the user moves around while issuing queries. In Chapter 8, we propose an improved technique based on *differential privacy* as a measure for a guaranteed privacy level.

Chapter 2

Location Privacy Mechanisms

In this chapter, we present existing privacy protection mechanisms in the form of a quick survey of existing literature. We can broadly categorize the privacy protection mechanisms that are in practice or proposed in the literature based on policy, anonymization, obfuscation, cryptography or a combination of these. While policy-based techniques require the user to trust the service provider, the other techniques offer various degrees of privacy even from the service provider. We discuss these issues in detail below.

2.1 Policy Based Protection

Policy-based privacy protection is arguably still the most prevalent in practice today. It gains importance as the focus of privacy protection shifts from protection against a third party eavesdropper to protection against a curious service provider itself. Currently, most LBS consumers have no choice but to trust the service provider and assume that the service provider adheres to the protections promised in the privacy policy. The policy-based controls are deployed into two different ways: a policy that regulates the access for various entities to private data and a policy that details how private information will be used and sets an expectation (promise) of privacy to the user.

2.1.1 Access control policy

Access control policy is a commonly practiced technique in organizations to ensure the security of their information systems. Role-based access control is proposed by Sandhu et al. [136, 137] as a large-scale access authorization model for database systems. Walking in the same steps, different research efforts attempted to use access control policies in order to protect the privacy of individuals. Agrawal et al. [2] proposed the concept of the Hippocratic database system as an architecture to regulate the privacy of database records. This architecture consists of two metadata tables. The first table consists of privacy policy attributes. External recipients and retention period are described for each attribute in the table. User authorizations are listed in the second table. Byun and Li [22] suggested a "purpose" based model of access management to handle advanced data management systems e.g. those based on XML. The purpose describes the reason(s) for accessing data that is organized in hierarchical relationships. Basically, a user is allowed to access the data item if the purpose of the request matches the intended purpose of that object.

On the other hand, Lalana and Hal [89] think that pure access restriction systems based only on information access are outdated and inadequate for addressing the privacy issues in recent technologies. As an example, the authors considered an access control policy that guards sensitive information such as SSN for an individual from being published. However, various researches showed that user identity can be recovered with a high degree of accuracy from auxiliary information available in public databases including government sources [61, 118, 120].

Access control policy, while plays a role in privacy preservation, cannot be the only measure. This is because access control controls the access to private information, among other things, to unauthorized entities but if the protection is needed from a service provider itself, these measures fail completely. Similarly, if third parties are involved in enhancing privacy, these third parties often need to have access to user's private information and are often given access. Any breach of security at the third parties will completely nullify if access control policy is the only protection available. In other words, access control policy is totally ineffective, if the entity that is given access is not completely trusted. Hence there is a need to look at other mechanisms that are more effective.

2.1.2 Privacy policy

Policy-based privacy preservation is arguably the most prevalent form of privacy protection mechanism today. Most LSPs and providers that collect location data publish an extensive privacy policy that tries to spell out exactly what private information is collected and how the data is used. These service providers collected and continue to collect huge volumes of data about their users, causing the advent of "big data" which essentially means, application of machine learning techniques to huge data sets of information about users to predict future behavior. Because of this, these service providers are able to monetize the private information of the users they have collected. So, most of these LSPs give away their service for free or very cheap, but make it a condition that the users of the LBS agree to the privacy policies that essentially give permission to them to collect and monetize private information of their users including their location data.

In the privacy policy-based preservation mechanism, within the system, there are two issues that are in play. One, the users trust the LSP to adhere to the policy they have published, which includes in most cases, a restriction that the data needs to be anonymized before being sold to third parties. Second, there is a trust placed on the LSPs by the users, that the LSPs implement proven, strong enough security and access mechanisms in place that prevents powerful attackers from forcibly obtaining the private information. Another expectation from the LSPs by the users is to assume that the third parties that do get the private information are properly scrutinized and adhere to privacy policies that are at least as strong as that of the LSP. Thus, one can imagine that if a benign or malicious breach of any of these different expectations placed on the LSPs is broken, the privacy of the user is completely breached.

There are however some external checks and balances that seem to push LSPs to strive hard to preserve the trust placed in them. First, a loss of trust by the users in the LSP's ability or willingness to preserve private information means loss or decrease of the LBSs provided by those LSPs. This means that they can collect less private data, which translates to a loss of revenue. The other way, a check is placed on the system because of activist and vigilant groups that scrutinize the privacy policies of major LSPs. Any change in the privacy policy that gives additional advantages to the LSPs at the cost of privacy of the users immediately becomes popular news and because of extensive usage of these services by large populations, they are often discussed and protection mechanisms published and implemented right away. LSPs on the other hand, often provide ways for their users to configure some of their privacy settings including tracking and use of location data so that they can set them to suit their comfort level. Any changes to this reconfigurability including new/additional ways to configure privacy at nuanced levels are again well published as far as popular LSPs are concerned. Essentially, user awareness of the privacy policy, being educated about what private data is used and learning how to tune the data collection and usage of their private information seems to be the major privacy protection measures available to the user in the case of policy-based privacy.

2.2 Anonymization

An early attempt to maintain the privacy of location data proposed by Beresford and Stajano [15]. They used pseudonyms during the communication transaction instead of the true identifier of the user so that even if an attacker was able to capture the communication between the user and LBS, the true identifier of the user is not directly revealed. But, long term utilization of the same pseudonym for the same user can make her location vulnerable to historical tracking attacks. To overcome this problem, the authors recommend that the pseudonym should be changed periodically. Thus, the attacker's opportunity for tracking the user and accumulating enough movement history to infer her identity will be reduced. The authors presented the concept of *mix-zones* to develop their method of updating the pseudonym of the user. A mix-zone is defined as a spatial region where the location of the user is not revealed to the applications. If the identities of the users are changed randomly (mixed) when users entered the mix-zone, then the application cannot distinguish them when they exit from that zone. An *anonymity set* is the group of users that are in the mix-zone in a given time period. An obvious measurement for location privacy in this context is the size of the anonymity set. The authors in that work assume the size of the anonymity set as a preference parameter that can be selected by the user to maintain her minimum level of privacy.

2.2.1 *k*-anonymity

Even when using a pseudonym instead of the actual identifier of the user, LBSs will disclose the position of the user at a certain point of time. In fact, the correlation of these two attributes reveals very sensitive information about the user. By collecting the location information of the user over a long enough period of time, the attacker can eventually, recover the true identity of the user. For example, a study by Golle and Partridge [74] shows that location traces for a pseudonym can be linked to the home/work address of an individual.

Alternatively, the user can hide her actual query in an anonymity set of dummy queries with incorrect location tags [94]. Yiu et al. [164] propose a framework, called "SpaceTwist", based on k nearest neighbor queries. The process starts with a location different from the user's actual location, then incrementally retrieve nearest neighbor locations until an accurate query result is reported. Gruteser and Grunwald [75] borrowed the concept of *k*-anonymity [134, 135] from privacy protection in the relational database and utilized it for protecting the privacy of locations in a typical POI search application. According to Samarati and Sweeney [135], *k*-anonymity in relational databases can be achieved by partitioning the records of the intended table into a set of groups based on the values of certain fields of that table, called quasi-identifiers (QI). Next, the exact values of the QI are replaced by more generalized values, e.g., numeric fields can be generalized to a range of values. A table satisfies *k*-anonymity if each group in that table includes at least *k* records. A quasi-identifier is an attribute that an attacker may use to determine the individual instead of the user identifier. It has been found that 87% of the population in the United States could be identified based on their Zip code, gender, and date of birth [150]. Since the QI can be accessed from publicly available data, most privacy protection architectures consider these identifiers as a background knowledge of the attacker.

For location privacy, k-anonymity is satisfied if the location of the user that is inferred from the sent query is indistinguishable from at least $k-1$ other users. The k users form the anonymity set. k-anonymity ensures that an attacker, without other background knowledge, cannot guess the real location of the user with probability greater than $\frac{1}{k}$. For a better understanding of this concept, we will use a simple example for illustration.

Example. Consider the location data for six users as shown in Figure 2.1a. Each record in the table consists of the following fields.

- The user identifier (ID) which uniquely identifies each individual user.
- The exact two-dimensional location data of the user that is formed by x-coordinate and y-coordinate fields.

user identifier	$x-$coordinate	$y-$coordinate
1	7	4
2	2	2
3	5	6
4	7	2
5	4	3
6	8	5

(a)

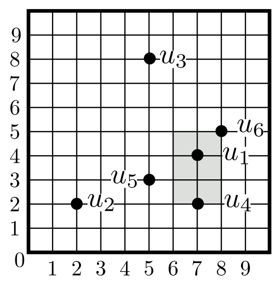

(b)

Figure 2.1: Location data for Example 2.2.1

Figure 2.1b shows the location for each user in a two-dimensional coordinate map. The attacker is assumed to know the contents of the query issued by the user or can guess it with a high level of confidence. In most realistic LBS scenarios, the location information of a user can be used by the adversary as a QI to infer the identity of the user. The privacy protection algorithm used in this example promises to preserve k-anonymity for each user with $k = 3$. In order to protect the location privacy, the algorithm will cloak the location data of the user before sharing it with other entities.

Let us suppose that the user u_1 is looking for the nearest night club from her location. Instead of sending the exact location data of u_1 along with the query, the anonymization algorithm determines the nearest two users to u_1, group them together in one generalized region and send the geolocation data of this region to the intended LSP. The generalization operation, shown in Figure 2.2, which groups exact location points into a region is referred to as *spatial cloaking*. This region is shown by the shaded square in Figure 2.1b.

user identifier	$x-$coordinate	$y-$coordinate
1	$7-8$	$2-5$
4	$7-8$	$2-5$
6	$7-8$	$2-5$

Figure 2.2: Location generalization for clocked region in Example 2.2.1

When an attacker observes the query and the cloaked region that contains u_1, without any other knowledge, the identity of u_1 is protected since all users in the cloaked region are indistinguishable from each other when looking at the query. From the attacker's point of view, the probability that the query was issued by u_1 is $\frac{1}{3}$. Thus k-anonymity achieved its goal and the privacy of user u_1 is protected.

Gruteser and Grunwald [75] suggested a quad-trees to build the cloaked region; this region could be any shape and it could be created by using any technique as long as it contains k users. The cloaking is performed at a TTP site. Several research based on the k-anonymity concept to satisfy location privacy used different techniques to build the cloaked region [80, 112, 115, 116]. Cloaking regions can be created with features such as a limited number of still objects [12] or a threshold level of entropy is maintained in the queries originating from that region [106]. Privacy level can be configured by using the popularity of public regions [161]. However, Marconi et al. [109] show that this method is futile if the attacker can track generated regions over time. An entropy-based dummy location selection algorithm with the objective of making the selected locations spread as far as possible is proposed by Niu et al. [122, 123].

Instead of requiring a TTP, Chow et al. [34] propose a peer-to-peer (P2P) algorithm to construct the cloaked region without involving a third party. They propose a P2P network of users that achieve k-anonymity together by forming groups. Before sending a request to the LSP, the mobile client creates a group of at least $k-1$ other users. Initially, the requesting mobile client propagates a special message called, FORM_GROUP, with *hop* sequence number of one. Any neighbor device that can detect this message will send the acknowledgment to the originator device. If the originator receives $k-1$ responses or more, then the k-anonymity requirement is satisfied and the client creates a cloaked region (the area that includes these devices) and uses it as part of the request. If no sufficient number of neighbors responded, the originator sends another request with *hop* number incremented. This request is forwarded by any receiver to their neighbors after decrementing the *hop* number. All the responses go back to the originator. This hierarchical group expansion continues till at least $k-1$ responses are received. They also eliminate one of the main disadvantages of k-anonymous algorithms, i.e., if k users are concentrated in a small identifiable region such a restaurant, the precise location is revealed. They do this by proposing a minimum area for the cloaked region. Shokri et al. [142] proposed a collaborative peer-to-peer model where mobile devices keep their previous search results to answer queries of their peers, thus no location data revealed to LSP. However, this approach is impractical in the sense that it requires two interfaces on each mobile device, one that communicates with the service provider and one that communicates with the peers. Another aspect of this proposal that makes it impractical is its need for a critical number of users that sign up for the system to have $k-1$ other users being available during query times. In fact, this problem is common among most k-anonymity based approaches.

Based on the number of users logged on Wi-Fi access points, Ahamed et al [4] proposed a probabilistic approach for building the k-anonymity set. The number of users located in the region of an access point in a certain period of time is predicted from the historic data of the logged on users. Each Wi-Fi access point represents a landmark on the map. The spatial locality around the landmark is defined as the *dominance space*. The proposed architecture requires an additional entity called Dominance Space Mapper (DSM) which has a database for location information of all access points on the map. The DSM is the operational component that can calculate the dominance space for each access point and estimate the number of users under it at specific time periods. Both user and LSP must subscribe with DSM to get an updated list of the access points and their dominance spaces.

2.2.2 Major problems with anonymization

As the attacker combines the observations with other background knowledge, k-anonymity starts breaking down. However, other anonymization models try to overcome this problem. The history of pseudonym user requests of a particular service could be used to link location information of the individual and act as a quasi-identifier. The notion of historical k-anonymity is introduced by Bettini et al. [16] to assess the risk of disclosure of sensitive personal information based on location data.

Sensitive attributes Machanavajjhala et al. [108] observed that some attributes are private to the individual and must be kept secret to protect the privacy, these attributes are called *sensitive attributes*. Consider the same dataset from Figure 2.1 with one more attribute "Age". This attribute is sensitive to all users in the database. The association between users and the age should be kept secret. For the cloaked region shown in Figure 2.1b, assume that the attacker can associate age attributes to the individuals in the dataset shown in Figure 2.3. Although the exact locations of the users are anonymized, the attacker can tell with high confidence that u_1 has issued the query "night club", because it is usually people in that age group that are generally interested in night clubs. To avoid this problem, Machanavajjhala et al. [108] proposed a new measure called l-diversity. A group of records created by the anonymization algorithm satisfies l-diversity if it contains at least l well-represented values for the sensitive attributes, i.e., the probability that an individual in this group can be linked to a sensitive attribute value is at most $\frac{1}{l}$. The group in Figure 2.3 satisfies 1-diversity for the query "night club". Li et al. [105] argue that l-diversity does not work in the cases of skewed distributions. If the attacker can classify the users into groups of homogeneous sensitive attribute values, he could infer the value of the sensitive attribute. So they proposed t-closeness to maintain same distribution of sensitive attributes for the entire dataset. To improve the diversity of the anonymized dataset, a different grouping strategy that considers such sensitive values could be used. Inheriting from both k-anonymity and l-diversity, Wong et al. [156] proposed (α, k)-anonymity to protect the location privacy. To satisfy (α, k)-anonymity, a data table must satisfy k-anonymity and the frequency of sensitive values for each group in the table must be αk. Multiple other suggestions are available to prevent sensitive attributes association [45,69,133,140].

user identifier	$x-$coordinate	$y-$coordinate	age
1	$7-8$	$2-5$	27
4	$7-8$	$2-5$	77
6	$7-8$	$2-5$	81

Figure 2.3: Cloaked dataset with sensitive attribute

Outliers From pure LBS perspective, k-anonymity tends to fail when there are *outliers* [90]. Consider Figure 2.4 . If the attacker knows the location of users u_1, u_2, u_3, u_4 and

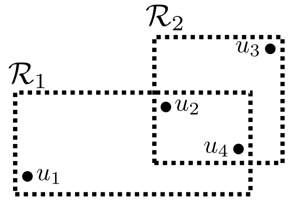

Figure 2.4: Outliers problem with k-anonymity

also that $k = 3$, then observes that a query comes from the region marked by the larger rectangle, $\mathcal{R}_1$, the attacker can figure out that the query must have come from u_1. This is because, if the query came from anyone else, the smaller rectangle, $\mathcal{R}_2$, will be observed in the query. To solve this problem, Chow and Mokbel [33] defined a new property called, k-sharing-region. This property requires that the cloaked region must be shared by at least k-users, i.e., at least k-users included in that region only. In the example of Figure 2.4, if the privacy algorithm chooses the region $\mathcal{R}_2$ for the users $u_2, u_3,$ and u_4 then the region $\mathcal{R}_1$ cannot be chosen for the users u_1, u_2, u_4 and the algorithm must find another two users sharing the same region with the user u_1. Kalnis et al. [90] discuss the importance of the *reciprocity* property and show how the quad-tree based algorithms for k-anonymity (discussed in Section 2.2.1) fail in the case of outliers. To maintain reciprocity, the cloaking algorithm must return the same cloaking region for all the queries made by any user in that region [70].

Cloak region size Even without assuming background knowledge for the attacker, k-anonymity still may fail to protect the location information of the user in some skewed distribution cases. For example, if $k = 3$ and all three users are using LBSs while sitting in a small room. The narrow region returned by the algorithm is granular enough for the attacker to locate the users. So, most of the location privacy algorithms guarantee that the size of a cloaked region is greater than some threshold area in addition to k-anonymity property.

Clearly, the above solutions add more restrictions on the privacy algorithm to determine the cloaked region and hence increases the chance of not satisfying the query, which degrades down the QoS. Finally, it has to be noted that, most of the problems common to k-anonymity based approaches also apply to techniques based on the anonymity sets if they consider the minimum size of the anonymity set as the main privacy parameter.

2.3 Obfuscation

Location obfuscation is a technique used in LBS to protect the location privacy of the user by degrading the quality of information about her location in order to avoid revealing the exact spatial location. Duckham and Kulik developed a formal model for spatial obfuscation and privacy [48]. They define obfuscation as: "introducing imperfection as the result of the deliberate degradation of spatial information quality." They refer to three types of imperfection: *inaccuracy*, *imprecision*, and *vagueness*. Inaccuracy is a situation in which the provided information is not true; imprecision occurs when the provided information is not specific; vagueness is the lack of definite boundary. For example, the position of the user shown in the map in Figure 2.5 can be obfuscated by giving an imprecise location data, such as saying that the user is located in the campus of the University of Denver, or an inaccurate position such as the intersection of Evans Ave and S University Blvd, or a vague location such as near to Daniels College of Business.

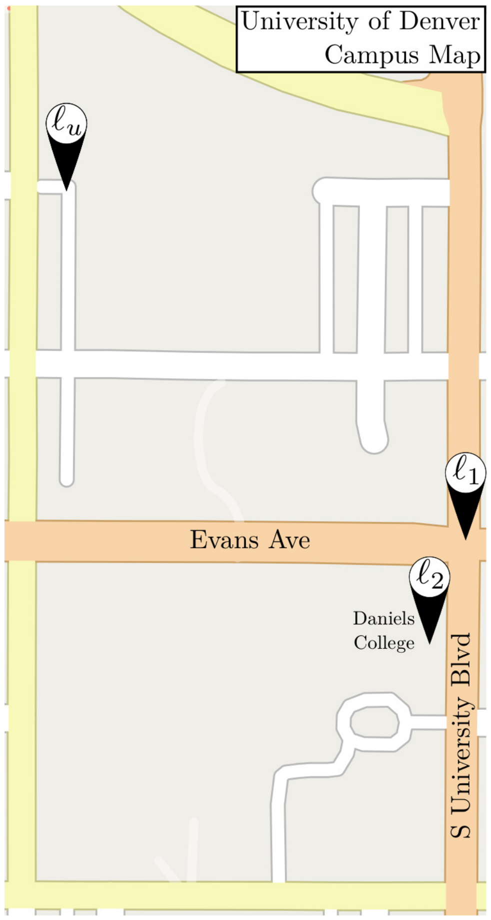

Figure 2.5: Spatial obfuscation types: ℓ_u is the user's location, the entire map represents imprecision obfuscation, ℓ_1 represents inaccuracy obfuscation, and ℓ_2 vagueness obfuscation.

The straightforward approach for implementing this technique is by creating a closed region around the client's location and send it to the service provider instead of revealing the exact location information in order to obtain a specific LBS [7,29,48,160]. The service provider returns the candidate result based on the given region. Obviously, this approach puts the onus on the client to determine and send a large enough region as part of the query to the LBS and to process the large dataset containing information about the large region coming back from the LBS as a response. With both processing power on mobile devices at that time and communication bandwidth being precious, this straightforward approach needs to be improved. This had led to several existing approaches that use TTP that does the obfuscation on behalf of the users and processes the bigger datasets obtained as part of the response from LBS for obfuscated region queries. In fact, these approaches impose a change to the current working structure of the LBSs. Additionally, in practice, it is difficult in real life scenarios to obtain a trusted third party and even then, get enough critical mass of users that trust the same TTP. Further, TTP has the major disadvantage of creating a bottleneck for data transmission and also become a single point of failure both in terms of utility and privacy. A breach of security on the TTP often results in total loss of privacy of all users utilizing that TTP.

There were several attempts to eliminate the use of TTP. For example, Yiu et al. [165] proposed the “SpaceTwist” algorithm to offer location privacy for n nearest neighboring POIs without requiring a TTP anonymizer. The client sends a fake location information called anchor to the server. The SpaceTwist on the server returns POIs to the client in ascending order based on their distances from the received anchor. The client iteratively processes the received POIs based on the actual location of the user until the nearest n-neighbor POIs are collected. For the same purpose of avoiding the TTP, Kim [95] proposed a framework based on Voronoi diagrams [1, 11, 101] to obfuscate the location of the user. Similar to Yiu et al. [165], the service of finding the best set of POIs for the user has been reduced to the problem of finding the nearest neighbor object and ignore any other possible user’s preferences for the POI. Another approach is the coordinate transformation by Gutscher [78, 152] where the mobile client applies a geometric transformation function over the user’s location and then sends it to the LSP. For example, in range query, after receiving transformed coordinates of the query area, the LSP selects all POIs located in that area and sends them to the mobile client. The client then applies inverse transforms to the locations of the returned objects. The main disadvantages of this approach were observed by Gutscher [78]: (1) additional processing complexity needed for transformation, and (2) it provides a relatively "weak" protection.

Hashem et al. [82] adopted obfuscation approach in order to answer a query of group nearest location of a meeting place. For example, consider a group of users who wants to meet in a restaurant where the total travel distance is minimized for all group members. The privacy of the user is protected by sending an obfuscated region to the LSP instead of the exact position in such a way that the results returned by the LSP will include the actual nearest neighbors of the user. The set of candidate answers is passed to each user individually in a random order to modify it. The actual answer is broadcast after all users modify the set of candidate answers. If the attacker already has a background knowledge about the targeted map he may be able to reduce the size of the obfuscated area by using this background knowledge.

Based on the geographic context of the map, Damiani et al. [37,38] proposed an obfuscation technique in which any POI on the map is abstracted as a feature of a specific type. The privacy profile of the user describes the sensitivity level for each type. The cloaked region covers both sensitive and non-sensitive areas. This is done in such a way that the probability of associating the user to a sensitive feature is below a configured threshold. Ardagna et al. [8] characterized the probabilistic requirements for a general model of geographic aware obfuscation mechanisms.

The literature discussed so far is based on giving imprecise information to the service provider in order to obfuscate the location information of the user. An alternative type of location information imperfection is when the user presents an inaccurate or a false position to other parties in a communication system. Using a Bayesian network model An et al. [5] shows how the user can choose the "right" false position, i.e., the position that seems reasonable to the attacker. The natural extension of this work is when the user needs to navigate a path from some source location to a destination. If the attacker can successfully trace some of the requested paths by the user, then the attacker may have a good chance of finding out the identity of the user and some of her activities based on the collected source and destination locations (see Section 1.3.2 & Chapter 3). To solve this problem, Krumm [98] proposes generating extra false trips that are indistinguishable from the true one to confuse the attacker that is trying to trace. Towards the same purpose, Lee et al. [103] suggested adding extra fake sources and destinations to path queries.

Most proposals that use obfuscation techniques, model an attacker and discuss various ways the attacker can gain more knowledge even in the case of obfuscation. Duckham et al. [50] model a geographic environment of road networks as a weighted graph where the user can move between adjacent nodes along the edges. The weight of the edge represents the distance along that edge. The authors presented in that work a formal model for different possible strategies for an attacker to enhance his knowledge about the user's location given an obfuscated location information over time.

Although they require some changes, most existing privacy preserving algorithms for LBSs are designed based on the mobile telecommunications infrastructure, e.g., base stations or cell towers and mobile phones in large geographical areas. Consequently, these algorithms cannot be applied to an ad-hoc environment such as mobile P2P networks, where a user can only communicate with other peers through P2P multi-hop routing without any support from servers. Several works [35, 81] proposed obfuscation algorithms for mobile P2P networks.

QoS vs LoP trade off. The main disadvantage of any obfuscation technique comes from the clear trade-off between QoS and Level of Privacy (LoP) that can be achieved by the obfuscation. Most proposals that use an obfuscation technique provide a configurable parameter or a tuning mechanism that achieves a balance between QoS and LoP based on the intended situation. For example, Duckham and Kulik [48] propose a negotiation algorithm between the user and the service provider to find a satisfactory balance of QoS and LoP. They present different negotiation strategies and simulate them [49]. They propose that the obfuscation region can be imagined as a set of discrete location. The negotiation process terminates if the proportion of the obfuscation set that is closest to each POI in the query is greater than or equal to some threshold value selected by the user. This threshold is a fraction ranges from 0.0 to 1.0, and it is called the confidence value. The confidence value reflects the satisfactory QoS chosen by the user where 1.0 means perfect QoS. Cheng et al. [29] also study this trade-off in their proposed probabilistic model for range queries.

2.4 Spatio-temporal Cloaking

Many researchers in the mobile location privacy field tried to combine both k-anonymity and obfuscation to benefit from the advantage of both approaches [64,75,167]. This involves creating a cloaked region of minimum area A_{min} which satisfies the condition of k-anonymity i.e., the clocked region is guaranteed to include $k-1$ users in addition to the user that generated the query. Usually, the parameters k and A_{min} are considered as the privacy requirements set by the user. The literature refers to this approach as spatial cloaking. Obviously, the main disadvantage of spatial cloaking is the need for TTP anonymizers inherited from the k-anonymity approach. Although spatial cloaking can protect the privacy of the user at specific time snapshot, it is not guaranteed to maintain the required k and A_{min} for a location trajectory of the user. An attacker may use the location trajectory data as a QI to discover the actual identity of the user. Different clustering and analysis algorithms for location trajectory data was developed e.g., [102,153,159].

The location trajectory in this context is the path that a moving object follows through a geographical area as a function of time. It can be represented by discrete timestamped location points (x_i, y_i, t_i) ordered in time. Consider a toy example of a dataset of trajectories that captures the movements of people as shown in Figure 2.6. Each record in the dataset has a unique pseudonym, ID, corresponding to a user. For instance an individual with $ID = 2$ visited the locations $(2,1), (5,5), (7,6)$ at timestamps $1, 3, 4$ respectively. Although this data set does not contain any identifier such as name or a QI such as age, the attacker may still be able to link the given spatiotemporal data points of a record to a certain user. Let us assume the attacker knows that the individual of $ID = 3$ was at work at time 1 and the work location is $(2, 2)$, then the attacker can link this path to that person and learn other locations visited by her. This shows that combining some background knowledge to

ID	Trajectory
1	$(1,3,1) \rightarrow (2,5,3) \rightarrow (4,3,4) \rightarrow (5,5,7) \rightarrow (5,7,8)$
2	$(2,1,1) \rightarrow (5,5,3) \rightarrow (7,6,4)$
3	$(2,2,1) \rightarrow (3,2,5) \rightarrow (4,2,6) \rightarrow (7,5,7)$

Figure 2.6: Movement trajectory data

a published spatial and temporal database creates threats to the privacy of the individuals in that database.

Different approaches for protecting spatiotemporal location privacy were developed. Ghinita et al. [67] propose a spatiotemporal cloaking that prevents the attacker from tracing exact locations based on prior knowledge about maximum user velocity. The attacker's background knowledge of the map represented by privacy sensitive locations is considered in that approach to improve the privacy. Chow and Mokbel [33] propose that cloaked regions need to be selected in such a way that the group of k-users selected for the cloaked region of the first query must be included in all cloaked regions of the subsequent queries. One obvious disadvantage of this approach is that the area of the cloaked region can become very large, eventually, after processing a sufficient number of queries as the users move farther. The cloaked region area can be reduced if the anonymizer was able to get movement directions and velocities of the users in addition to their locations beforehand. An algorithm to cluster queries based on the mobility patterns of the users proposed by Pan et al. [129]. The algorithm tries to balance between the offered level of privacy and the incurred distortion from the anonymization. Other alternative approaches are also proposed for protecting spatiotemporal location information, such as mix-zone [126–128], path cloaking [87,88] and dummy paths [104].

2.5 Cryptography Based Mechanisms

Privacy protection mechanisms discussed so far, except for the policy-based ones, suffer from the following general disadvantages.

- QoS/Privacy level trade off.

- The area of the obfuscation region can be reduced if the attacker has a background knowledge about the map.
- Heavy dependence on the distribution of other mobile users over the geographic space.
- Requires a critical mass of users to sign up for the service so as to ensure the timely formation of anonymity sets.
- Dropped/unanswered queries if the required privacy parameters cannot be met with threshold time limits.
- Trusted third party requirement, which requires major changes to the current communication network topologies, represents a performance bottleneck and can be a single point of attack or failure.

In contrast, the cryptographic approaches try to apply cryptographic techniques to the query/answering mechanism to achieve location privacy. In this section, we review the proposals in this area.

Khoshgozaran and Shahabi [92] give a method to process private queries for n nearest neighbor objects by transforming all static and dynamic objects of the map to another space using Hilbert curves. The proposed method preserves the privacy of the user in a relatively efficient manner in terms of computational cost compared to the classical encryption techniques. The Hilbert curve is a type of space-filling curve that can preserve the closeness of points in the transformation. For a query from the user, the privacy aware database returns the set of points that are nearest to the queried point in the Hilbert curve space. Another cloaking algorithm that uses Hilbert curve is proposed by Kalnis et al. [90] also preserves the reciprocity property.

A combination of Private Information Retrieval (PIR) technique [32] and Hilbert curve proposed by Ghinita et al. [68] to achieve location privacy. The database initially is populated with approximate neighbors using Hilbert curve and the clients use PIR to retrieve nearest neighbors without revealing the query. The biggest drawback of private query methods is the requirement of a preprocessing step that encrypts the entire database at the service provider. This is very impractical in typical LBS scenarios. Moreover, such encryption and lack of visibility into the contents of the user's query is a tough sell, where the service provider has to blindly answer the queries. We compared the performance of different PIR methods and suggest some performance enhancing heuristics in our paper [57]. To overcome the difficulties that come along PIR implementation, Khoshgozaran et al. [93] and Papadopoulos et al. [130] suggested a secure processor on the server side to ensure that the content provider is oblivious of the retrieved answer of the query. Further discussion on PIR techniques and their implementation challenges in Chapter 5.

To protect the location privacy in proximity service where the LSP alerts the user if one of her friends is in her vicinity, Mascetti et al. [113] proposed two protocols called C-Hide&Seek and C-Hide&Hash. The two protocols rely on the symmetric cryptography concept. Because it uses symmetric key cryptography, it is assumed that users are sharing the same secret key. Each user has to send an update of her location to the LSP periodically, but since this update is encrypted it is guaranteed that the LSP cannot determine her position. Regarding the privacy with respect to other users, i.e., friends, the user will express her position by specifying a region of a geographical space with a spatial granularity that satisfies her privacy preferences.

Marias et al. [110] proposed an approach based on the secret sharing scheme of Shamir [139]. The main idea of Shamir's scheme is to express the secret information by some random polynomial of any degree n, $f(x) = a_0 + a_1x + \ldots + a_nx^n$. Let the secret information be the number a_0, then compute the secret shares which are the evaluation of the polynomial at $n+1$ points such as $f(1), \ldots f(n+1)$. Clearly, all the shares are required to reconstruct the polynomial and then compute the secret information, $a_0 = f(0)$. The approach requires a different architecture where the location information needs to be partitioned into a number of shares and distributed among a set of LSPs. The user that is interested to find the location information of an object must access all the servers holding the shares of that object's location. The main disadvantage of this approach is the requirement of keeping synchronized information among all the servers.

2.6 Differential Privacy

Anonymization and obfuscation mechanisms discussed previously are describing a method for concealing the user's data; but, do not give a measurement tool for the advertised privacy level. Although different evaluation methods are proposed e.g., [7, 29], yet they lack for a precise measurement of the amount of leaked information that could be useful for the adversary [144]. Furthermore, anonymity and entropy-based metrics could produce inaccurate assessments of the privacy levels offered by the algorithms [141]. Recently, the research tends toward *differential privacy* as an alternative mechanism to protect the privacy of location data. Differential privacy was first proposed by Dwork [52], and then later enhanced in several works [25, 65, 107] to avoid many of the weaknesses and suit different types of applications. Different implementation techniques and application areas for differential privacy have been studied [51, 53, 114, 157].

The most important feature of this technique is the disciplined statistical analysis for evaluating the protection level of privacy. On the other hand, the attacker's background information is one of the biggest challenges that faces any privacy protection mechanism in general. Substantial background information for LSP are publicly available today with sufficiently high reliability and detail, which makes this problem remarkable for a privacy protection mechanism. Based on strong mathematical theory, differential privacy ensures that the attacker cannot identify individuals from a protected dataset regardless of the amount of background information that he has.

First, the main concept of differential privacy technique is introduced, then we will explore different methods suggested in the previous research to implement this technique in the realm of location privacy preservation.

2.6.1 Intuition of differential privacy

In statistical databases, the communication with the database typically occurs through aggregate queries. The main idea of differential privacy is that, instead of publishing the original database, another copy is created in a way so that the statistical accuracy of the

Name	Age	HIV
Peter	27	1
John	50	0
Mary	45	1
Sally	32	0
Luis	60	0
Helen	28	0
Iris	33	1

Figure 2.7: Sample of medical dataset.

answer to the aggregate query against the released (modified) database is degraded to guarantee non-disclosure of any information related to any specific record in the database. Consequently, the attacker cannot determine whether or not a certain record from the original database changed in the released database. For a deep discussion of the method with related mathematical proofs, the reader is referred to Dwork and Roth [54]. We present here a quick overview to give an intuition about the main concept. In Chapter 8, we discuss differential privacy further and present our implementation for protecting privacy in LBSs using this technique. We use the following trivial example to illustrate the idea of compromising a statistical database. Assume a database table, T, shown in Figure 2.7 for medical records, where the value 1 for the field HIV indicates that the corresponding person has that disease and 0 is not. Assume the attacker knows that Mary's age is 45, then he can execute the query,

$$Q_1 : \, select\, sum(\text{HIV})\, from\, T\, where\, \text{AGE} = 45,$$

to find out if Mary has HIV or not. Similarly, even if the attacker does not know the exact age, his knowledge about the victim could be enhanced by using this attack. For instance, if the attacker knows that Peter is one of the patients in the database and he does a query as follows

$$Q_2 : \, select\, sum(\text{HIV})\, from\, T,$$

he will get an answer 3. Based on that, his guess of Peter being HIV positive is $\frac{3}{7}$. If the attacker knows that, Peter is between age 25 and 35, he can issue the following queries

$$Q_3: \textit{select count}(*)\,\textit{from}\,T\,\textit{where}\,\text{AGE} \geq 25 \text{ and } \text{AGE} \leq 35,$$

$$Q_4: \textit{select sum}(\text{HIV})\,\textit{from}\,T\,\textit{where}\,\text{AGE} \geq 25 \text{ and } \text{AGE} \leq 35.$$

The attacker will gather that there is a total of four records that match Q_3 and the query Q_4 returns 2. So, the attacker can conclude that the chance of Peter being HIV positive is now $\frac{1}{2}$, which is greater than his previous conclusion. One way to enhance the privacy in this situation is to introduce a perturbation mechanism in the answer. When the attacker who is expected to know the privacy enhancing techniques in place sees the answer for query Q_4, he cannot be sure about his probability assignment of Peter being HIV positive anymore. We formalize this concept as *differential privacy* as follows.

Consider a statistical database where, instead of returning the exact answer, it uses some random perturbation mechanism that takes a dataset T as input and produces output $y \in Y$. A mechanism, $\mathscr{M} : T \to Y$, is applied to the answer before it is returned. The mechanism $\mathscr{M}$ is called $\epsilon-$differentially private if

$$\frac{\Pr\left[\mathscr{M}(T) = y\right]}{\Pr\left[\mathscr{M}(T') = y'\right]} \leq \exp(\epsilon) \forall y, y' \in Y, \tag{2.1}$$

where the datasets T and T' differ in at most one record. It is obvious from Equation 2.1 that the smaller the value of ϵ the higher the privacy level. If both numerator and denominator were 0, then by convention the ratio is assumed 1.

Let T' be a copy of T with Mary's record removed. Assume now that the attacker can access this new copy, T', and he knows how the mechanism $\mathscr{M}$ works. The attacker sends the query Q_1 to the server and gets the answer as perturbed by the privacy mechanism, $y = \mathscr{M}(Q_1) \in Y$. Given y, T', and $\mathscr{M}$, the question now *is the attacker able to determine whether Mary is HIV positive or not?* Since the returned value, y, is chosen at random from the output set Y, the attacker may add Mary's record to the dataset T' and execute Q_1

for each possible value of HIV field, which is $\{0, 1\}$ in this example. Let the answers be y_0 and y_1 for the inputs 0 and 1, respectively. From Equation 2.1, $\frac{\Pr[y_0=y]}{\Pr[y_1=y]} \leq e^{\epsilon}$, which means that the chance for the attacker to *differentiate* between the two possible values of HIV is not greater than the threshold value, e^{ϵ}. The concept can be generalized for any range of the output set as long as the condition in Equation 2.1 is satisfied for each possible output $y \in Y$. From this example, it is clear that differential privacy does not put any limitations on the attacker's power.

2.6.2 Differential privacy for location data

To the best of our knowledge, Machanavajjhala et al. [107] is the first work that formally proposes differential privacy to protect location data. It suggests an enhanced version of the differential privacy, called the probabilistic differential privacy, which is utilized to create synthetic datasets from the US Census Bureau data for the purposes of statistical analysis for mobility patterns of individuals. The basic idea was centered on building a statistical model derived from the original data, and then use this model to replace some of the points in the original data.

Applying differential privacy to protect spatial data is not easy due to the difficulties that may arise from the sensitivity of these applications. Perturbing location data without carefully calibrating the added noise, usually, yields to a meaningless result. Another problem faced by differential privacy technique in LBS is that differential privacy was designed to deal with applications in which the published information is collected for many users. While in the case of LBS, what is required is to protect the data for a single user. Instead of directly applying differential privacy, Dewri [42] introduced the idea of creating a set of k anonymous locations, and then a random location drawn from a Laplace distribution is selected for the query. The advantage is that the probability of choosing any one of these locations does not exceed certain threshold e^{ϵ}. To protect the spatiotemporal data of a moving object Assam and Seidl [10] require a TTP that uses a Kalman filter to generate an optimized set of differentially private obfuscated nearby locations. The query's location is chosen from that set and sent to the LPS.

A new privacy metric, $\epsilon-$geo-indistinguishability, is introduced by Andrés et al. [6]. The authors argue that a user normally will demand higher privacy in his near perimeter while she is going to be less interested in privacy as this perimeter is increased. To achieve this, they add planar Laplace noise to the location data of the user. As a result, the amount of noise shall be higher in locations closer to the true location of the user and progressively less as we move away from it. Many other approaches extend the concept of $\epsilon-$geo-indistinguishability [18,26,121,158] to build location privacy protection mechanisms.

2.7 Motivation

Location privacy loss has been a recognized problem for several years and hence several attempts have been made by the research community in coming up with algorithms that preserve location privacy while not giving up the utility of LBSs. LPPMs come in various flavors. Initially, these LPPMs were one-size-fits-all solutions that offered enhanced privacy to all users of the system at an equal level. Soon, researchers realized that privacy needs are different for different users, and even for the same user, privacy requirements are different in different situations. The most recent LPPMs proposed in the literature provide their users configurable levels of privacy that are balanced against QoS.

A common theme emerges when one looks at the survey of existing techniques. TTP-based techniques suffer from several disadvantages. They are impractical as they require fundamental changes to current architectures and revenue models. In real life, it is difficult to find a trusted third party that is cheap or free. Payment-based third parties can become expensive. Also, most TTP-based techniques require a critical mass of customers for them to achieve reasonable privacy levels. This requirement of TTP has a significant impact on QoS as users often have to wait till k other users accumulate. Some algorithms even proposed discarding the user's query if it cannot be answered by the TTP within a specified threshold time period [63]. Third parties become additional attack targets and in many cases a breach of a TTP results in total loss of privacy for the customers. TTP-based techniques evolved during a time when mobile devices had a very limited processing power and can only be considered thin clients. So, third parties not only played a role in enhancing privacy, but also in taking most of the client side processing burden. This creates a performance bottleneck in the architecture at the third parties. A third party with performance problems will impact all the clients connected to it. Although one might assume that these bottlenecks can be avoided by using redundant third party servers, it will only exacerbate the other problems such as cost of building trust, waiting for critical mass of clients on the failover server, reconfiguration of clients etc., So there is a need for the research community to look into third party free protocols, study them and propose new techniques.

Later developments in hardware have resulted in mobile devices that are powerful enough to implement efficient algorithms. Thus newly proposed privacy preserving techniques that take advantage of the superior, although limited, power of current mobile devices should be practical for current day user. The techniques need to work within the framework of current service providers without requiring them to make huge architectural changes. This will eliminate single points of failure and distribute the computing requirements more efficiently. Moreover, they need to be practical in terms of the kind of data expected from service providers. In recent years, LBS search often results in richly tagged POIs that not only contain location information, but also other interesting information such as ranking, customer reviews, business hours etc., Without other meta-data about POIs, the POI search boils down to nearest neighbor search problem and there are several proposals in the literature that address this problem. So, techniques proposed should do more than just rank the result set only based on distance from the user.

Eliminating the requirement of trusted third party does not eliminate the threat to user's location privacy. Now, the techniques have to deal with a sophisticated attacker that can be the service provider itself. Thus techniques are needed that enhance user's location privacy in the presence of a semi-trusted LSP.

2.8 Problem Statement

Lots of existing proposals in the LBS privacy area require trusted third parties that have their own problems as explained earlier. These proposals assume a very limited mobile devices hardware and don't properly utilize the capabilities of modern mobile hardware. Moreover, most of these techniques fail if the attacker is a semi-trusted service provider itself. So our problem statement can be summed up as follows.

We need a set of LBS privacy preserving techniques with the following properties.

TTP needs to be avoided. As discussed earlier, a TTP introduces inherent problems such as single point of failure in terms of availability, performance, security, and privacy.

Take advantage of the modern mobile hardware. Modern mobile hardware can be compared with personal computers from a few years ago in terms of their performance capabilities, programmability, and available resources. Any proposal should take advantage of these advances.

Does not require extensive changes in existing architectures. Any proposal should not require extensive changes in existing LBS architectures. Such proposals immediately become impractical as they require huge expenditures from the service providers, where customer privacy may not be the top most priority.

Provide for configurable LoP. Privacy requirements, even for the same user changes based on the situation. The user may not care if she is placed accurately in a sports stadium, but may care even if placed inaccurately when traveling across town by an attacker. So any technique proposed should be able to take this into consideration and be configurable using some parameters.

QoS cost. The privacy achieved often comes with a cost of degrading quality. Often in the form of delay between request and response. So any technique proposed should be practical enough that, the noticeable delay should still be in the acceptable range for the given parameters.

Should address both single and multiple query scenarios. The proposed techniques should, of course, preserve the privacy of the user when making a single query to the LBS. Most users though use the LBS in a repeated fashion as they move around . As we show later in Chapter 7, multiple query scenario poses its own risk to the privacy. So any technique should consider both scenarios.

Measurable improvement in privacy. Any technique proposed should be implemented using openly available standard libraries. Their practicability needs to be proven (or disproven) based on the observations and measurements made on this implementation. Moreover, specific privacy measures need to be considered and shown that the implementation has actually improved these privacy measures.

Realistic top-K ranking. The majority of proposed privacy preservation mechanisms for location-based services in the existing research ranks the result set of POI based only on distance. Since this approach boils down the problem of calculating the result set of POIs to the nearest neighbor search, it has an advantage of less demanding computations. But, real providers for location based services rank the result set of POIs based on the distance and the prominence value of each POI on the set.

Chapter 3

State of User's Location Privacy

In this chapter, we present the current state of location privacy in terms of LBSs by presenting how powerful the service provider can be in determining accurate user locations even with incomplete data. By showing this, we wish to drive the point on the need for equipping the client with defensive privacy protection mechanisms that are practical and do not rely on trusted third parties.

Location privacy is an important expectation by the users of LBS. Location privacy can be lost when an attacker eavesdrops and monitors communication between the users and the service provider. There are several techniques proposed and implemented in the communications security space that address this problem. In this dissertation, we are mainly concerned with loss of location privacy in spite of an assumption of secure communication between the user and service provider. We are concerned with the case where the user has a certain expectation of location privacy when using the LBS from the service provider. But in these days, where, accurate information about the user including her location is treated as an asset and can be easily monetized by service providers, many users pay attention to what data is being collected about them and often interested in implementing LPPMs that reduce the accuracy of location inference by the service provider to acceptable levels. In this chapter, we present our work done in this regard, which shows that the user's expectation if not being tracked can be easily breached by a resourceful service provider without directly collecting location data. The example we pick is the driving habits data, that is commonly being collected by automobile insurance companies. Most of these programs do not directly collect user's location, but collect driving habits data, in exchange for which they offer the opt-in users a potential discount. We show that, by using few techniques, these companies are capable of inferring user's location with reasonable accuracy breaching the expectation of the user of her location privacy. Using this, we argue that, similar to the modern techniques being developed to enhance location privacy, the service providers have access to data and techniques that enhance the accuracy of inference of user's location. This builds a case for the importance and urgency of location privacy preservation techniques presented in this work.

3.1 Collecting Driving Habits Data: Problem Definition

To demonstrate such a situation, we use the case of pay-how-you-drive programs. Many automobile insurance providers these days offer programs where they collect driving habits data from their customers in exchange for discounts in their premiums. Many auto-insurance owners are probably familiar with the insurance discounts one can get by enrolling in telematics-based pay-how-you-drive programs. Examples of such programs include Progressive's Snapshot[1] , AllState's Drivewise[2], Safeco's Rewind[3], Aviva's Drive[4], and many others. These programs rely on the collection of *driving habits data* (time of driving, speed, mileage, etc.) during a monitoring period, which is later analyzed to offer a customized discount to the policy holder [43].

These pay-how-you-drive programs offer many advantages to both insurers and the consumers. Insurers can offer more accurate pricing to consumers based on their driving habits. This increases affordability for safe drivers, and motivates others to adopt safer

[1]www.progressive.com/auto/snapshot

[2]www.allstate.com/drive-wise.aspx

[3]www.rewindprogram.com

[4]www.aviva.co.uk/drive

driving habits. Given the incentive to drive less, these programs also help reduce road accidents, traffic congestion, and vehicle emissions. Telematics have also proven useful in monitoring driver safety (e.g. the OnStar program), evaluating accident liability, preventing vehicle theft, tracking fleet movement, and routing traffic efficiently. For the customer, the advantage, particularly for a safer driver, is that their premium matches the risk profile more closely and they are usually promised that their premiums will not increase due to the participation in these programs.

While few programs disclose that their data collection devices track the driver, most do not (or at least claim not to) track exact GPS locations, and imply an expectation of privacy that the customer's destinations are not tracked. Please note that all insurance companies are required to collect their customers address, so they already know the source of most user's trips. So, privacy of the destination location is expected by most users of these programs. Privacy policies clearly state what information is collected, the possibility of sharing the data with third-parties, using it for fraud prevention and research, or to comply with the law. Even if the service provider itself is trusted, the sharing of the data with third parties for processing, fraud prevention, compliance etc., increases the risk to location privacy from entities that are authorized to get the data.

Our goal is to show that, service providers or authorized third parties, are capable of breaching user's location privacy even if GPS location data is not directly part of the collected data. A number of researchers have shown that privacy cannot be guaranteed simply by avoiding sharing or avoiding the direct collection of private data. The possibility of linking using quasi-identifiers, or other sophisticated methods, always remain (Section 1.3.1). Half of the individuals in the U.S. population can be uniquely determined if their home and work locations are known at the level of a census block [74]. In GPS logs, people can be identified based on the last destination of the day and the most populated cluster of points [86, 97]. We treat driving habits data as quasi identifiers in our technique, but our goal is to identify the destination of the trip instead of the identity of the user.

To achieve this, we develop a location inference attack that executes on real traces of driving habits data, and attempts to identify the destinations of the trips during which the data were collected. Our techniques extract potentially quasi-identifying information such as traffic stops, driving speed and turns from the data, and match them to publicly available map information to determine potential destinations of a trip. In the rest of the chapter, we describe the implementation of these techniques and demonstrate that a number of trips can indeed be geographically matched to their destinations using simple driving features. Our conclusions are based on a probabilistic ranking of the possible destinations of a trip. Although not a foolproof method, this study shows that the destinations of certain trips can be very easily identified, thereby raising concerns about current expectations of privacy set by the data collection agencies. Of greater concern is the relatively unsophisticated (often common sense) nature of the concepts underlying our inference algorithm. We can only imagine, in the hands of a resourceful attacker with access to better databases, the accuracy of the destination inference can be further improved.

3.2 Location Privacy Model

In this section we model the user's location privacy in the context of driving habits data. Location tracking enables inferences about an individual's lifestyle and social circles, most of which may be considered private. Although the decision to share one's location is a personal one, such decisions can only be made when the intent to collect location data is fully disclosed. Therefore, location data collection and sharing practices should be explicitly stated in the privacy policies of pertinent businesses. The difficulty arises when the location information is inferable from other types of seemingly unrelated data, in which case, either the possibility of inference is unknown to the business, or the location data is inferred and used without consumer's consent. We make the conservative assumption that if inferences are possible, they will be made.

We study the threat of location data in Section 1.3. Location inference is a deduction about the geographic location of an event from other known facts. We focus on the problem in the context of driving habits data collected *with* the consent of the driver. The collected data has no direct tracking of the user's location. Therefore, user's are led to have an expectation that the data collection agency, or an adversary with access to the data, is unable to track the driver using this data. Consequently, we assume that obtaining knowledge of the destinations of travel is a clear violation of the location privacy expectations of the driver. This also implies that if a destination can be reached via more than one route, an inference of the correct destination is considered a violation even if the correct route is not inferred. We also assume that the driver has typical driving habits, such as staying within reasonable speed limits and taking best possible routes.

3.3 Driving Habits Data

In the pay-how-you-drive context, the intent of collecting driving habits data is to assess the risk of the driver, not necessarily to determine where the user is driving to. So driving habits data includes features such as time of driving, speed, acceleration/deceleration patterns, distance traveled, braking practices, and others. Unless the associated service explicitly requires customer tracking, collection of location data is avoided for privacy concerns. We explain a typical data collection exercise by using an auto-insurance discount program as an example. Typical auto-insurance discount programs (propelled by driving habits data) are opt-in programs where the driver has to enroll to be evaluated for a discount in her insurance premium. Upon enrollment, the driver receives a data collection device that can be plugged into the on-board diagnostic (OBD) port of the vehicle. The device collects driving habits data over a period of several days to few months. Some devices can periodically upload the data to a background server using consumer telecommunication networks. The device is returned to the agency at the completion of the data collection phase. Based on factors such as distances driven, time when driven, and absence of hard brakes, the driver is issued a discount in the insurance premium for the current and future terms.

3.3.1 Data collection

Often some insurance companies let the user view near real time plots of the driving habits data collected on them. Unfortunately, the data underlying these plots is not available for download. With the ability to read most of the data from the vehicle's on-board computer, the collected raw data is expected to be precise and frequent. Therefore, we used a commodity tracking device (LandAirSea GPS Tracking Key) to collect the raw data pertinent to this study. This battery powered device logs detailed driving data such as vehicle speed and GPS position, which can be later extracted into a computer through a USB connection. Note that a device connected to the OBD port can easily obtain more than ten samples per second; our tracking device operates at a much lower resolution of one sample per second. Although the device collects the GPS location (useful for validation later), the only data fields used in the inference process are: *time stamp* (t), *driving speed* (s), and *distance traveled* (d). We introduce here the term "trip" to mean a subset of the collected data, signifying a drive from one point of interest (e.g. home, office, hospital, store, friend's home, etc.) to another. Each $\langle t, s, d \rangle$ tuple of a trip is a data point of the trip.

We kept the devices in our vehicles for a period of 15 days in order to collect data from regular home-office trips, occasional shopping trips, and visits to infrequent places. We also collected a few trips between random locations at varying distances. During these trips, normal driving habits were maintained.

We use a total of 30 trips in this study. All trips are in the Denver, Colorado area, and includes home to work and work to home drives, visits to the airport, the downtown area, local grocery stores, school drop-offs, social visits, and others. Length of trips range from 1 mile to 25 miles, and spanned interstates, state highways, city roads and residential areas.

3.3.2 Pre-processing

Pre-processing is the first step in our inference attack. The idea in this step is to clean the data and remove anomalies that are a result of traffic stops and occasional zero-speed points we attribute to device errors. Our inference algorithms currently do not account for slow or “stop-and-go” driving resulting from heavy traffic; removal of data points collected during such conditions help infer locations accurately in more number of trips.

Two steps are performed in this process. In the first step, we identify the data points where the driving speed is zero (possible stop in traffic). Thereafter, all data points between two zero-speed data points (inclusive) are removed if the total distance traveled between those two points is less than a threshold (0.5 mile used in this study). In the next step, consecutively time-stamped zero-speed data points are removed if they do not span a time interval of at least 3 seconds.

After the traffic pre-processing, we note the unique distance values corresponding to the remaining data points with a zero speed value. We refer to these distances as *stop-points*, possible distances from the beginning of a trip where the driver had to halt due to traffic stops at signals or stop signs at intersections.

3.4 Location Inference Method

Our location inference method works under the hypothesis that the stop-points of a trip can be used as a set of quasi-identifiers for the destination of the trip. Therefore, if the start-location of the trip is known, we can search a map of the area for paths that begin at the start-location, and have traffic stops at distances given by the stop-points. The assumption of a known start-location is not unrealistic, since the data collectors are typically aware of the street address where the vehicle is parked overnight. Start-locations in subsequent trips can be obtained from the destinations of previous trips. Unless the roadways in the area are very regular, it is expected that a relatively smaller number of paths will satisfy the constraint to match every stop-point. The end-points of these *candidate paths* are potential destinations of the trip. We will employ a ranking process when multiple candidate paths are identified. In the following, we give a step-by-step account of the inference process as executed by us.

3.4.1 Area map as a graph

The first step in identifying candidate paths is to obtain a reliable map of the area. We obtained the map data available from the crowd-sourced OpenStreetMap project. The map data is collected for the greater Denver area, where our experiments took place. The data comes in the form of XML formatted .osm files. These files are processed to generate a graph with 323928 nodes, and 639395 directed edges representing motorways, trunks, primary/secondary/tertiary/residential roads, and corresponding link roads. Nodes are typically placed at intersections. Nodes are also placed between two intersections if the road in between is curved. Therefore, the length of a road segment can be accurately computed by aggregating the distances between successive nodes placed on the road segment. Each node is labeled with its latitude and longitude coordinates. Each edge is labeled with the geodesic distance between the two nodes of the edge. Distances are computed using the Vincenty inverse formula for ellipsoids, available as part of the gdist function in the Imap R package. Edges are also annotated with a road type extracted from the downloaded XML files. This map data[5] covers an area of more than 1500 sq. miles in Denver, Colorado and its suburbs, spanning between latitudes $39.41015^o N$ and $39.91424^o N$, and longitudes $105.3150^o W$ and $104.3554^o W$.

Speed limit information was difficult to obtain. Although it was available with some commercial providers, we were not able to obtain that information. After experimenting with some free data we obtained from Denver county, we figure out that precise speed data for each road segment does not improve the accuracy much compared with when we assign an estimated speed limit based on the road type. So we assigned speed limit values to the edges of the graph based on the road type indicated in the OpenStreetMap xml data. For example, for internal roads we assigned a 25 mph speed limit and 65 mph for the highways. A capable adversary can obtain more accurate speed limit data from commercial sources.

[5]crisp.cs.du.edu/datasets

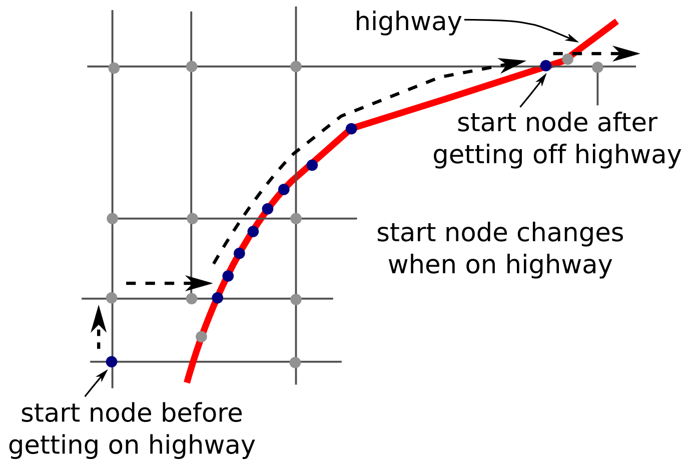

Figure 3.1: Disabling of shortest path constraint while exploring highway nodes.

3.4.2 Generating candidate paths

Candidate paths are generated by performing a standard depth-first search (DFS) of the map graph. The DFS starts at a node corresponding to the start-location of a trip and outputs all paths that satisfy the constraints discussed next.

Stop-point matching

During the DFS traversal, we keep track of the length of the path from the start node. This constraint requires that, at any stage of the traversal, the current path must have an intersection node (3-way or more) at all stop-points less than the current length of the path. However, since traffic stops often happen a few feet away from the signal (the exact coordinates of the intersection), we allow for a *slack* while matching the path length to a stop-point. The slack is set to 500 feet in this study. Stop-point matching is not performed for the last stop-point, since the last stop-point appears due to the vehicle being parked, rather than due to a traffic stop.

Shortest path

The second constraint requires that, at any stage of the traversal, a path to a node must always be the shortest one (within a slack of 0.1 miles) from the start node to that node. The constraint is motivated by typical driving behavior where a shortest path is preferred when traveling short distances inside the city. In such cases, shortest paths are often fastest paths too. This is a reasonable assumption in lieu of traffic conditions data at the time of the trip. However, the assumption fails when traveling long distances, where the driver is likely to take a faster (not necessarily shorter) route through the highway. Nonetheless, we can make the assumption that the driver would take the shortest route up to the highway, and then again from the point of exit on the highway to the destination. We incorporate this assumption by changing the start node to be the currently explored node, if the current node is part of a highway segment. As a result, the shortest path constraint remains disabled as long as the exploration continues on the highway nodes; the constraint is enabled when the exploration enters non-highway nodes, although the start node now is the last highway node (point of exit) on the path (Figure 3.1).

Turn feasibility

The third constraint requires a path to always satisfy feasible speed limits at points of right and left turns. At every point of the exploration, we compute the angle by which a vehicle would have to turn when moving from the current node to the next node(Figure 3.2). An angle higher than 60^o is considered a turn, in which case we consult the trip data to ensure that the speed at that point of time was under 25 mph. We use the current length of the path to extract the closest data point from the trip, and use the speed in that data point as the current driving speed.

Length

The length constraint terminates the exploration along a particular path when the path length exceeds the trip length. The path is then a candidate path if all stop-points (except the last one) have been matched in the path. When multiple candidate paths to the same end node are discovered, we retain the one with the least number of turns.

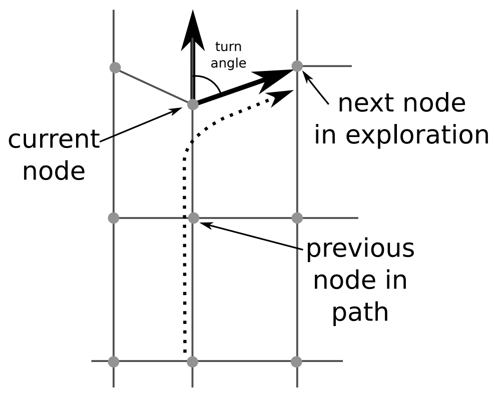

Figure 3.2: Turns along an explored path.

The nodes in our map graph correspond to points on roadways. However, the initial few data points (and the last few as well) of a trip may correspond to driving on a parking lot or a driveway. We used the GPS coordinates logged by the tracking device to manually discard some of these initial data points such that the first data point of a trip always corresponds to a node of the map graph. This processing is not required when more elaborate map data is used to generate the graph; many online services (e.g. Google Maps) already use commercial maps with data for parking areas, bikeways, and pedestrian paths.

3.4.3 Candidate ranking

The output of the DFS traversal above subject to the four constrains presented is a list of candidate paths. The candidate paths in our experiments ranged from as few as 4 to as many as 196. We process the candidates through a ranking procedure to arrive at the top inferred destination of a trip. This is where the speed limits assigned by road types come into picture again. The ranking procedure makes use of information on typical speed limits along the candidate paths to find ones that best match the speed changes observed in the trip data points. We begin by first creating an ideal speed model for each candidate, then augment the model with driving behavior typically seen when making turns, and then compute a probability for the observed trip data to have been generated from the model. The candidates are ranked based on decreasing order of the probabilities. In other words, we create a speed profile of a typical driver for each candidate path and compare it against the actual speeds observed.

Ideal speed model

The ideal speed model of a path P is a representation of the speeds that an ideal driver would follow when driving along the path under ideal conditions. An ideal driver is considered to be one who drives at exactly the speed limit, and ideal conditions imply no acceleration or decelerations in the driving speed. The model can be formally expressed as a function M of distance d and a path P. The output of such a function is the legal speed limit at distance d from the beginning of path P (assuming speed limit is same along both directions of travel).

$$M(d, P) = s^{limit} \tag{3.1}$$

In a discrete representation, the ideal speed model is an array of distance and speed pairs at points where the speed limit changes along the path.

Augmenting the model

An ideal speed model can be improved by correcting the output speed in parts of the path where the vehicle would be performing a turn. Even an ideal driver in ideal conditions will decelerate to a reasonable speed to make a right or a left turn. A turn is assumed to happen exactly at the node joining the two edges that make the turn. We assume that all left turns happen at a speed of 15 mph and all right turns happen at 10 mph. The augmented model, denoted by M_{aug}, gradually reduces the output speed to the turning speed over a distance that depends on the acceleration and deceleration capabilities of the vehicle. Similarly, the model also incorporates the required acceleration behavior after the turn is complete. For all vehicles in this study, we use a fixed deceleration rate of 25 $feet/s^2$ ($= 7.8m/s^2 = 0.8g$, g being the acceleration of gravity), and a fixed acceleration rate of 6.5 $feet/s^2 (= 2m/s^2)$.

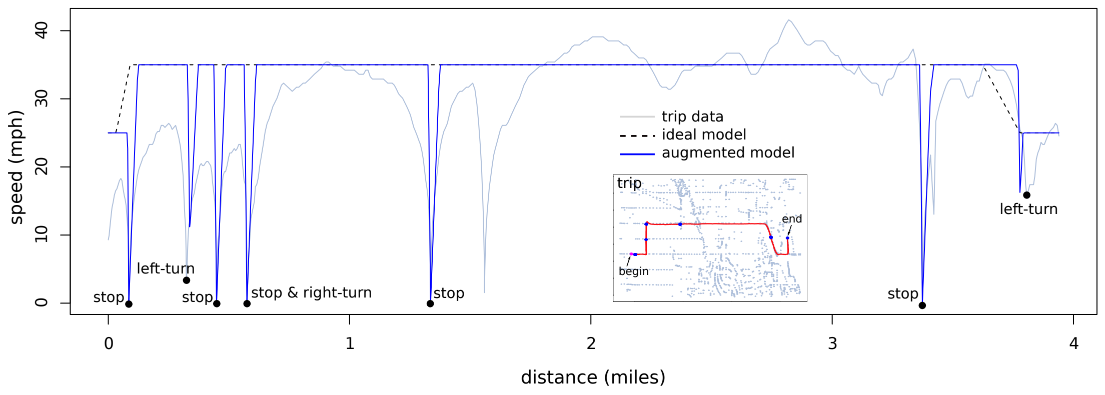

Figure 3.3: Speed profile for a trip, along with that generated from the ideal and the augmented models for a different path.

The augmented model also incorporates the information that the vehicle must have come to a complete halt at all stop-points. Similar to the turns, the output speed is corrected around the vicinity of the stop-points as well. Figure 3.3 compares the speed values from a trip, and the values generated from the ideal speed model and the augmented model along a similar path to the same destination.

Probability of a candidate path

Given a trip $\mathcal{T}$ with n data points, $\langle t_i, d_i, s_i \rangle$; $i = 1, ..., n$, and a path P, we obtain the speed values generated by the augmented model along path P at distances $d_1, ..., d_n$. We denote these values by $s_1^{'}, ..., s_n^{'}$. The probability we seek is

$$Pr\left[\mathcal{T}|M_{aug}(d_i, P) = s_i^{'};\ i = 1, ..., n\right]. \tag{3.2}$$

We assume independence of speed values across time and distance, which gives us the probability as

$$\prod_{i=1}^{n} Pr\left[\langle t_i, d_i, s_i \rangle | M_{aug}(d_i, P) = s_i^{'}\right]. \tag{3.3}$$

Therefore, for each time instant t_i, we seek to compute the probability of observing speed s_i when the speed should have been $s_i^{'}$ at distance d_i along the path. The probability is computed from speed variation models based on standard Gaussian distributions. For speed value $s_i^{'}$, the distribution used is

$$f = \begin{cases} \mathcal{N}(s_i^{'} + \frac{s_i^{'}}{10}, \frac{s_i^{'}}{30}) & , s_i^{'} \geq 20\text{mph} \\ \mathcal{N}(s_i^{'}, 1) & , otherwise \end{cases}, \tag{3.4}$$

where $\mathcal{N}(\mu, \sigma)$ signifies a Gaussian distribution with mean μ and standard deviation σ. The distribution implies that, for speed limits of 20 mph or more, the mean driving speed is 10% higher, and 99.7% of the drivers drive between speeds of $s_i^{'}$ and $s_i^{'} + s_i^{'}/20$. For example, in a road with speed limit 60 mph, most drivers are assumed to drive at speeds between 60-72 mph, with 66 mph being the mean. For lower speed limits, we assume that drivers are more likely to stay close to the limit. The probability is then computed as

$$Pr\left[\langle t_i, d_i, s_i \rangle | M_{aug}(d_i, P) = s_i^{'}\right] = \int\limits_{s_i-\epsilon}^{s_i+\epsilon} f(x)dx, \tag{3.5}$$

where ϵ is a negligible number (10^{-5}). To avoid issues of precision, we take the sum of the logarithm of the probabilities instead of the product of the probabilities at different time instances. The ranking is not affected because of this transformation.

3.5 Empirical Observations

We applied the inference algorithm to the data from 30 trips. Inference correctness depends on factors such as stop-points, abidance to the shortest path assumption, ability to drive at speed limits, accuracy of the data collection device, and the correctness of the map data. The algorithm was unable to generate any path leading to the actual destination in 12 out of the 30 trips. However, in 16 of the remaining 18 trips, the actual destination was always in the top three destinations generated after the ranking. In fact, in 11 of the 30 trips, the actual destination of the user is also the destination indicated by the first ranked path generated by our attack. Table 3.1 lists the trip length, number of candidate paths,

Table 3.1: Rank of actual trip destination from amongst the candidate paths.

trip length (miles)	number of candidates	rank of actual destination
1.48	12	1
1.59	12	1
2.60	50	1
3.23	15	1
3.78	11	2
3.85	23	1
3.93	52	1
3.93	49	1
3.95	37	3
5.47	11	2
5.89	18	1
5.84	20	1
7.95	196	2
9.42	26	4
13.15	37	3
14.10	53	1
14.57	68	1
24.10	42	13

and rank of actual destination for the 18 trips with successful inference. We are unable to find a correlation between the number of candidate paths and the ranking performance.

3.5.1 Illustrative example

Figure 3.4 shows five candidate paths identified for one of the trips. A total of 196 candidate paths were found for this trip. All candidate paths match the four stop-points of the trip (7.95 miles in length). Candidate path 118 is also the actual route taken during the trip. The last plot in the figure shows the end nodes (destinations) of all candidate paths. Irrespective of the large number of candidate paths identified for this trip, most destination nodes cluster around a small number of localities. This is worth noting, since only four stop-points are involved over a distance of 7.95 miles in this trip; yet the ways to match them to an actual map are quite limited!

Figure 3.5 compares the speed profiles of the actual trip and that generated by the augmented model for a path. It is clear that the more similar the speed limits and turns

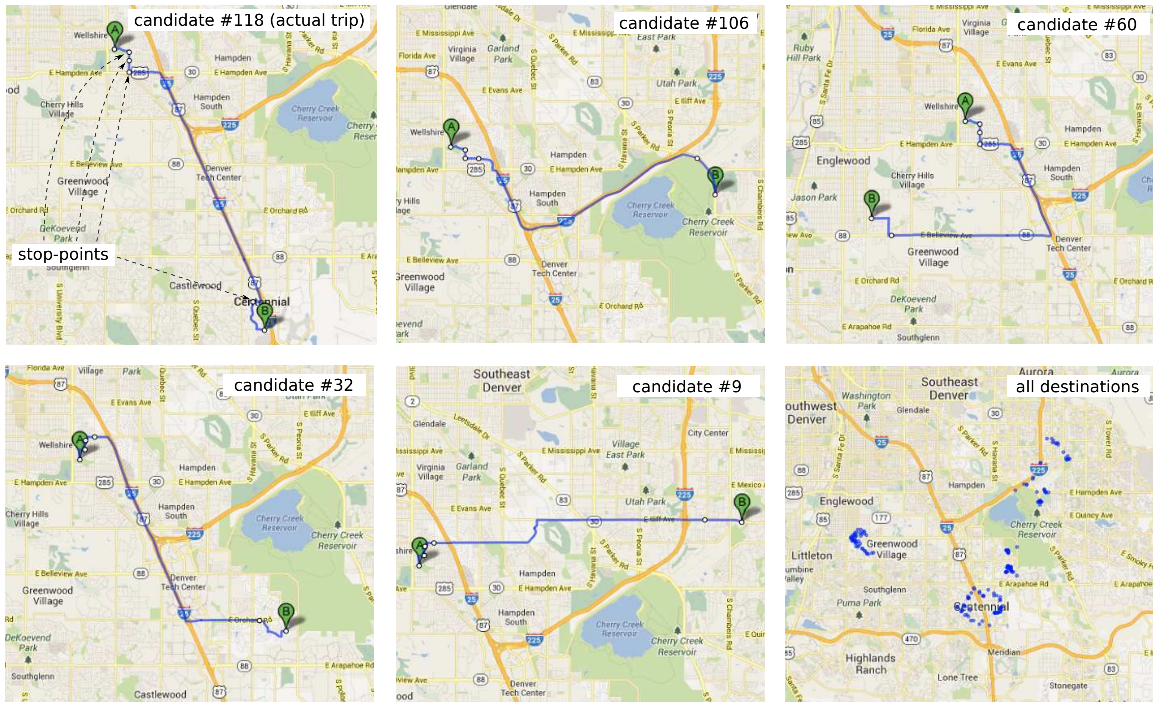

Figure 3.4: Sample candidate paths generated for a trip. Candidate path 118 is the actual route taken during the trip. The bottom right plot shows the destinations of all (196) candidate paths generated for this trip. A: start node; B: end node. Map data: Google (2013).

along a path are to that of the actual route, the higher is the ranking. Candidate paths 9, 32 and 118 progressively cover more of the highway, thereby increasing the match probability.

3.5.2 Ranking performance

In spite of our attack operating with less accurate and detailed data (device limitations) and with lesser environmental data (such as traffic conditions for the day of the trip), the ranking method is found to be robust in identifying the actual destination of a trip. If the destination is the end point of a candidate path, the path is often found in the three most likely paths that match the speed profile of the trip. Note that the ranking procedure does a point-by-point probabilistic comparison of the speed values observed in the trip and that along an entire path. Therefore, although we are not interested in the actual route followed during a trip, the obtained paths often represent the exact driving route. An

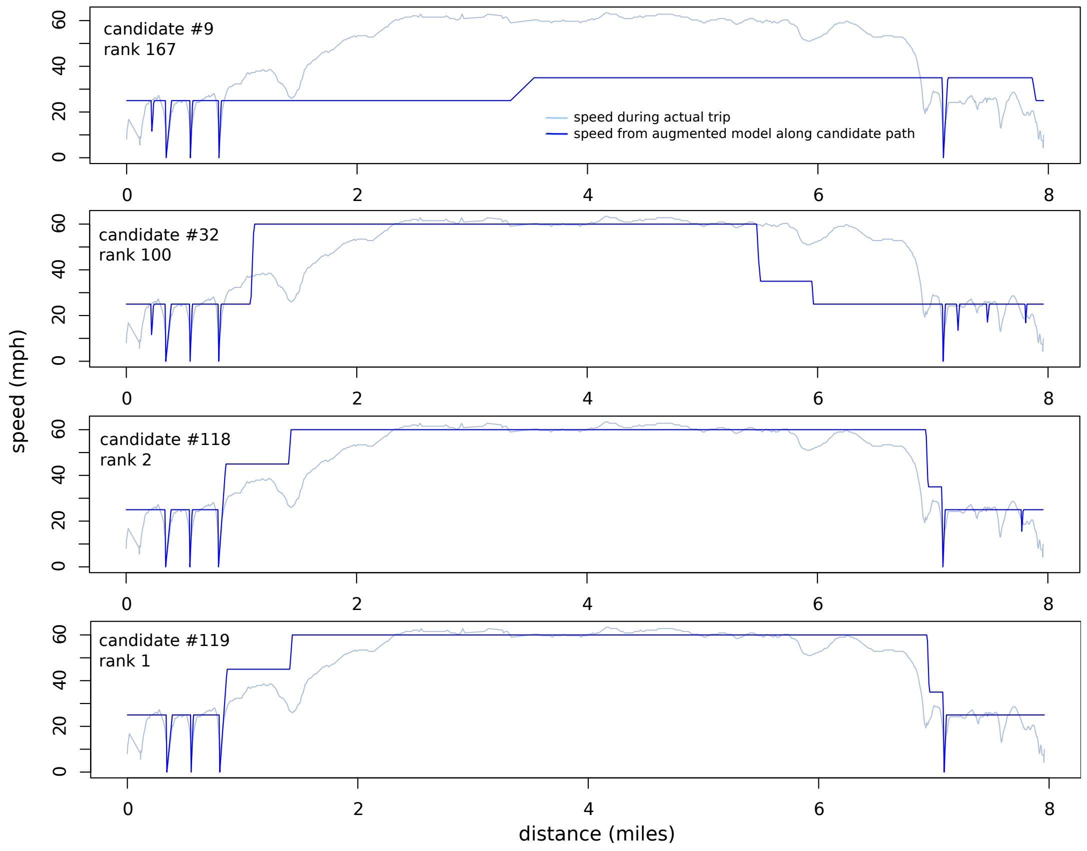

Figure 3.5: Speed profile during actual trip and that generated by augmented model for sample paths.

interesting observation is that, even if the top ranked destination is not the actual one, they are usually very close (within 0.5 miles) to each other. Therefore, the locality of the destination can be inferred almost always! The ranking method suffers when speed limits are not reasonably followed, either due to excessive speeding or slow movement in traffic, and another candidate path matches this noisy speed profile. Again, a capable adversary with insurance risk information based on user demographics can come up with a more realistic speeding model for the user e.g. based on age or make/model of the car, traffic density information of the locality etc. In addition, the attacker can easily get access to commercially available information such as traffic conditions on day of the trip, actual speed limit information, road blockages, whether intersection has signal or a stop sign etc., which can be utilized to improve the accuracy.

3.6 Summary

We developed an inference algorithm to demonstrate that inferring the destinations of driving trips is possible with access to simple features such as driving speed and distance traveled. The algorithm does fail in some cases. However, we believe that communicating the existence of this threat to privacy is a priority over perfecting the algorithm. We summarize our observations in this study in the following points.

- Although multiple candidate paths may satisfy the stop-points and turn feasibility constraints, the number of neighborhoods where the paths end can still be limited.
- A robust ranking method can easily identify candidate paths that do not conform with the speed profile of the trip, possibly leaving behind ones that end near the true destination.
- The speed attribute in the collected data is a crucial component in the inference process. It is worth exploring how the data collection process can be modified to introduce noise in this attribute, of course, without affecting its intended use.
- Finally, it is possible to infer the destination (often the full route) of a trip from driving habits data such as speed and distance traveled. It is crucial that agencies that collect such data acknowledge this fact and inform their customers about it.

Through in this work, we showed that keeping the GPS location private is not sufficient, especially if the attacker is someone that has authorized access to the data such as the service provider itself or an authorized third party, thus highlighting the need for developing LPPMs that protect against a curious service provider itself. For a reader interested in studying this attack further with the intention of developing a method to prevent this specific attack, we direct them to concentrate on the failed inferences in our experiments. In other words, determine what features of the data made the inference fail and incorporate those features into the OBD device.

Chapter 4

Architecture

In this chapter, we present the sequence of interactions between the user's mobile device and service provider, a high-level overview of the data exchanged and exactly what part of the interaction needs protection in order to maintain a configured level of privacy when the user consumes local search services. First, we briefly discuss the current typical setup. The rest of the discussion elaborates on our proposed architecture. The changes we propose while disruptive will not require any new physical asset installations such as towers and are confined to software changes. The fact that physical changes to the topology are not required makes our proposal practical. The overall flow of interactions between the mobile device and the service provider in our proposal is common across all the protocols presented in the rest of the dissertation. We also, maintain the practicality aspect when we propose the data that is exchanged i.e. to allow for detailed meta-data of points of interest to be exchanged, not just their geographic location.

4.1 Privacy in Local Search

Substantial development of technologies in mobile devices has led to the emergence of many applications that take advantage of multiple capabilities of such devices. Most mobile devices these days come with a positioning chip, so much so that it has become an integral part of these devices. Taking advantage of the location information that is available via this GPS chip has become a major focus of software companies in the mobile space. Among the most popular applications is local search. Local search applications such as Google Places[1], Yelp[2], AroundMe[3], and others, appeared in the last decade to meet a wide range of users' demands. Providing useful local search based on user's location has become a major offering and is considered an important revenue stream for these service providers. These applications are essentially web searches for points of interest, except that the query the user enters is appended with her location tag. The service provider responds with a list of POIs sorted based both on the distance and the prominence value, decided by the service provider. In spite of the development of these applications and excellent utility they provide to users, collecting location data raises various concerns about the privacy of individuals. Indeed, we find a large portion of users demand to protect their location privacy, yet consider local search applications to be an invaluable tool in their devices [19]. Unfortunately, the current design of the local search applications fails to meet the privacy requirements of the user who asks for pragmatic guarantees for non-disclosure of her location data. In today's real scenarios the service provider undertakes to abide by a privacy policy toward the user, which often prevents the user from taking full advantage of the local search application, or give up her expectations about maintaining her location data private (Section 2.1). We start our discussion here by the following example.

Alice is located at Point A, 5 Av & w 43 St, New York, NY, USA, and wants to find neighboring pizza locations. She uses a local search platform such as Google Places to perform the search on her mobile device. Figure 4.1a shows the top ten locations retrieved by Google based on their prominence and distance from the true location of Alice. However, Alice is unwilling to reveal her true coordinates. Hence, she denies permission to access her GPS coordinates and instead executes a search query for pizza from point B. Results of this query are shown in Figure 4.1b. Note that, only 30% of POIs are common between the two results. Therefore, results returned in this search are inaccurate. On the other hand

[1]www.google.com/search/about/features/02

[2]www.yelp.com/mobile

[3]www.aroundmeapp.com/

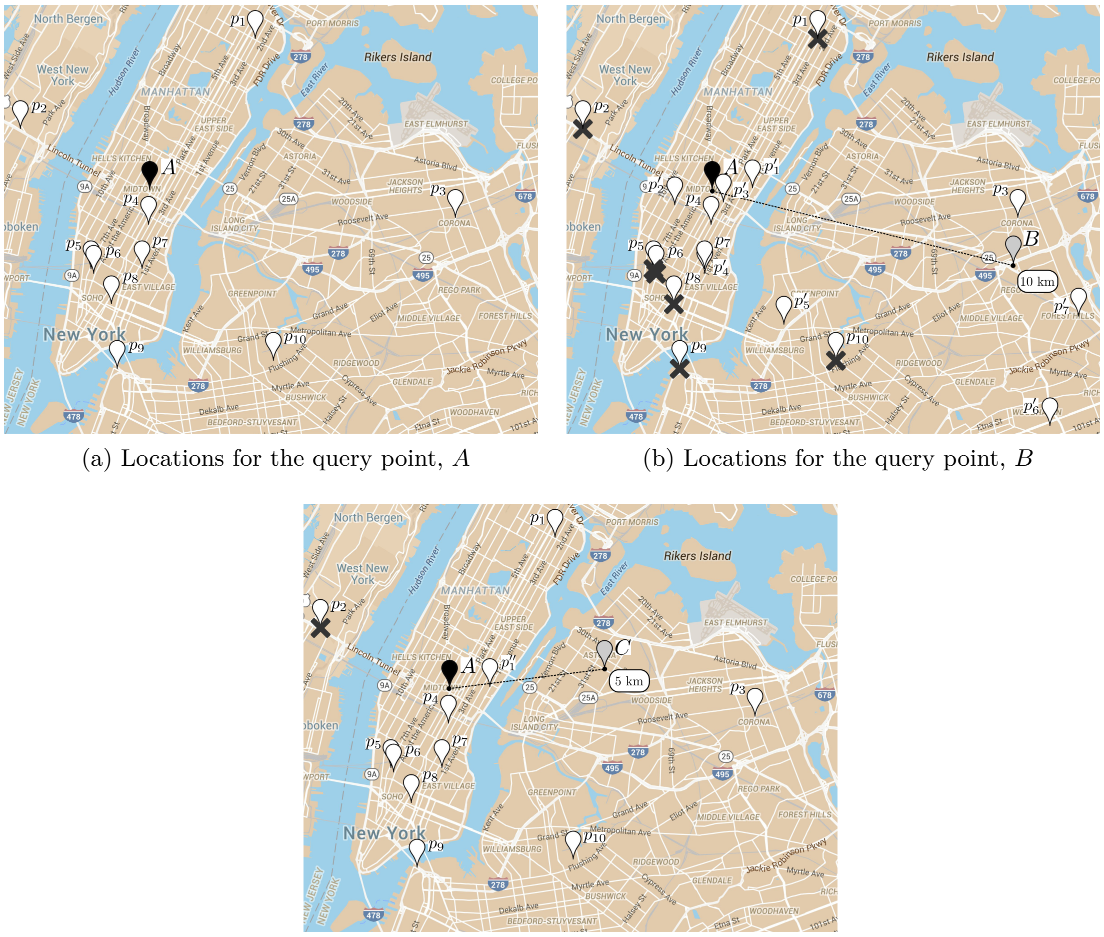

(a) Locations for the query point, A

(b) Locations for the query point, B

(c) Locations for the query point,C

Figure 4.1: Pizza locations returned by Google search in 5 Av / w 43 St, New York, NY, USA.

point B is 10 km away from Alice's true location, A. From the standpoint of QoS, in this case, Alice is unaware of the level of degradation in the result. Figure 4.1c shows the top ten pizza locations from another pseudo location point, C, which is 5 km away from A. The results now differ from the query of the actual location only in one POI.

This example illustrates the existence of a trade-off between QoS and the level of privacy protection in location-based applications. Notice that Alice can ensure her location privacy and at the same time, obtain an acceptable QoS level as the ratio of common POIs between the two locations is 90% although the point C is five kilometers away from the true location. A recent study on privacy for location-based search (2014) [46] determines that the form of information exchanged between the user and the service provider plays an important role in the QoS/privacy trade-off in LBSs. Empirical results of that study show that it is unlikely to obtain accurate results while maintaining privacy at the same time if a high density of queried objects were in the search area. So, an LPPM should allow the user to aggressively trade off the QoS for a large enough area to achieve a sufficiently perturbed location. Shokri et al. [143] considered the QoS/privacy trade-off as one of the fundamental elements of any LPPM. The authors model user–attacker objectives by using the framework of Stackelberg Bayesian games. They developed an optimization algorithm to determine the best pseudo location that minimizes the chance for the attacker to discover the user's location while maintaining the minimum distance between true and pseudo locations. Along the same line Bordenabe et al. [18] develop a method that maximizes the QoS for a threshold degree of geo-indistinguishability. Both of these works assume that the POI list from the server is sorted only by distance. An arbitrary ranking function for local search results, instead, is proposed by Dewri and Thurimella [46]. If one were to observe most popular POI search providers these days, the list of POIs is not necessarily sorted only by the distance from the location of the user. In fact, most popular providers, e.g. Google, use three main factors for object determination in local search [124]. First factor is the relevance, which involves the semantic matching of search keywords and object descriptions. Prominence value is the second factor, which is expressed as the relative importance of the relevant objects regardless of their location. The third factor is the distance from the query point. The prominence of a POI is derived from multiple sub-factors such as reference counts, the highest score of objects that refer to this object, the number of user reviews, and the extent of services offered, among others. Interestingly, in the earlier example we can clearly see the effect of the prominence value on the search results. The POI p_2 is replaced by p'_1 when the query is issued from point C; p_2 appears in the search results in Figure 4.1a although it is farther than p''_1 from A. The same scene is repeated in Figure 4.1b. For instance, it is very clear that the POIs p'_1, p'_2, p'_3, p'_4 are closer to A than the POIs p_1, p_2, p_9, p_{10}. However, we see in Figure 4.1a that p_1, p_2, p_9, p_{10} show up in the search results instead of p'_1, p'_2, p'_3, p'_4.

4.2 Non-private Architecture

The interaction with the service provider starts with the user, using some mobile application, typing in a query (e.g. pizza restaurant in Denver) and submitting it to the application. The application uses the GPS chip that is commonly found on all modern mobile devices to obtain the geographic location of the user. It adds this location tag to the query that the user typed and sends the request to the service provider. Note that, the more accurate the user's location that is sent along with the query, the more useful (relevant) the results the service provider returns. In the current LBS model, the service provider returns not just one, but a sorted list of POIs (typically 10–20) to the requesting application on the user's mobile device. Points of interest data that service providers maintain nowadays contain lot more data than just a name and geographic location. It contains metadata such as detailed description of the business, business hours, user reviews etc. These additional attributes are combined together into a single value called the *prominence*, which represents the importance of the POI. The user is not just interested in the nearest POI, but a POI that is optimum based on both distance from the current location and its prominence. So, the sort order of the returned list is based not just on the distance, but also the prominence value of the POIs. The user then picks one of these POIs for her purpose.

One has to note that the location privacy in this scenario is based entirely on the privacy policy of the service provider. If the service provider is assumed to be *semi-honest,* i.e. honest but curious, then the location privacy of the user is completely lost, as it is exposed to the service provider directly. In this case, one of the LPPMs such as the ones discussed in Chapter 2 needs to be implemented to enhance the location privacy. Our objective in this chapter is to come up with a general architecture for a TTP free LPPM that allows for the prominence value to be transmitted and be used.

4.3 Request–Response Protocol

We use a different request-response architecture which is performed in two round-trips. The first round-trip is to get a list of POIs with just their names, locations, and their prominence values. In the second round-trip, the mobile application sends a set of POIs that are of interest to obtain detailed information about the POIs that are chosen. That is, initially, the user sends a query that includes the keyword(s) along with her location tag to the service provider. Location tags help the server define a wide geographical area wherein objects relevant to the search are identified. The location tag could be the name of a public area, a postal code, a street address, or an exact latitude/longitude of the location. LSP then responds by sending the set of matching POIs with respect to the user's location. In order to prevent unwarranted data collection and protect the privacy of the user, we adopt a TTP less protocol where the client and server ends of the application perform intermediate meta-data exchanges to calculate the final result set. The client end application uses the meta-data to assess the results with respect to some geographic cloaking area or multiple pseudo location points. Given this information and the user's privacy preferences, the client-end application can now retrieve, privately, the query's answer.

One has to note that, in this model, during the first round-trip, the location information is sent as coarse as possible so that the service provider cannot accurately determine the location of the user. However, when a smaller set of POIs are included in the second round-trip, whose detailed information is desired, the service provider can easily pinpoint user's location to a more granular level. So, preventing the service provider from learning a more accurate location of the user when the second query is issued is the core goal of our proposal. In this dissertation, we deal with two approaches to this problem.

1. Encrypting the query in such a way that the service provider cannot tell exactly what POIs the user is looking for extra information on, but still be able to respond with valid results.

2. We propose several approaches to anonymize the queried set of POIs in the second round-trip.

In either approach, the first round-trip of getting a list of POIs over a large region remains the same. The second round-trip is where LPPMs come into play. Although the techniques used and the exact query differs in the approaches presented, the idea remains common; *the attacker should not be able to gain more than an acceptable level of knowledge about the user's location from the second round-trip.*

4.3.1 First round-trip

The user starts the process by specifying the search keyword through the client application interface. The client application determines a large geographical area that includes the current position of the user. This can be done by randomly select a sufficiently large area (say $500km^2$) around the user's location, which could be obtained using the onboard GPS unit. We will refer to this area as retrieval area, A_R. An example of this query format will be a query such as "cafe in Los Angeles, CA," as is supported by the Radar Search method of the Google Places API[4]. We require such a large A_R to prevent inference attacks against the user's location during this step. The client sends the coordinates of the generated A_R along with the search keyword to the server. After it receives the query, the server compiles it and determines the matching set of POIs. The location information and prominence value of each obtained POI are sent to the client. We aim to reduce the communication overhead by sending only the location and the prominence information instead of entire features (e.g. object names, phone numbers, addresses, etc.) corresponding to each POI at this point. It is assumed that the user does not care if the attacker places her in the large area picked in this step. If the user requires better privacy than this, then the size of A_R can be increased. But beyond some point, the user is better off using an offline approach such as using downloaded maps or offline GPS locators.

[4]developers.google.com/places/web-service/search

4.3.2 Second round-trip

In the second round-trip, an LPPM considers the current user location and the list of POIs and their prominence information obtained from the first round-trip to produce a smaller list of POIs that are preferable based on their location and prominence. These preferred POIs are then used in a query to the server to obtain detailed information about them. The number of preferred POIs that the user wishes the algorithm to pick can be configured, represented by a number K. Naturally one can argue that just by increasing K, the user can increase her privacy, as more POIs generally seem to get distributed across larger areas. But this method works only to an extent. Our assumption is that the attacker knows the algorithm and most of the parameters used in the LPPM, and he can pre-calculate the top-K POIs for each location on the map and keep the list ready. Now, his job, if he is able to see the exact top-K POIs used in this step is to match them against his pre-calculated list and determine the exact location of the user. If the LSP is semi-trusted, more sophisticated algorithms are needed. This is because, a semi-trusted LSP can easily determine the exact location of the user (or at least narrow it down to a very small area) if it has the knowledge of the top-K POIs, as the LSPs have access to vast amounts of geographical data at their disposal [56].

So, based on desired sensitivities, the user configures the application with an area large enough that she does not care if the attacker locates her there. In the application, this is usually specified by the user in the settings screen where she can pick a block, mall, subdivision etc., indicating the large enough acceptable area. This coarseness specification is internally translated into a number representing the side of a square area. Now, the goal of the LPPM is to prevent the attacker from determining the location of the user in an area smaller than the configured square. In order to do this, we present two sets of techniques. One based on encryption and second based on heuristics. These approaches are presented at a high level in the next two sections, with just enough detail to show the differences in the contents of the second query produced in this step.

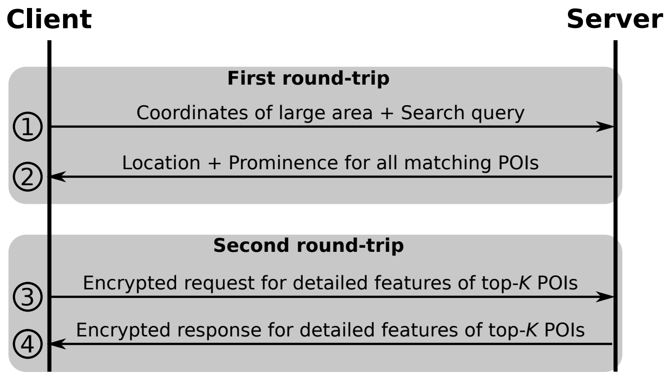
Client
Server
First round-trip
① Coordinates of large area + Search query
② Location + Prominence for all matching POIs
Second round-trip
③ Encrypted request for detailed features of top-K POIs
④ Encrypted response for detailed features of top-K POIs

Figure 4.2: Client/Server communication steps in PIR based LPPM.

4.4 PIR Based Approach

The PIR method mentioned in Section 2.5 seems like a plausible candidate solution to our problem. This method uses cryptographic techniques based on rigorous mathematical assumptions that allow the user to privately download information from a database provider, i.e., the content provider cannot tell which information had been accessed by the user. Figure 4.2 shows the protocol steps.

In these techniques, the query for the top-K POIs is encrypted using some private key and sent to the server. The server performs its computation on the encrypted query and returns the answer to the client. Notice that, the private key is required to decrypt the answer, so the server cannot decrypt the query nor the answer. Once it has the answer from the server, the client can decrypt this answer using its private key and hence get the required detailed information about the top-K POIs.

The PIR approach offers a high level of privacy protection and in fact, it solves this problem both in the single query and multiple queries scenarios. A single query scenario is where the user issues a single query and a subsequent query is issued after enough time that the attacker assumes both queries to be independent. In a multiple query scenario the user keeps issuing queries as she moves around. The multiple query scenario carries with it higher risk and will be explained in detail in Chapter 7. Since the attacker cannot observe the contents of a query at all (because of encryption), he cannot narrow down the user's location to an area smaller than the A_R selected by the client application in the first step,

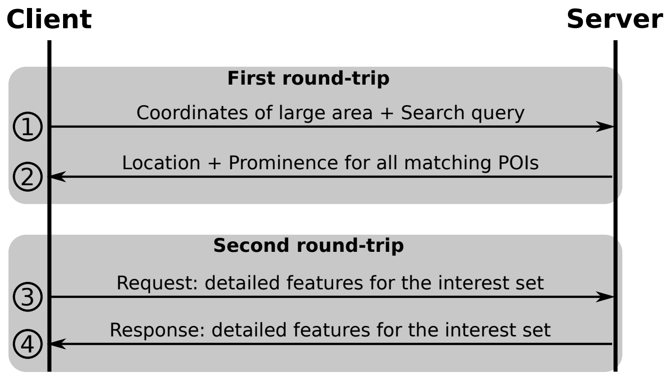
Client
Server
First round-trip
① Coordinates of large area + Search query
② Location + Prominence for all matching POIs
Second round-trip
③ Request: detailed features for the interest set
④ Response: detailed features for the interest set

Figure 4.3: Client/Server communication steps in heuristic based LPPM.

no matter how many subsequent queries are issued by the client. Therefore, the attacker cannot learn any additional information about the user's location.

4.5 Statistical Based Approach

As we will see in Chapter 5, PIR suffers from a problem of very high demand for computation and bandwidth resources, making this method impractical as a solution to our problem. Thus, we propose a new architecture for LPPM based on statistical privacy guarantees. Figure 4.3 summarizes the steps of the communication between the client and the server for this new protocol. Steps 1 and 2 are identical to the previous one (Figure 4.2). For Step 3, we develop a method that will run on the client device to determine a set of POIs in such a way that the semi-trusted LSP cannot easily estimate the precise location of the user. The POI set that is generated by the local privacy algorithm must include the top-K POIs, so as to not reduce the utility of the LBS to the user. This set of POIs obtained by running the algorithm locally is called the *interest set*. The interest set is a set of POIs that contains the top-K POIs with respect to the user's current location and few additional POIs to guarantee privacy preservation for the user. The client now requests the detailed feature information about the interest set and the server will respond by sending back the requested details. Requesting detailed information about specific POIs is already widely supported by major service providers, e.g., the Google Places API[5] has a Place-Details call that provides detailed information including user reviews.

Compared to the conventional process, this protocol incurs slight additional communication and computation overhead. However, as demonstrated later, the overhead can be maintained within levels that does not have a noticeable impact on user experience.

4.6 Ranking the POIs

The query in the second round-trip needs to be built in such a way that it contains all the POIs that the user may be interested in. The first step in this process is to rank the POIs obtained in the first round-trip based on their distance and prominence and pick the top K POIs. Towards this goal, we model the broad geographical area (A_R) selected in Step 1 of the protocol by a square grid $\mathcal{G}$ of size $Z \times Z$ cells. The set of all cells is denoted by C. A geographic location is then signified by a cell $c \in C$. A *cell* is defined as the smallest amount of distance the user has to move to be recognized as existing in a different location. This means, as long as the user moves within the boundaries of a cell, she will be considered as staying in the same location. A user located in the cell c_u sends a search keyword to the server for a specific type of POI. Suppose that $P = \{p_1, p_2 ..., p_n\}$ represents the set of POIs within the broad area and corresponds to the search keyword sent by the user. Let $0 < \mathscr{P}_i \leq 1$ be the prominence value of the POI $p_i \in P$ and assume that p_i is located in a specific cell c_i in the grid $\mathcal{G}$. Let the user be currently located at the cell c_u. The rank of p_i is computed as a weighted combination of its prominence value and the normalized distance from c_i, given as

$$rank'(p_i, c_u) = \alpha \times dist_{norm}(c_u, c_i) + (1 - \alpha)(1 - \mathscr{P}_i). \tag{4.1}$$

The length of the diagonal of $\mathcal{G}$ is used as the normalization factor for the distance. The parameter α is a weighting coefficient such that $0 < \alpha \leq 1$. Thus, the ranks of objects

[5]developers.google.com/places/documentation/

are between 0 and 1, with lower ranks implying better choices. In most situations, values of α and $\mathscr{P}_i$ are not revealed to the user. Hence, we redefine the ranking function as

$$rank(p_i, c_u) = dist_{norm}(c_u, c_i) + \gamma_i, \tag{4.2}$$

where $\gamma_i = \frac{1-\alpha}{\alpha}(1 - \mathscr{P}_i)$. Since α is a constant, both functions result in the same ranked ordering of the objects.

Therefore, in the first round-trip, the server sends the tuples $T = \{\langle id_i, l_i, \gamma_i\rangle \, | i = 1...n\}$ to the client, where l_i is the POI's location[6] and id_i is a unique identifier for the POI. Using T and the current location of the user, the privacy-preserving algorithm can sort the set P based on the rank of its items and extract out the subset of top-K POIs.

The key difference between the PIR-based and the statistical-based LPPMs when it comes to privacy is that PIR uses encryption and keeps the query secret from the attacker, i.e. the attacker does not *know* the contents of the query in the second round-trip, whereas in statistical/heuristic approaches, the attacker can observe the contents of the query in the second round-trip, but still cannot determine the user's location precisely. Hence, for PIR, the privacy guarantee is straightforward. But with statistical-based LPPMs, such as the ones presented in chapters 6,7, and 8, the privacy achieved needs to be quantified in order to prove their efficacy. Towards that goal, in the rest of the sections of this chapter, we build the model and symbols needed as a background to discuss the statistical-based approach.

4.7 Threat Model

The main privacy requirement for the client in the context of our problem is to not disclose the location information of the user when the query is sent to the server. This privacy requirement arises from the model of a *semi-trusted* service provider. In this model, the trust on the service provider is defined in terms of two dimensions, (i) answering the

[6]Locations are typically provided as latitude/longitude pairs; we convert them to cell coordinates as per the A_R discretization setting.

client's query and (ii) discovering private information about the client. A semi-trusted service provider is trusted in the first dimension, which is the query answer, where it is clear that the service provider is not interested in giving a malicious answer for any query. On the other hand, the service provider can collect the user's queries and infer some private information about her from these queries. Similar to what is typically assumed in the literature, the security protocol is publicly known. So everyone, including the attacker, knows details of the LPPM algorithm utilized by the user. In addition, the attacker:

- has the ability to eavesdrop and observe the contents of the query and interest set;
- is also assumed to have some information (background knowledge) on the initial location of the user, e.g., the attacker may know the user's residential or work address;
- knows the map of the geographical area and has access to the POI database;
- knows (or can accurately guess) the user's selection of privacy preference parameters;
- can pre-process a POI database to map the observed interest set to the corresponding smallest geographic area;

The service provider or an eavesdropping adversary, defined above, will try to figure out the location of the user from the exchanged messages between the client and the server when they process the protocol steps shown in Figure 4.3. So, ultimately, his goal is to determine the cell the user is in, based on the observed interest set.

At this point we will focus on the single query scenario and the enhancements to the attacker model required in the case of multiple queries will be presented in Chapter 7. Let the probability distribution Φ represent the adversary's knowledge about the user's location. We denote the prior probability estimate of the attacker for the user being located in the cell c by $\Phi_0(c)$. Since the adversary knows the details of the utilized LPPM, by observing the interest set, he can update his probability distribution as follows:

$$\Phi_1(c) = Pr\,(c|I) = \frac{Pr\,(I|c)\,\Phi(c)}{Pr\,(I)}\,\forall c \in C,$$

where $Pr(I|c)$ is the probability of generating the set I if the user is at cell c and $\Phi_1(c)$ is the posterior estimate of the attacker for the user being at the cell c. Note that Φ_0 models the knowledge of the adversary before the query is issued to the LBS. A common form of this knowledge is a uniform distribution spread over a subset of cells in the grid $\mathcal{G}$. It is also reasonable to assume that Φ_0 spreads over an area larger than the area inferable from an LPPM; otherwise, the background knowledge of the adversary is already stronger than the guarantees of the LPPM. The inferable area from an LPPM is the smallest area which the attacker can restrict the probability of the user's location inside. We formalize this inferencing process in Chapter 6.

4.8 Abstract Model for LPPM

The privacy preserving algorithm in this context can be abstracted as the composition of two functions $\mathcal{A}(\mathcal{R}(\cdot))$, such that $\mathcal{R}$ maps a cell to a region (set of cells, i.e. an element of the power set of C) and $\mathcal{A}$ maps that region to a (sub)set of the matching POIs, i.e. $\mathcal{R} : C \to 2^C$ and $\mathcal{A} : 2^C \to 2^P$. The domain of the function $\mathcal{A}$ is determined by the range of $\mathcal{R}$, denoted as $C_1, C_2, ..., C_m \in 2^C$. Correspondingly, let $I_1, I_2, ..., I_m$ be the POI (sub)sets that are mapped to these regions by $\mathcal{A}$. Without loss of generality, assume an arbitrary set $I_u \in \{I_1, I_2 ..., I_m\}$ that is generated as the interest set for a user located in region C_u. Consider the case when $I_u \neq I_t, t = 1, ..., u-1, u+1, ...m$. Given I_u, the attacker can determine C_u. For all cells $c_j \notin C_u$, we have $\Phi_1(c_j) = 0$, then for all cells $c_i \in C_u$, the posterior probability is

$$\Phi_1(c_i) = \frac{Pr\left(I_u|c_i\right)\Phi_1\left(c_i\right)}{Pr\left(I_u\right)} = \frac{Pr\left(I_u|c_i\right)\Phi_0\left(c_i\right)}{\sum_{c_j \in C_u} Pr\left(I_u|c_j\right)\Phi_0\left(c_j\right)}. \tag{4.3}$$

4.8.1 Assessments

We use a set of metrics to assess the privacy and the QoS of the LPPM. Following is a detailed explanation for each of these metrics.

Obfuscation

This technique has been applied to protect the location privacy in LBS in various other research (Section 2.3). It is based on hiding the user's location within a geographical area of the site that contains the real location of the user, rather than accurately revealing the exact location when requesting the service. So, the user can have access to the information related to her location, while upholding the privacy. In order to achieve obfuscation, we should have a "large" number of cells (including the cell of the user) in the region C_u with positive probabilities. This number may be specified as part of the privacy policy of the user. However, the user specified requirements cannot be achieved if the adversary has a prior probability knowledge that allows him to narrow the user's location down to a smaller area. Hence, a precise statement (such as the Φ_0 function) is necessary for the adversary's knowledge.

The adversary can sample one cell at a time (without replacement) based on the distribution Φ. The expected number of cells that the adversary would sample before arriving at the user's actual location creates an obfuscation area for the user. We call this the *expected inexact* privacy metric. It can be computed using the following closed form expression

$$expected\_inexact(\Phi, c_u) = \sum_{c \neq c_u} \frac{\Phi(c)}{\Phi(c) + \Phi(c_u)}. \tag{4.4}$$

Expected *inexact* privacy can be viewed as the smallest obfuscation area one can expect if the attacker is *successful* in learning an approximate presence area using the sampling method. The area can be obtained by multiplying the metric's value with the area of one cell. We will refer to this measure by the *areal privacy metric.* On the other hand, the expected *exact* privacy reflects the probability of *not* arriving at the user's location in one single attempt. The *expected estimation error* of the adversary measures the average distance between the true location of the user and the location estimated by the adversary [143]. When Φ is a uniform distribution over a subset C of cells, expected inexact privacy is equal to $\frac{|C|-1}{2}$ cells. For example, for a uniform distribution over an area of 32×32 cells, the expected inexact privacy is 511.5 cells. Say that the cell area is $0.01km^2$, then the *areal* privacy of the user is $5.115km^2$.

Convergence

Based on the prior probability distribution of the attacker, the chances for the user being in some cells may be higher than the chances of the other cells within the region C_u. In fact, the disclosure of the interest set I_u, which is part of the execution of the protocol proposed in the Section 4.3, gives the attacker some additional information about the current position of the user. The attacker is now able to build a new posterior probability distribution based on I_u and his prior probability distribution (Equation 4.3). However, if the posterior probability distribution of the attacker for the region C_u is directly proportional to the prior probability distribution, then this will ensure that the set I_u has no contribution to improving the attacker's knowledge about the new location of the user within the boundaries of the region C_u. We refer to this as the *convergence* property of the algorithm. In Equation 4.3, convergence is achieved if $Pr(I_u|c_i)$, for any $c_i \in C_u$, is a constant. Therefore, the probability of producing the output I_u should be equal for all cells in the region C_u.

The convergence condition is hard to satisfy for the case of multiple queries. So in order to measure the contribution of an LPPM in improving the attacker's knowledge about the new location of the user, we use a metric called *nearness privacy.* This metric is based on the adversary's best guess according to the distribution Φ. Given a probability distribution Φ over the cells in the grid and the user's current location c_u, nearness privacy is computed as

$$nearness(\Phi, c_u) = distance(\max_c \Phi(c), c_u). \tag{4.5}$$

We use Euclidean distance in our evaluation. If multiple cells have the most probable value, then we pick the cell closest to c_u as the adversary's guess. Note that when Φ is a uniform distribution, nearness will be zero.

The quality of service

To achieve a high level of obfuscation, the region C_u must contain the largest possible number of cells; in other words, a trivial solution is to always use the entire grid $\mathcal{G}$ in the query of the second round-trip. But, this may degrade the QoS by increasing the expected communication overhead (Steps 3 and 4 in Figure 4.3). Therefore, the privacy algorithm must choose the smallest possible set of POIs that covers the area of the region C_u. Ideally, the sets $I_1, I_2..., I_n$ should each have only K elements.

4.9 LPPM implementation

It is difficult to identify all the forms that can be taken by the privacy algorithm that offers an acceptable level of obfuscation, convergence, and high QoS. Here we present the formulation of the problem and give an outline for designing an LPPM model that preserves the desired properties.

Let's assume that C is partitioned into regions $R_1, R_2, ..., R_q$, such that the top-K POI sets for each cell in a given region are the same. Let the sets $P_1, P_2, ..., P_q$ represent the top-K POIs for these q regions. The function $\mathcal{R}$ is responsible for the creating disjoint groups $C_1, C_2, ..., C_m$ of the q regions such that, $C_i = R_{i_1} \bigcup ... \bigcup R_{i_t}$. The interest set of a given group of cells C_i is obtained by the function $\mathcal{A}$, $I_i = \mathcal{A}(C_i) = P_{i_1} \bigcup ... \bigcup P_{i_t}$. Ideally, the m groups created using the $\mathcal{R}$ function should satisfy the following constraints.

1. For all groups C_i, $\Big|\{c \in C_i | \Phi(c) > 0\}\Big| \geq \delta$. The parameter δ indicates the obfuscation level requested by the user. The trivial method to meet this requirement is to create a single group of the union of all q regions. However, this solution may negatively impact the quality of service of the application, which motivates us to include the second constraint.

2. Suppose that the function $f(C_1, C_2..., C_m)$ determines the effect of grouping the different regions on the quality of service. The function f may be defined as

$$f(C_1, C_2..., C_m) = \max_{i=1,2,\cdots,m} |I_i|, \tag{4.6}$$

where I_i is the interest set corresponds to the group C_i. What is commanded here is to minimize f. In our setting, it decreases the communication overhead.

Therefore, given a cell c_u, a privacy algorithm using $\mathcal{R}$ and $\mathcal{A}$ returns the set I_u as the interest set if $c_u \in C_u$. Note that $\mathcal{R}$ is a many-to-one function, i.e. a cell can belong to only one of the $C_1, C_2, ..., C_m$ regions. The function $\mathcal{A}$ also is not necessarily a one-to-one mapping but is many-to-one. The obfuscation and convergence requirements hold for this algorithm. Assuming I_u is unique ($\mathcal{A}(C_i) = I_u \iff i = u$), for all cells $c_i \in C_u$, we have $Pr(I_u|c_i) = 1$.

$$\therefore \forall c_i \in C_u, \Phi_1(c_i) = \frac{Pr\left(I_u|c_i\right) \Phi\left(c_i\right)}{Pr\left(I_u\right)} = \text{constant} \times \Phi\left(c_i\right). \tag{4.7}$$

For all cells $c_j \notin C_u$, we have $\Phi_1(c_j) = 0$. By virtue of the first constraint of our problem, we have $C_i, \Big|\{c \in C_i | \Phi(c) > 0\}\Big| \geq \delta$; therefore, at least δ cells (including the cell of the user) in C_u have positive posterior probability (obfuscation). Also, the posterior probabilities associated with this reduced set of cells is directly proportional to the background knowledge (convergence). The observations trivially hold when I_u is not unique.

The function $\mathcal{R}$ is required to create m partitions from the regions $R_1, R_2, ..., R_q$, and each partition C_i has at least δ cells with probability $\Phi > 0$. Let the number of cells with probability $\Phi > 0$ for each region R_i is x_i, where $i = 1, 2, \cdots q$. So, we can represent the set of regions $\{R_1, R_2, ..., R_q\}$ by the set of integers $X = \{x_1, x_2, ..., x_q\}$. The problem that the function $\mathcal{R}$ should solve is: *find* $\{C_1, C_2, \cdots C_m\}$ *partitions for the multi-set of positive integers* X *such that the sum of the numbers of each partition* $C_j \geq \delta \, \forall j = 1, 2, \cdots m$. The function $\mathcal{R}$ takes three input parameters; namely, the set X, the number of partitions m, and minimum sum threshold parameter δ. By invoking $\mathcal{R}\left(X, \delta, m\right)$ we should either get the required partitions or a flag which tell us that no such partition is possible. We claim that if there is a computationally efficient algorithm to solve the problem of the function $\mathcal{R}$, then this algorithm can solve the number partitioning problem. Number partitioning is an NP-complete problem [62]. The problem asks for deciding whether a given multiset S of positive integers can be partitioned into two subsets such that the summation of the numbers in both sets are equal. The algorithm that can solve number partitioning using $\mathcal{R}$ is described as follows.

> Given a set S of integers we compute the sum L of the numbers in S. If L is odd then no partition exists for S, so we stop. If L is even we invoke $\mathcal{R}\left(S, \frac{L}{2}, 2\right)$. Then S has a partition if $\mathcal{R}$ succeeded; otherwise, S has no partition.

Verifying an instance solution of the problem $\mathcal{R}$ is trivial and we just show its NP hardness; thus, the problem is NP-complete. We introduce in later chapters our heuristics based techniques that achieve acceptable performance in terms of privacy achieved without giving in too much of QoS.

4.10 Summary

In this chapter, we briefly describe the current prevalent communication architecture and describe the changes we propose in order to implement a TTP free LPPM. The general architecture we proposed, consisting of two communication round-trips, can be commonly used across both PIR based techniques and heuristic-based techniques discussed in this dissertation.

In the case of statistical-based techniques, we presented an abstract model that will be used to quantify the privacy achieved and presented few metrics that can be used. One may think of this abstract model as an outline to design a heuristic based LPPM. We show that in heuristic based approaches, achieving privacy without compromising much of quality of service boils down to creating an efficient partition of grid regions to improve obfuscation and convergence while not losing too much QoS. We also showed that a technique that tries to achieve the optimum solution is NP-complete, and motivate the need for using heuristic-based approaches that can efficiently partition the cells of the grid $\mathcal{G}$ into regions that satisfy both privacy and QoS requirements.

In the next chapter, we present the first TTP less protocol, using PIR, as it has got considerable attention from the research community. Our goal there is to study and implement two representative PIR schemes and assess their feasibility for real life applications.

Chapter 5

Investigation of PIR As a Candidate Solution

PIR techniques allow users to query and retrieve records from a database without revealing the query to the database. These techniques gather more importance as more and more users rely on on-line services and at the same time demand better privacy. *Computational* PIR (cPIR) is a category of PIR that uses mathematical techniques to achieve its goals. It requires the database to be pre-processed in some way at the service provider. Once honestly followed, the PIR protocols ensure that it is computationally expensive for the attacker, or the service provider itself, to decrypt the query, at the same time, be able to respond with correct answers to it. The high level of privacy achieved using these techniques comes at the cost of added computational and communication overhead. As new mathematical techniques such as fully homomorphic encryption emerge, so does adoption of them into cPIR. The effort has been trending towards making cPIR efficient enough for a practical implementation. There have been a few notable proposals in cPIR in recent years.

In Section 4.4 we characterize a protocol architecture (Figure 4.2) that adopts PIR to preserve the location privacy of the user. We argue that, a PIR based protocol may represent an ideal solution for our problem since the LSP will not be able to draw any additional information about the user's location through that protocol. In this chapter we present a brief survey of PIR methods and then we pick the most promising of these proposals, implement them, run them against typical database and block sizes, and compare their performance. The last such comparative study was done in 2007 by Sion and Carbunar [147] and there is a need to take into account recent advances, and check if the performance of the latest proposals come close to practical adoption. Although each algorithm proposed has its computational and communication complexity measures presented in terms of database size, anyone that implements it will quickly realize that, because of the multiplier parameter associated with each order term, the performance achieved "in reality" using standard implementations on practical hardware and network technologies can be quite different from what one expects by just looking at the big O terms.

5.1 Preliminaries

In typical client/server scenarios, the user sends a query to the database, and the database locates the relevant records and responds with the data i.e. the database server has to know the query to be able to respond. In contrast, PIR is a protocol aimed to protect the client's privacy by allowing the user to still retrieve relevant information but without revealing the query to the database. The need for such protocols to protect the privacy of the clients arises from the model of semi-trusted service providers, where our problem (location based search) exemplify this scenario.

A trivial protocol to solve this problem is for the server to send a copy of the entire database to the client, who can then choose the required record(s) from this copy. It is obvious that this solution offers ultimate privacy to the client, since the server has no idea about which record(s) the client is actually interested in. It is also obvious that this approach is impractical as the transfer of the entire database has high communication cost. The problem now is to determine some approach that guarantees almost the same privacy but with lesser communication overhead. Chor et al. [32] introduced the term PIR to define this problem and propose the *information-theoretic* PIR scheme (itPIR). This scheme actually provides an absolute privacy guarantee (the same level as the trivial solution provides) for the client with more reasonable communication cost. The main drawback of this scheme is that it requires an identical copy of the database available with at least two non-colluding servers. In fact Chor et al. [32] shows that nontrivial itPIR is not possible in the case of a single database server. Another scheme to implement PIR is to use mathematical (cryptographic) techniques known as *computational* PIR (cPIR). Here "computational" means to guarantee that the server can compromise the privacy of the client only if it can solve a computationally hard problem. The main advantage of this scheme is that it waives the requirement of multiple servers. Unfortunately, the protocols that attempt to satisfy this approach, in general, introduce high communication and computational overheads. We mentioned the two major schemes of PIR viz., itPIR and cPIR. We discuss the details of various proposal in each scheme below.

5.1.1 Information theoretic PIR techniques

In a simple itPIR scheme, the database is modeled as an n-bit string, x, replicated among k servers where $k \geq 2$. In order to retrieve a certain bit x_i from the database, the client will send a uniform random bit string S_j of length n to each server such that $S_1 \oplus \cdots \oplus S_k = \mathrm{e}_i$, where all the bits of e_i are zero except for the bit at the i^{th} position. Each server responds by sending the result of bitwise XOR of x and S_j. The client then XORs all the responses together to recover the bit x_i. To reduce communication costs Chor et al. [32] proposed embedding x in a d-dimensional cube, so the server can cover its string S_j and all strings at Hamming distance 1 from it by d-bit long strings. For instance, by embedding x in a 3-dimensional cube, two servers can emulate up to eight servers with a total communication complexity $O\left(\sqrt[3]{n}\right)$. Unfortunately, to emulate any larger number of servers, it is required that the emulating server cover all possible codes with a Hamming distance > 1, which adds more communication overhead.

Another set of proposals to reduce the number of servers use locally decodable codes (LDC) [27,55,96,162]. LDCs are error-correcting codes in which a message x is encoded into a codeword $C(x)$ such that any bit of x_i can be recovered efficiently, with high probability, by querying only k coordinates randomly in $C(x)$. For PIR protocols based on this technique, all the k servers are supposed to store the encoding of x. In order to retrieve the bit x_i, the client requests a uniform random coordinate (ideally one bit) in $C(x)$ from each server. Although the k coordinates requested by the client must be sufficient to recover the bit x_i, each server can see that the client is just interested in one uniformly selected coordinate in $C(x)$.

Although bit retrieval theoretically is extensible, retrieving a block (or a record) of several bits from the database is a more realistic scenario. Here a linear algebraic query model is used where the database is modeled as a matrix D of n blocks, $b_1, \cdots b_n$, each block b_i is m-bits long. By generalizing the simple itPIR scheme explained above, if k servers have exactly the same replica of the database, the client can retrieve the block i privately with total communication cost of $k \cdot (n+m)$. The first step is the same, where the client generates k uniform bit strings of length n, such that $S_1 \oplus \cdots \oplus S_k = \mathrm{e}_i$, and sends one bit string to each server. The server j now returns the vector $v_j = S_j \times D$. The client recovers the i^{th} record by computing $v_1 \oplus \cdots \oplus v_k = \mathrm{e}_i \times D$. This scheme is based on a simple secret sharing mechanism. The secret is the index of the interested record, i, and the secret shares are the bit strings $S_1, \cdots, S_k$, since i can be determined only if we know all of these bit strings. But this scheme will fail if one of the servers does not respond, or even worse, replies with a false answer. This problem can be described in general as follows. Given total number of servers ℓ, only k of them answers the client's query. From these k servers, h servers reply honestly, and the rest could lie. The goal is to retrieve the client's query privately for up to t non-colluding servers. Goldberg [71] addressed this problem and proposes a protocol based on Shamir's secret sharing [139] to generate the query's secret shares and then recover the answer code words using the Guruswami-Sudan error correcting algorithm [77]. Devet et al. [41] improve the computation speed of Goldberg's protocol, as well as the minimum bound for the number t of non-colluding servers. Devet used dynamic programming to decide the answer recovery algorithm among Berlekamp-Welch [155], Guruswami-Sudan [77] or brute force methods. Henry et al. [83] also built on the Goldberg's protocol to develop a method for retrieving multiple blocks simultaneously from the database.

itPIR is reasonably fast (negligible computation cost) and can guarantee privacy if the servers are trusted. But, the major problem with itPIR schemes is the vulnerability of query exposure when the replicated servers collude. In the most simple case, colluding servers can totally nullify query privacy. This requirement of multiple non-colluding servers makes itPIR impractical in most real scenarios.

5.1.2 Computational PIR techniques

The first attempt to solve the PIR problem without the need for multiple non-colluding database servers was made in 1997 by Kushilevitz and Ostrovsky [100]. The proposed solution is based on the assumption that the server cannot solve the quadratic-residuo problem efficiently (i.e., in polynomial time) [72]. In 2005 Gentry and Ramzan [66] constructed a cPIR algorithm that is based on the ϕ-hiding assumption, introduced by Cachin et al. [23]. The algorithm has a communication complexity of $O(k+d)$, where $k \geq \log n$ is the security parameter and d is the length of the database block. This protocol achieves the best performance in terms of reducing the communication cost compared to other known cPIR protocols. However, it necessitates expensive computational operations, especially on the server side, to generate the query response, which limits the practicality of the protocol [3, 130]. In fact, it turns out that the major deficiency in all cPIR protocols is the high computational cost. In 2007, Sion and Carbunar [147] showed that the trivial PIR protocol is more efficient than any other PIR protocol proposed by that time, when implemented on realistic hardware and communication networks. The authors have focused only on the protocol of Kushilevitz and Ostrovsky [100] in their analysis for cPIR schemes and completely rejected itPIR by assuming that the requirement of replicating a database is an unsatisfiable condition in real scenarios. Aguilar-Melchor and Gaborit [3] proposed a linear algebra based protocol that aims to achieve high computation throughput. A later study by Olumofin and Goldberg [125] similar to the one done by Sion and Carbunar [147] conclude that this protocol is an order of magnitude more efficient than the trivial PIR. Although, the query size for this protocol is large, the protocol has significantly reduced the computational overhead compared to the previous protocols. Unfortunately, in 2012, Jingguo Bi et al. [17] show a possible attack against the Aguilar-Melchor and Gaborit [3] protocol by uncovering the secret linear relationship between the public keys and the secret keys.

Xun Yi et al. [163] uses some variant of Dijk et al. [154] Fully Homomorphic Encryption (FHE) to offer a cPIR. For a database size of n-bits and consisting of m records each of the same length, the total communication and computational overhead of the protocol are $O(\gamma \log m + n\gamma/m)$ and $O(m\gamma^2 \log m + n\gamma/2)$, respectively, where γ is the cipher text size, which is determined by specific security parameters. Changyu et al. [47] also proposed a scheme based on fully homomorphic encryption in which they take advantage of the inherent parallelism in the BGV algorithm [20] to reduce the communication complexity to $O(\log \log n)$. However, the authors describe the protocol for single bit retrieval and left the more practical block retrieval protocol to be addressed in later work.

When one looks at the existing research, a clear pattern emerges. Efficiency achieved on the communication overhead is balanced out by often increased computational complexity. Even though newer proposals are clever and improve on both dimensions, further improvements are needed for these to become really practical. In order to evaluate the improvements achieved in cPIR performance over the years, we compare the first major proposal [100] based on the quadratic residuosity assumption (QRP) against the latest[1] proposed protocol based on fully homomorphic encryption (FHE) [163].

5.2 PIR Protocol Model

In this section, we present just enough background of the protocols, QRP and FHP, to keep the discussion complete. Also, we present them with common symbols so readers get a better feel for their performance when represented in those common terms. In our

[1]At the time of this writing

implementation for both QRP and FHP, we assume that the database consists of n blocks (records) of equal length. Each block $\mathbf{B}_i$ is m-bit long. So the database is viewed as an $n \times m$ matrix, where each row in the matrix corresponds to one record in the database. Before going into the details of the QRP and FHP protocols, it would be better to give an overview of the general structure of cPIR schemes.

A cPIR protocol consists of three polynomial time algorithms; QueryGenerator, ResponseGenerator and ResponseDecoder. First, the client uses the QueryGenerator algorithm to create an encrypted query and a private secret for a specific block of index, j, and sends the query to the server. The server computes the response for the "encrypted" query on the database by using the Response-Generator algorithm, and then sends this response back to the client. The client shall be able to retrieve the block j from the received response using the Response-Decoder. In this chapter, we call execution of all three algorithms, starting with query generation to response decoding on the client, as a *round-trip* (this should not be confused with the previous definition for the round-trip in Chapter 4). Two conditions must be satisfied by the cPIR scheme – *correctness* and *privacy*. Correctness means that for any query generated for a block j by the QueryGenerator algorithm, the correct block must be recovered back from the response generated by the ResponseGenerator algorithm by using the algorithm ResponseDecoder. The privacy requirement stipulates that for any two queries for different blocks i and j in the database, the server cannot distinguish one from the other with a non negligible probability. The communication overhead and computational cost of a cPIR scheme are measured in terms of n and m (the size of the database) and the size of the overhead induced by the privacy protocol.

5.2.1 Description of QRP

Since this protocol is based on the intractability of the quadratic residuosity problem, we will introduce the problem briefly before we describe the protocol.

Given an integer N and an integer $x \in \mathbb{Z}_N^*$, x is said to be a quadratic residue modulo N if there exists an integer $y \in \mathbb{Z}_N^*$ such that $x \equiv y^2 \pmod{N}$. Otherwise we say it is a quadratic non-residue. We denote the set of quadratic residues modulo N by $\mathcal{QR}_N$ and the set of quadratic non-residues modulo N by $\mathcal{NR}_N$. The Jacobi symbol is defined over the set $\mathbb{Z}_N$ as the product of the Legendre symbols corresponding to the prime factors of N, and it can be computed in polynomial time [36]. The Legendre symbol is defined in Equation 5.1. If the modulus is a prime, p, then it is easy to decide whether an integer $x \in \mathbb{Z}_p^*$ is quadratic residue or not by just computing the Jacobi symbol, $\left(\frac{x}{p}\right)$. For composite modulus, the Jacobi symbol cannot be directly used to decide the quadratic residuosity of an integer $x \in \mathbb{Z}_N^*$. Consider a composite modulus, $N = p.q$, where p and q are unknown primes. We can still compute the Jacobi symbol $\left(\frac{x}{N}\right)$, but in this case $\left(\frac{x}{N}\right) = \left(\frac{x}{p}\right)\left(\frac{x}{q}\right)$ and $x \in \mathcal{QR}_N \iff \left(\frac{x}{p}\right) = \left(\frac{x}{q}\right) = 1$. Half of the integers $x \in \mathbb{Z}_N^*$ have Jacobi symbol equal to -1 where $\left(\frac{x}{p}\right) \neq \left(\frac{x}{q}\right)$, and we know certainly that they are not quadratic residues modulo N. But, the other half have Jacobi symbol equal to 1 where $\left(\frac{x}{p}\right) = \left(\frac{x}{q}\right)$. Notice that, if $\left(\frac{x}{p}\right) = \left(\frac{x}{q}\right) = 1$, then $x \in \mathcal{QR}_N$; and, if $\left(\frac{x}{p}\right) = \left(\frac{x}{q}\right) = -1$, then $x \in \mathcal{NR}_N$.

$$\left(\frac{x}{p}\right) = \begin{cases} 0 & \text{if } a \equiv 0 \pmod{p}\text{;i.e., } a \notin \mathbb{Z}_p^* \\ 1 & \text{if } x \in \mathcal{QR}_p \\ -1 & \text{if } x \in \mathcal{NR}_p \end{cases} \tag{5.1}$$

Therefore, if the Jacobi symbol is 1, $\Pr[x \in \mathcal{QR}_N] = \Pr[x \in \mathcal{NR}_N] = \frac{1}{2}$. A *hard-set* of quadratic residuosity, H_k, is defined in Equation 5.2

$$\begin{aligned} H_k = \{x | x \in \mathbb{Z}_N^*, N = p.q \\ \text{where}\, p, q\, \text{are } \tfrac{k}{2}\text{-bit primes and } \left(\tfrac{x}{N}\right) = 1\Big\} \end{aligned} \tag{5.2}$$

The quadratic residuosity assumption states that *for any integer $x \in H_k$, if the factorization of N is unknown, there is no efficient algorithm to decide whether x is a quadratic residue modulo N or not.* In addition to the hardness of deciding quadratic residuosity for

$x \in H_k$, the set H_k maintains a useful XOR property. That is, $\forall x, y \in H_k$, the product $x \cdot y \pmod N$ is a $\mathcal{QR}_N$ if both x and y are $\mathcal{QR}_N$ or $\mathcal{NR}_N$; otherwise the product is $\mathcal{NR}_N$.

Now that we have sufficient background, we describe the *QRP* PIR protocol. Steps of QueryGenerator, ResponseGenerator and ResponseDecoder routines are described in Algorithm 5.1. The round trip starts at the client side, when the QueryGenerator routine is invoked to create the query vector $[q_1 \cdots q_n]$ for a database record j, using the private key (p_1, p_2) and a public key N. The client then sends $[q_1 \cdots q_n]$ and N to the server which computes the response $[z_1 \cdots z_m]$ and sends it back to the client. Using the response received from the server, the client will recover the record $\mathbf{B}_j$ using the ResponseDecoder routine, thus completing the round-trip. Notice that, deciding whether

Algorithm 5.1 *QRP* algorithms.

```
1: function QueryGenerator($\lambda, n, j$)
2:     $p_1, p_2 \leftarrow$rand_prime, where $|p_1| = |p_2| = k/2$
3:     $N \leftarrow p_1 \cdot p_2$
4:     for $i = 1$ to $n$ and $i \neq j$ do
5:         Choose random $q_i \in H_k$ s.t. $q_i$ is $\mathcal{QR}_N$
6:     end for
7:     Choose random $q_j \in H_k$ s.t. $q_j$ is $\mathcal{NR}_N$
8:     return $(p_1, p_2, [q_1, \cdots, q_n])$
9: end function
10: function ResponseGenerator($N, [q_1, \cdots, q_n], \mathbf{DB}$)
11:     $[z_1, \cdots, z_m] \leftarrow 1$
12:     for $i = 1$ to $n$ do
13:         for $t = 1$ to $m$ do
14:             if $b_{i,t} = 1$ then
15:                 $z_t \leftarrow z_t \times q_i \pmod N$
16:             end if
17:         end for
18:     end for
19:     return $([z_1, \cdots, z_m])$
20: end function
21: function ResponseDecoder($[z_1, \cdots, z_m], p_1, p_2$)
22:     for $t = 1$ to $m$ do
23:         if $z_t$ is $\mathcal{QR}_N$ then
24:             $b_{j,t} \leftarrow 0$
25:         else
26:             $b_{j,t} \leftarrow 1$
27:         end if
28:     end for
29:     return $([b_{j,1}, \cdots, b_{j,m}])$
30: end function
```

an integer z_t is $\mathcal{QR}_N$ or not (line 17 in Algorithm 5.1) is a polynomial time operation because the client knows the primes (p_1, p_2) which form the private key.

We will not present detailed proofs for the correctness and privacy of either algorithm here. The interested reader may refer to the original references. However, the security of QRP, intuitively, follows from the quadratic residuosity assumption. The correctness is based on the XOR property of H_k. As it is obvious, if $b_{j,t} = 0$ in the original database, then z_t is the accumulated product of $\mathcal{QR}_N$ integers, which results in a $\mathcal{QR}_N$ integer. On the other hand, $b_{j,t} = 1$, means the accumulated product of z_t will include *one* $\mathcal{NR}_N$ integer, which results in a $\mathcal{NR}_N$ integer.

5.2.2 Description of FHP

This protocol is based on a variant of the Fully Homomorphic Encryption (FHE) scheme proposed by Dijk et al. [154]. In FHE, mathematical operations can be performed on encrypted inputs to produce an encrypted version of the result. Thus, a semi-trusted party can perform computations on encrypted inputs and produce correct results without knowing the plain values of the inputs. In Dijk et al. [154] scheme the user chooses a security parameter λ and determines a parameter set $\rho = \lambda, \eta = (\lambda + 3) \lceil \log n \rceil, \gamma = 5(\lambda + 3) \frac{\lceil \log n \rceil}{2}$. The secret key, sk, is a random odd integer of length η-bit. The public key is $pk = sk \cdot q_0$, where q_0 is a random odd integer chosen from $[1, 2^\gamma / sk)$. To encrypt $M \in \{0, 1\}$, the user, who knows sk, chooses two random integers $p \in \left(-2^\lambda, 2^\lambda\right)$ and $q \in [1, 2^\gamma / sk)$. The ciphertext, $c = E\left(M, pk\right) \equiv M + 2 \cdot r + q \cdot sk \pmod{pk}$. With the secret key sk, the user decrypts a ciphertext as $M = D\left(c, sk\right) \equiv \left(c \pmod{sk}\right) \pmod{2}$.

The protocol consists of the three algorithms given in Algorithm 5.2. In the QUERY-GENERATOR, the client calculates pk and sk based on the security parameter λ. In line 6, r_s and q_s are random integers chosen as specified by the FHE scheme described above. Notice that, in line 6, $\alpha_s \in \{0, 1\}$ is the plaintext and $\hat{\alpha}_s$ is its encryption. So the query basically is nothing but an encryption of the index of the required block. For the RESPONSEGENERATOR algorithm, each block $\mathbf{B_i}$ is viewed as a bit vector $[b_{i,1}, \cdots, b_{i,m}]$. Before it

Algorithm 5.2 *FHP* algorithms.

```
1: function QueryGenerator($\lambda, n, j$)
2:     Generate $pk$ and $sk$
3:     $\ell \leftarrow \lceil \log n \rceil$
4:     $\alpha_1, \cdots, \alpha_\ell \leftarrow$binary_representation of $j$
5:     for $s = 1$ to $\ell$ do
6:         $\hat{\alpha}_s \leftarrow E(\alpha_s, pk) = \alpha_s + 2 \cdot r_s + q_s \cdot sk \pmod{pk}$
7:     end for
8:     return $(sk, pk, [\hat{\alpha}_1, \cdots, \hat{\alpha}_\ell])$
9: end function
10: function ResponseGenerator($pk, [\hat{\alpha}_1, \cdots, \hat{\alpha}_\ell], \mathbf{DB}$)
11:     $\ell \leftarrow \lceil \log n \rceil$
12:     for $i = 1$ to $n$ do
13:         $\beta_{i,1}, \cdots, \beta_{i,\ell} \leftarrow$binary_representation of $i$
14:         $\hat{\omega}_i \leftarrow \prod_{s=1}^{\ell} \hat{\alpha}_s + (\beta_{i,s} \oplus 1) \pmod{pk}$
15:     end for
16:     $[z_1, \cdots, z_m] \leftarrow 0$
17:     for $i = 1$ to $n$ do
18:         for $t = 1$ to $m$ do
19:             if $b_{i,t} = 1$ then
20:                 $z_t \leftarrow z_t + \hat{\omega}_i \pmod{pk}$
21:             end if
22:         end for
23:     end for
24:     return $([z_1, \cdots, z_m])$
25: end function
26: function ResponseDecoder($[z_1, \cdots, z_m], sk$)
27:     for $t = 1$ to $m$ do
28:         $b_{j,t} \leftarrow (z_t \pmod{sk}) \pmod{2}$
29:     end for
30:     return $([b_{j,1}, \cdots, b_{j,m}])$
31: end function
```

can create the response, the algorithm must compute the encryption values corresponding to each record $\hat{\omega}$ (lines 10–12 in Algorithm 5.2). This additional computation cost comes as a penalty for the reduction that has been made in the communication cost. Hence, in this protocol, the query size is logarithmically proportional to the number of records where as it is linear in the case of *QRP*. Finally, recovery of queried record j at the client is straightforward as shown in the ResponseDecoder routine.

5.3 Implementation Details

In implementing both QRP and FHP algorithms, we used open source, peer validated libraries that implement the underlying arithmetic. A not too old, not too modern hardware platform is chosen to represent a typically available hardware architecture. Also, normally available Ethernet based LAN connections are used between the server and the client. Our goal is to be realistic in terms of hardware and network platform selection. We implemented both protocols using C++ on Ubuntu 14.04.3 LTS virtual server machine with 4 core Intel® Xeon® CPU E5 – 2695 v3 @ 2.30GHz with cache size of 35MB and Debian GNU/Linux 7 client machine –Intel® Xeon® E5405 @ 2.00GHz. We use the NTL (version 9.4.0) library [145] to perform big integer modular operations. NTL is a high-performance free open source C++ library that offers algorithms for processing arbitrary length integers.

Each of the algorithms was first validated for correctness, by making sure the retrieved block of data on the client side exactly matches the corresponding block in the database. The performance characteristics of each algorithm are verified independently. We used similar techniques to test the performance as those used by the original authors of the algorithms. This is so that we can compare our results with those published by the authors and ensure that our implementation performs at least as good as those obtained by the original authors.

After ensuring the correctness and satisfactory performance, the algorithms were normalized by adjusting the parameters so that the privacy offered by each algorithm is similar, i.e., if the semi trusted server were to break the privacy and figure out the index j that is queried by the client, the amount of work needed should be similar for both algorithms. For FHP protocol, the authors [163] propose $\lambda = 60$. This gives $\gamma = 2205$ and a public key length of 2205 bits, so all the integers exchanged between the client (queries) and the server (responses) are going to be of length 2205 bits. In fact setting $\lambda = 60$ gives us a low security level $\approx 2^{60}$. We set $\lambda = 85$, so we have a security level of 2^{85}. With $\lambda = 85$, the public key length is 3080 bit. For the quadratic residue protocol, we choose $k = 500$, so the moduli N is 1000 bits long. The fastest known algorithm for integer factorization,

Table 5.1: Average Computation Time and Round-trip Time in minutes for QRP and FHP for different database sizes. Database Size is represented as number of records $\times$ record size.

Database Size	Computation		Roundtrip	
	QRP	FHP	QRP	FHP
$10000 \times$ 10kB	2.041	1.361	2.111	1.366
$10000 \times$ 25kB	5.041	5.637	5.214	5.651
$10000 \times$ 50KB	10.353	11.308	10.698	11.335
$10000 \times$ 100kB	21.189	22.409	21.878	22.465
$20000 \times$ 10kB	4.068	3.070	4.137	3.076
$20000 \times$ 25kB	10.146	10.862	10.319	10.877
$20000 \times$ 50kB	21.239	22.721	21.583	22.752
$20000 \times$ 100kB	42.019	44.649	42.711	44.711
$30000 \times$ 10kB	6.034	4.553	6.103	4.558
$30000 \times$ 25kB	15.281	16.284	15.454	16.299
$30000 \times$ 50kB	31.349	33.126	31.701	33.157
$30000 \times$ 100kB	63.274	68.699	63.965	68.761

number field sieve [21], can factorize an integer of length 1000 bits (under some heuristic assumptions) in a time $\approx 2^{85}$. With these settings we compare the performance of both protocols under the same level for privacy.

5.4 Results and Analysis

Table 5.1 shows experimental results for both protocols running on different sized databases. To generate the query, the QRP client creates n random integers of k bits long, which gives a total computation complexity of $k \cdot n$. FHP client encrypts $\log n$ bits using DGHV a somewhat homomorphic encryption scheme, which require two multiplications and two additions for γ bits long integers. So the total computation complexity of the query generation algorithm is $2 \cdot \gamma \cdot (\gamma + 1) \cdot \log n$.

For response decoding, the QRP client will test the quadratic residuosity of each received integer from the server. Given the factorization of N, the residuosity check requires $O\left(\log^3 N\right)$ [146]. So the total computational complexity of the decoding algorithm is $m \cdot k^3$. For FHP, the response decoding algorithm is nothing but a long integer devision performed iteratively over m integers; each of these integers is γ bits long, so the total cost of the algorithm is $m \cdot \gamma^2$ bit operations.

The QRP client query consists of n integers and the response generated by the server is m integers. Since each of these integers is k bits, the total communication cost of the protocol is $k \cdot (n + m)$ bits. On the other hand, the client using FHP sends $\log n$ integer numbers for each query and receives m integers representing the response from the server, where the length of each number is γ bits. In order to address the problem of large query size for QRP, Kushilevitz and Ostrovsky [100] suggested a recursive technique to implement the protocol. Unfortunately, this technique leads to exponential increment in both the response size and the computational cost. Therefore we skip this technique in our implementation and we choose to implement the QRP server using the classical producer/consumer pattern. The server could start computing the elements of the response array as soon as the first query element is received from the client, and then accumulatively update the response array when new elements of the query array are available. Since the time for uploading the query from client to server is negligible compared to the response computation time, this implementation of the server would eliminate the impact of the large query size on the overall roundtrip of the protocol. Clearly the query size of FHP is much smaller than the query size of QRP. In Table 5.1 the difference between the roundtrip time and the server computation time represents the total communication and the client computation costs. Notice that this difference for QRP is ~ 10 times larger than that for FHP. But as we will see shortly that this gain in the query size of FHP comes at the cost of increased computation overhead at the server side which can significantly impact the overall performance of the protocol.

The most expensive part for both protocols is the response generation that happens on the server side. In the process of generating a response, both algorithms examine each single bit in the database. If the bit is 1, the QRP server performs a modular multiplication for two integers of k-bit, while the FHP server performs a modular addition for two integers of γ-bit. Even though $\gamma = 3 \cdot k$, NTL (on our server) performs modular addition of two 3000-bit integers 10 times faster than a modular multiplication of two 1000-bit integers, which gives a worthy advantage to FHP over QRP. But, since the query generated by the FHP client represents the encryption of the address of the required record, the server now must compute an encryption $\hat{\omega}$ corresponding to each record in the database. This step includes additional $n \cdot \log n$ modular multiplication and addition operations for integers of size γ bits at the FHP server (lines $11, 12$ in Algorithm 5.2). We solve this problem also by implementing the producer/consumer pattern as we did in the QRP server. The response array elements are computed accumulatively as the next encryption value $\hat{\omega}$ becomes ready. But, one should notice that the computation cost of $\hat{\omega}$ is significantly higher than the communication cost of sending k-bit numbers. Specifically, in our settings the communication cost of sending 1000 bits is 0.01 msec while the computation cost of $\hat{\omega}$ is 0.8 msec. The effect of this additional computational cost of FHP increases with the number of records in the database, which explains the performance degradation for FHP in our experimental results when the number of the database records is increased (Table 5.1). Another observation is that the FHP performance decreases as the size of the record increases. Notice that, the FHP server needs to maintain two arrays, the size of each array is $3080 \times n$ bits, while the QRP server will maintain one array of size $1000 \times n$ bits. This larger amount of memory (~ 6 times) requirement by FHP causes a higher rate of cache misses; which in turn will increase the computation time of the ResponseGenerator algorithm. We summarize the pros and cons for both protocols in the following points.

- The QRP query size increases linearly with the number of records in the database, n, while FHP offers a good solution to this problem since the query size increases logarithmically with n.
- The FHP protocol demands larger bit size for the security parameter γ than the security parameter k for the QRP protocol. This causes a negative effect on the computation time and the response size for FHP.
- In general, the FHP performs better than the QRP for smaller databases while QRP outruns FHP when the database is large.

- Unfortunately, neither protocol is efficient enough to be practical. Both protocols are much slower than a trivial protocol in which the server will transfer the entire database to the client.

5.5 Summary

In this chapter we have implemented and evaluated both Quadratic-Residuosity based and Fully-Homomorphic Encryption based cPIR protocols that represent earliest and latest work in this area. We have used standard middle-of-the-ground hardware, software and open source libraries to implement them. Our goal has been to study the performance characteristics of each of these algorithms with a focus on testing if the latest improvements in cPIR schemes give enough performance gains as to make them useful in practical applications. We have normalized the protocols to offer similar acceptable privacy and run them against various representative sizes of databases and records. We have compared the performance statistics against that of the most trivial cPIR protocol. Our conclusion is that, even though there are improvements in communication and computation costs, cPIR protocols still require lot of work before they become efficient enough for practical applications, especially, TTP less protocol for LBS.

Moreover, when one observes the already prevalent LBS architecture, one can see that PIR techniques (both cPIR and itPIR) cannot be practically implemented on the current LBS architecture. Even if one were to ignore the client side processing and the communication costs, cPIR requires extensive processing overhead at the server side and itPIR requires replication of the service provider databases. Service providers may not be inclined to these changes that are counter intuitive to their revenue models in the LBS business. The alternative, which is transferring the entire database to the client, is even more counter productive for the service provider's business model, not to mention the communication and capacity costs imposed on the client and the entire system in general. Hence, having considered and studied carefully, we rule out PIR as a feasible method for our purpose, the TTP less LBS protocol. In the next few chapters, we propose our own protocols that use statistical privacy techniques and apply heuristics to achieve that goal. While proposing these techniques, our goal is not only to develop a proven technique in achieving guaranteed privacy levels, but also impose as minimal changes to existing prevalent architectures as possible.

Chapter 6

Single Query Scenario

Continuing the discussion from Chapter 4, we present in this chapter implementation details of an efficient heuristic based LPPM. The goal is to implement optimizations and heuristics with a focus on reducing processing times that makes it practical on mobile devices. Even though mobile devices have come a long way in terms of processing power, optimizations are required in order for the privacy protection methods to finish quickly enough to preserve quality of service. Algorithms along with heuristics of the proposed LPPM presented here are based on our work in [44]. Later, we present the implementation details and assess the performance characteristics of the proposed LPPM.

First, we consider a simple scenario where the user issues a single query. In the next chapter we enhance this architecture to be able to provide strong and efficient privacy guarantees when multiple queries are made by the user. However, the model and symbols introduced in this chapter are maintained and extended throughout the rest of the dissertation.

6.1 Proposed LPPM

High levels of privacy measures discussed in Section 4.8 serve as an objective that one may try to achieve while designing a search algorithm for local search. However, the question remains open whether the computational cost associated with implementing this solution on a mobile device will be practical or not. Alternatively, instead of obtaining the optimal regions $C_1, C_2, ..., C_m$, (Section 4.9) we have taken the engineering approach and divide the set of cells C into predefined regions. These regions are created by overlaying the grid $\mathcal{G}$ with a coarser grid of size $\hat{Z} \times \hat{Z}$. All cells contained within a coarser cell then form a region. We will refer to such a region also as a *box*. In this case, we have $m = \left(\frac{Z}{\hat{Z}}\right)^2$ (assume Z is a multiple of $\hat{Z}$) and each box B_i is simply a sub-grid of the grid $\mathcal{G}$ with size of $b \times b$, where $b = \frac{Z}{\hat{Z}}$. Note that, in this formulation, the user configures her required level of obfuscation by setting the value of the parameter b indicating that she does not care if the attacker narrows her location to an area greater than or equal to a b cells by b cells ($b \times b$ box). This is often specified in real life approximations such as a mall, block and sub-division that is usually translated by the application into the parameter b that represents their size. So, pinpointing the user's location to an area that is less than a $b \times b$ box will be considered a breach of her expected privacy.

If the box B_u happens to be the $b \times b$ box where the user is located, then the interest set, I_u, is the union of the most highly ranked K POIs (top-K POIs) for each cell in B_u. The need is to compute a set of top-K POIs for each cell in a subset of cells C_u and return the union of these sets. Here, the subset C_u is a set of cells that form a box B_u which contains the user's cell, c_u. Clearly, the obfuscation requirement is satisfied for this algorithm, since for each cell $c \in C_u$, $\Phi_1(c) > 0$. Equation 4.3 for the probability that the user exists in a cell $c_i \in C_u$ can be rewritten as follows

$$\Phi_1(c_i) = \Pr(c_i|C_u) = \frac{\Pr(C_u|c_i)\,\Phi_0(c_i)}{\sum_{c_j \in C_u} \Pr(C_u|c_j)\,\Phi_0(c_j)}. \tag{6.1}$$

Since the grid $\mathcal{G}$ has been pre-partitioned into non-overlapping boxes of size $b \times b$, for any box B, $\Pr(C|c_i) = 1, \forall c_i \in C$, where C is the subset of cells included in B. By substituting into Equation 6.1, we have $\Phi_1(c_i) =$ a constant $\times\ \Phi_0(c_i)$; hence convergence holds as well.

Service loss minimization is also not performed explicitly; nonetheless, we expect the union size of the top-K sets to be relatively low since neighboring cells are collected together to form the regions. The interest set computation for the user is then performed in two steps:

1. $\mathcal{R}$: determine the box B_u where the cell of the user belongs.

2. $\mathcal{A}$: obtain the union of the top-K POI sets of the cells in B_u.

Following the steps of the architecture presented in Section 4.5, the client determines a large geographical area that includes the user's location (A_R), and sends the coordinates of this area along with search keywords to the server. The server finds the list of matching POIs within A_R from its database, and sends back only the location and the prominence information of the obtained POIs. The client locally ranks the received list of POIs and determines the interest set I_u corresponding to the box B_u. The client then queries the server for detailed information about the POIs in the set I_u. The server responds with details of those POIs.

To determine the interest set, a brute force search is the trivial solution to compute the union of the top-K POIs of the cells in a box. But it is computationally impractical to implement on the client end, i.e., the mobile device. Hence, a faster algorithm to calculate the interest set locally on the client end has been proposed.

6.2 Interests Set Computation

The top level procedure of our method is given in Algorithm 6.1. The algorithm starts with the following pre-computations:

1. Partition the set C_u into two subset C_{border} and $C_{internal}$. The set C_{border} is a set of cells that occur at the border of the box B_u; $C_{internal}$ is the set of the remaining cells of B_u.

2. Determine subset $P_{box} \in P$, the set of POIs that occur inside, or on the border of the box B_u.

Algorithm 6.1 Compute the top-K set of POIs for the user's box.

```
Input: Set $P$ of all POIs; Set $C_u$ of all cells in the box $B_u$; Prameter $K$
Output: Interest set $I$: the unioun of the top-$K$ POIs for all cells $c_i \in C_u$
 1: function CreateTopK-List($P$, $C_u$, $K$)
 2:     $C_{border} \leftarrow$ border cells of $B_u$                    ▷ subset of $C_u$
 3:     $C_{internal} \leftarrow$ non-border cells of $B_u$              ▷ complement of $C_{border}$
 4:     $P_{box} \leftarrow$ POIs included in the box $B_u$              ▷ subset of $P$
 5:     $I \leftarrow \varnothing$
 6:     $root \leftarrow$ BuildTree(Data($P$), 1)
 7:     for all $c_i \in C_{border}$ do
 8:         $I \leftarrow I\cup$ CellTopPOIs($root$, $c_i$, $K$)
 9:     end for
10:     $P_{reduced} \leftarrow P_{box} \cup I$
11:     $root \leftarrow$ BuildTree(Data($P_{reduced}$), 1)
12:     for all $c_i \in C_{internal}$ do
13:         if $I = P_{reduced}$ then exit for
14:         $I \leftarrow I\cup$ CellTopPOIs($root$, $c_i$, $K$)
15:     end for
16:     return $I$
17: end function
```

Stage-I

Build the interest set for the border cells cumulatively by iterating through the cells of C_{border}, computing the top-K POIs for each cell and add it to the interest set I. In order to obtain the set of the top-K POI for a cell, we use a kd-tree based branch-and-bound search algorithm. The details of constructing the tree and modifying this technique to satisfy our problem requirements are going to be discussed later in this chapter. For this stage we build the kd-tree using the full set of POIs, P. In the next stage we will use a reduced search space (POIs set) to build the kd-tree with less number of nodes, which leads to a smaller tree and so improves the search time. Moreover, at this stage we do the computation for a smaller partition of C_u cells, namely the border cells, while the small tree is used for the larger partition.

Stage-II

By the end of Stage-I we have the set I that represents the top-K POIs for the border cells of the box B_u. We create a new reduced search set of POIs, $P_{reduced}$, for this stage by computing the union of the sets I and P_{box}, where P_{box} is the set of POIs that are located within the box. Now a new kd-tree is built using the set $P_{reduced}$. We use this kd-tree and iterate through the cells of the set $C_{internal}$ to obtain the top-K POIs for each cell. Again we cumulatively add the top-K POIs from each cell to the interest set, I. The algorithm ends after either exhausting all the cells in set $C_{internal}$ or if $I = P_{reduced}$, since we cannot add any more POIs to I.

6.3 kd-Tree Branch-and-bound Search

A kd-tree data structure is chosen, because it is a data structure that gracefully adapts the distribution of k-dimensional points and also can be used "efficiently" for range searching and range counting queries. We built the kd-tree using the search set of the POIs, and then used it to determine the top-K POIs for a cell c_{ref} in the grid. The tree built here is a slightly modified version of the standard 2d-tree data structure (in our application $k = 2$). So the concept of a 2d-tree is briefly reviewed here before the implementation of the proposed 2d-tree is explained.

The main idea of a 2d-tree is that it recursively partitions the plane into two half planes. Let's take as an example a set of points that are distributed in the xy-plane as shown in Figure 6.1a and build a 2d-tree based on these points. Consider any random permutation of the points, say $(c_3, c_2, c_7, c_9, c_6, c_4, c_{10}, c_1, c_8, c_5)$. Take the point c_3, which is the first point that appears in the random list, and set this point as the root of the tree. The plane is divided into two parts based on a vertical line through this point. In the tree, all points that fall to the left of the point c_3, i.e., the points with smaller x-coordinate values must be added to the left subtree of the node c_3. Similarly, every point with x-coordinate value greater than the x-coordinate value of the point c_3 must be in the right subtree of the node c_3. At this point the x-axis is referred to as the *cutting dimension* of the node. Then we get the next point c_2 where we switch our partitioning of the plane according to the horizontal line that passes through this point. At the node c_2 in the tree the left subtree consists of the set of points that are below the horizontal line (smaller y-coordinate values) and the

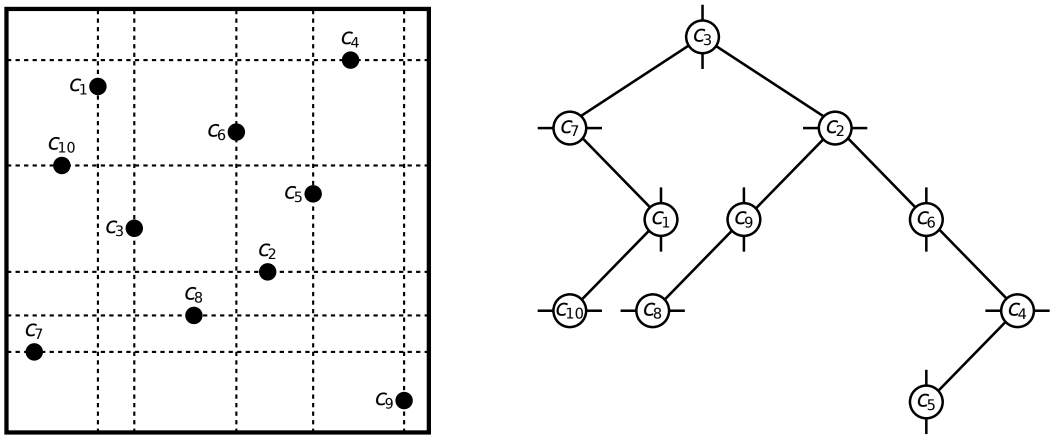

(a) Data points (b) 2d-tree

Figure 6.1: Building a 2d-tree example.

right subtree will include only the points above the horizontal line (greater y-coordinate values). In this step, the cutting dimension is the y-axis. Continuing the same process for the rest of the points we end up with the tree shown in Figure 6.1b. The left subtree for any node c_i represents the set of all points in the plane with a cutting dimension coordinate values less than the value of the point c_i, and the right subtree will contain all the points that have values greater than the value of the point c_i. The resulting tree is nothing but a binary search tree in which the key is alternated based on the cutting dimension (axis) of the node.

6.3.1 Building augmented kd-tree

Clearly, keeping a binary search tree balanced will significantly reduce the search time. In Algorithm 6.2, the kd-tree is built by using a composite array, *data*, for the set P of POIs that is sorted based on both x and y coordinate values. To create the first node (root) of the tree the median point from the data set is chosen based on the current cutting dimension. Then, branches of the tree are built recursively by considering all points and placing them on either side of the root node. This ensures a more balanced kd-tree compared to building it iteratively using randomly ordered points. Additionally, in Algorithm 6.2, each node in the tree is augmented with the minimum possible γ value of POIs included in the subtree rooted at that node including the node itself (recall from Section 4.6 that $\gamma_i = \frac{1-\alpha}{\alpha}(1-\mathscr{P}_i))$. We denote this value by $\gamma_{min}(.)$.

Algorithm 6.2 Build kd-tree.

Input: Composite array *data* of all POIs sorted based on both x and y; Index of cutting dimension *cd*

Output: The root of kd-tree for the given set of POIs

```
1: function BuildTree(data, cd)                                    ▷ cd is the cutting dimension
2:     if size(data) = 1 then
3:         t ← kdNode(data[cd, 1], cd)
4:     else
5:         median ← size(data)/2
6:         t ← kdNode(data[cd, median], cd)
7:         if median > 1 then
8:             t.Left ← BuildTree(LeftPoints(data[cd], median), ((cd + 1)%2) + 1)
9:             t.MinLeftGamma ← Min(t.Left.Gamma, t.Left.MinChildGamma)
10:        end if
11:        if median < size(data) then
12:            t.Right ← BuildTree(RightPoints(data[cd], median), ((cd + 1)%2) + 1)
13:            t.MinRightGamma ← Min(t.Right.Gamma, t.Right.MinChildGamma)
14:        end if
15:    end if
16:    return t
17: end function
```

6.3.2 Find the top-k POIs

Algorithm 6.3 shows how to calculate the top-K POIs for a given query cell c_{ref}. Two lists are maintained – (i) a list T representing the top-K nodes (POIs), ordered according to the rank of the nodes with respect to c_{ref}, and (ii) a list L of nodes to be explored, sorted by a *lower bound* value. The lower bound value for a node represents the minimum possible rank achievable for the subtree rooted at that node.

To compute the lower bound value for a node we associate two distance estimates to every node c, $d_x(c)$ and $d_y(c)$, representing the minimum possible distance we expect to find in the subtree rooted at node c, along x- and y- dimensions, respectively. Equation 6.2 gives the lower bound of the rank values in the subtree at node c.

Algorithm 6.3 Compute the top-K set for reference cell.

```
Input: Root node $root$ of kd-tree; Reference cell $c_{ref}$; Parameter $K$
Output: Ordered list of top-$K$ POIs with respect to the cell $c_{ref}$
 1: function CellTopPOIs($root$, $c_{ref}$, $K$)
 2:     $T \leftarrow$ empty list
 3:     $L \leftarrow$ empty list
 4:     $L$.Append($root$)
 5:     while $L$ is not empty do
 6:         $n_{test} \leftarrow L$.Remove-And-Return-Head()
 7:         $i \leftarrow 1$
 8:         if $T.size = K$ and $\nexists i$such that$n_{test}.lbound \leq T[i].rank$ then exit while
 9:         $n_{test}$.CalcRank($C_{ref}$)
10:         $T$.PriorityInsert($n_{test}$)                          ▷ $rank$ based.
11:         if $T.size > K$ then $T$.RemoveLast()
12:         If there exists $n_{test}.left$ node then
13:             $L$.PriorityInsert($n_{test}.left$)                 ▷ $lbound$ based.
14:         If there exists $n_{test}.rigth$ node then
15:             $L$.PriorityInsert($n_{test}.rigth$)                ▷ $lbound$ based.
16:     end while
17:     return $T$
18: end function
```

$$LB(c) = \frac{\sqrt{d_x(c)^2 + d_y(c)^2}}{N} + \gamma_{min}(c), \tag{6.2}$$

where N is normalization factor for distance (see Section 4.6). Both distance estimates are initialized to zero for the root of the tree and then updated as we explore the tree. Let c_{ref} be (x_{ref}, y_{ref}) and we want to calculate the lower bound for the left and right child nodes of the node $c_i = (x_i, y_i)$. Further, assume that x-axis is the cutting dimension at the node c_i.

- If $x_{ref} < x_i$, then the minimum possible x-distance for the nodes in the "right" subtree of c_i with respect to c_{ref} is $d_x(right) = |x_{ref} - x_i|$, because all nodes in the right subtree of c_i have x-coordinate values greater than x_i. We cannot estimate the minimum y-distance for the right subtree here because we split on x-dimension at this node. However, we can still retain the estimate from the node c_i itself, effectively giving us $d_y(right) = d_y(c_i)$. For the left subtree we will retain the estimate for both x and y distances from the node c_i, i.e., $d_x(left) = d_x(c_i)$ and $d_y(left) = d_y(c_i)$.

- If $x_{ref} \geq x_i$, then the minimum possible x-distance for the nodes in the "left" subtree of c_i with respect to c_{ref} is $d_x(left) = |x_{ref} - x_i|$, because all nodes in the left subtree of c_i have x-coordinate values less than x_i. As in the previous case, $d_y(left) = d_y(c_i)$, $d_x(right) = d_x(c_i)$ and $d_y(right) = d_y(c_i)$.

The same line of reasoning can can be applied if the splitting dimension on node c_i was y-axis instead of x-axis.

During the search, we explore the nodes in L in their order of appearance, and terminate when L becomes empty (line 5 in Algorithm 6.3), or it is determined that no node in the subtree can potentially change the existing T list (line 8 in Algorithm 6.3). The latter case can happen when the lower bound value of the first node in L is greater than the rank value of the last node in T. Exploring a node involves the steps of checking if the node can be inserted in the T list based on its rank (lines $[9-11]$ in Algorithm 6.3), computing the lower bounds for the left and right children, and then inserting them in L (lines $[12-15]$ in Algorithm 6.3).

Example. We present this example for further illustration of the process. In this example, a grid size is assumed to be 320×320 cells, giving us a normalization factor $N = \frac{1}{320\sqrt{2}}$. We consider a top-3 search query for the cell c_{ref}. In *state*–1, the first node c_1 in L is the root of the subtree shown in Figure 6.2. The minimum distance estimates for the root node c_1 are assumed as $d_x(c_1) = 15$ and $d_y(c_1) = 5$. The location and the γ values for c_{ref} and for each node in our example subtree are listed below.

	Location (x, y)	γ	γ_{min}
c_{ref}	$(204, 115)$		
c_1	$(190, 72)$	0.26	
c_2	$(180, 125)$	0.25	
c_3			0.47
c_4			0.38
c_5			0.35

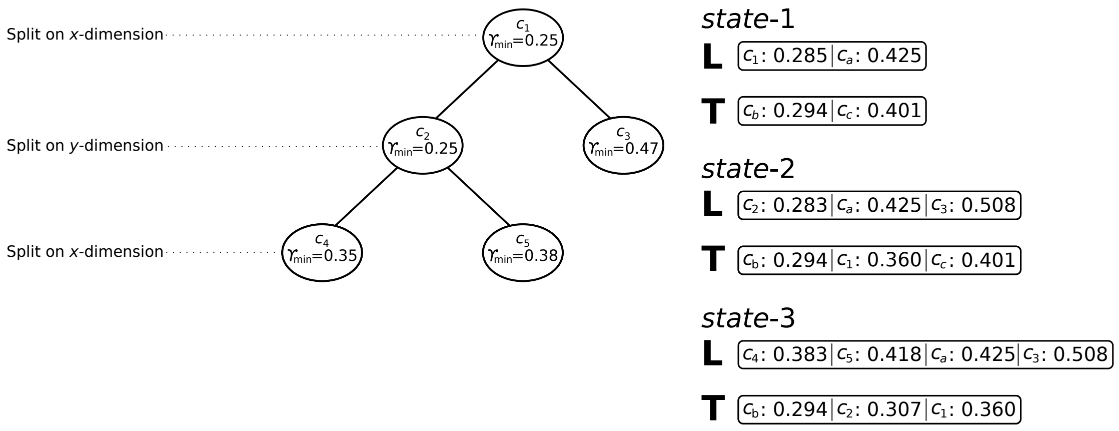
Split on x-dimension
Split on y-dimension
Split on x-dimension
c_1 Υ_{min}=0.25
c_2 Υ_{min}=0.25
c_3 Υ_{min}=0.47
c_4 Υ_{min}=0.35
c_5 Υ_{min}=0.38
state-1
L c_1: 0.285 | c_a: 0.425
T c_b: 0.294 | c_c: 0.401
state-2
L c_2: 0.283 | c_a: 0.425 | c_3: 0.508
T c_b: 0.294 | c_1: 0.360 | c_c: 0.401
state-3
L c_4: 0.383 | c_5: 0.418 | c_a: 0.425 | c_3: 0.508
T c_b: 0.294 | c_2: 0.307 | c_1: 0.360

Figure 6.2: Example of kd-tree search

Following Algorithm 6.3, if L is not empty we remove the first node, c_1, and check whether is it possible to add this node to T. Since the rank of c_1 is $\frac{\sqrt{(204-190)^2+(115-72)^2}}{320\sqrt{2}}+0.26 = 0.360$ it will be inserted into T, after the node c_b, as shown in *state*–2. Then we look for the left and right children of c_1. Since on c_1 we split on x-dimension, all nodes on the left subtree of c_1 have x-coordinate values < 190. Since the x-coordinate of c_{ref} is greater than the x-coordinate of c_1, the minimum x-distance for the left subtree of c_1 is $d_x(c_2) = |204 - 190| = 14$. The same argument is not possible for the minimum y-distance of c_2, so we retain this value from the parent node, $d_y(c_2) = d_y(c_1) = 5$. Thus, the lower bound for c_2 is $LB(c_2) = \frac{\sqrt{14^2+5^2}}{320\sqrt{2}} + 0.25 = 0.283$. For the right child, c_3, we can only retain the values from the parent, i.e., $d_x(c_3) = d_x(c_1) = 15$, $d_y(c_3) = d_y(c_1) = 5$. Thus, the lower bound for c_3 is 0.508. Now, nodes c_2 and c_3 are inserted into L based on their lower bound as shown in *state*–2. In the next iteration, we remove the node c_2 from L, so the cutting dimension this time is the y-axis. Since y-coordinate of c_{ref} is less than the y-coordinate of c_2, all nodes on the right subtree of c_2 will have y-coordinate > 125, giving $d_y(c_5) = |115 - 125| = 10$. With $d_x(c_5) = d_x(c_2) = 14$, the lower bound for c_5 is $\frac{\sqrt{14^2+10^2}}{320\sqrt{2}} + 0.38 = 0.418$. For the left child, c_4, $d_x(c_4) = d_x(c_2) = 14$, $d_y(c_4) = d_y(c_2) = 5$ and the lower bound is 0.383. The rank of c_2 is 0.307. The node c_2 is inserted into T based on its rank, and the nodes c_4 and c_5 are inserted into L based on their lower bound. The status of both L and T at the end of this iteration is shown in *state*–3 in Figure 6.2. Once we observe that the lower bound value for c_4 (the first node in L) is greater then the rank of the last node in T, we can terminate the search and return the list T.

6.4 Improving the Grid Search Time

Even though optimized using a kd-tree, any reduction we can do on the number of the top-K POI calculations could further improve the performance of our algorithm.

6.4.1 Skip top-k search for equivalent cells

We observe that when top-K POIs are being determined for consecutive cells (e.g. a row or column of cells), it may be possible to skip the top-K search for certain cells. So whenever Algorithm 6.1 iterates through a set of cells, it will take them either by rows or by columns and invokes the actual determination of top-K POIs for that cell (function CellTopPOIs) only when it is necessary.

Assume that T is the vector of top-$(K+1)$ POIs obtained for a cell c_s using the kd-tree search. Let c_t be a subsequent cell in the same row or column. Given the structure of the ranking function, the rank of any POI with respect to c_s can at best reduce by $dist_{norm}(c_s, c_t)$ (the γ values are constant) when computed with respect to c_t . Consider the $(K+1)^{\text{th}}$ top POI for c_s , i.e. $T[K+1]$. The rank of this POI, and any other POI not in T , can at best be $\psi = rank(T[K+1], c_s) - dist_{norm}(c_s, c_t)$ when computed with respect to c_t . Therefore, if we reorder T based on the ranks of the POIs with respect to c_t , and observe that the K^{th} POI rank is less than or equal to ψ, then no other POI can replace the first K POIs in the reordered T. In that case, the kd-tree search for c_t can be skipped, and the first K POIs in the reordered T are the top-K POIs for c_t . Note that the $(K+1)^{\text{th}}$ POI is only known for cell c_s, the last cell where a full search was performed. Hence, ψ should always be calculated using the last fully searched cell.

6.4.2 Reducing the search space for non-border cells

An improvement can also be achieved if the number of nodes in the kd-tree itself can be reduced. A smaller set of POIs ($P_{reduced}$) is used in Stage-II of Algorithm 6.1 to construct a new kd-tree for this purpose. One can easily verify that in the plane $\mathbb{R}^2$, the top-K POIs of a point inside any given box is either inside the box, or is the same as the top-K POIs of some point on the boundary of the box. The same argument also applies to our discretized grid, provided the discretization is fine enough that, for any real-valued query point between two cells on a border of the region, the top-K set matches the top-K set of either one of the neighboring cells. For example, if set T_1 is the top-K set of cell $(1, 1)$ and T_2 is the top-K set of cell $(1, 2)$, then the top-K set of any point $(1, y); 1 < y < 2$ is either of T_1 or T_2. The physical distance between two cells in our empirical evaluation is 100 meters, which is reasonably small to maintain the accuracy of this heuristic.

6.5 Evaluation

In this section, we discuss a set of experiments aimed to estimate the runtime performance and the expected privacy overhead of the proposed architecture.

6.5.1 Experimental setup

We consider a 320×320 grid over a 32×32 km^2 broad area (A_R) centered at Los Angeles, CA downtown $(34.0522^O\text{N}, 118.2428^O\text{W})$. This area is divided into a grid of cells measuring $100m \times 100m$. Default values of $\alpha = 0.8$ and $K = 10$ are used, and all distance computations are Euclidean. We use multiple search keywords to obtain different POI distributions, in terms of size and density. The business listings are obtained from the SimpleGeo Places database. The SimpleGeo database does not include prominence values for POIs; we assigned values to the POIs from $\{0.95, 0.90, ...,0.2, 0.25\}$ using a Zipf distribution with exponent 0.8. Lower prominence scores are more frequent under this distribution.

Experiments are performed on a 2.8 GHz quad-core Intel Xeon$^{\text{TM}}$system running Mac OS X$^{\text{TM}}$10.8.2 with 8GB memory. Run times of the algorithms to be executed on mobile devices are obtained on an Android$^{\text{TM}}$emulator running a virtual device with an ARM Cortex-A8 processor ($\sim$ 800 MHz) and 512MB memory. We also run the algorithms on a virtual device using the Intel Atom system image (with 1GB memory). All implementations are single-threaded.

6.5.2 Runtime performance

Table 6.1 lists the average time to compute the interest set across the different regions for a given coarse grid $\hat{\mathcal{G}}$ consisting of $\hat{Z} \times \hat{Z}$ regions. The number of cells in each region is $b \times b = \frac{Z}{\hat{Z}} \times \frac{Z}{\hat{Z}}$. For example, a 10×10 coarse grid results in 100 regions (sub-grids) of 32×32 cells. The execution time for each region is taken as the average of 10 identical runs. Each cell in the table shows the time for the two different devices (ARM and Atom). Except for when large regions (a 5×5 coarse grid) are created for some high density POIs, the execution time using the ARM processor is within one second; in fact, it is less than 500 milliseconds for a majority of the cases. We get almost a five fold improvement in the computation time by using the Atom processor, with most computations in the 20 to 100 ms range. Although the Atom processors are currently more suitable for tablet computers, efforts have already been successful in porting them to smartphones. We also tested our algorithm on a physical Samsung Galaxy Note smartphone with a dual-core 1.5GHz Snapdragon S3 processor. The observed run times for the 10×10 coarse grid are a three fold improvement over the emulated values on the ARM device. In addition to the overhead associated with the interest set computation, our architecture also incurs a communication overhead. This overhead appears in the first round-trip of the architecture (Figure 4.3), where the client has to obtain the locations and γ values of the matching POIs inside the A_R. However, the overhead is negligible if—the latitude, longitude and γ values of a POI are encoded as 32-bit numbers, and 1000 matching POIs exist inside the A_R, then a total of 12KB of data needs to be downloaded before computing the interest set. Assuming a 3G connection with 320 KB/s speed [148] , this download will incur an additional 37.5 ms to the process. Observe the average times the algorithm took to run on a real android device in Figure 6.3 on a

Table 6.1: Average time (milliseconds) to compute interest set for different sizes of the coarse grid ($\hat{Z} \times \hat{Z}$). Top and bottom values correspond to the ARM processor and the Atom processor virtual devices respectively.

search query	no. of POIs	computation time (ms) given a coarse grid					
		80×80	40×40	20×20	10×10	8×8	5×5
bus station	32	10.83	15.32	24.41	43.47	49.65	76.96
		2.0	2.9	4.71	8.62	9.84	15.18
farmers market	50	24.99	31.93	45.69	74.04	92.25	140.88
		4.03	5.4	8.12	13.62	17.32	26.78
police	84	35.12	46.72	71.25	128.58	179.54	396.82
		5.82	7.93	12.41	22.93	31.9	70.38
starbucks coffee	92	33.73	43.51	63.26	117.24	156.18	478.98
		5.5	7.21	10.79	20.57	27.49	84.84
grocery	95	34.49	44.11	64.43	119.55	178.24	386.67
		5.89	7.84	12.02	23.03	34.48	75.34
restaurant italian	124	46.1	57.39	81.74	155.23	206.6	539.14
		7.29	9.3	13.77	27.02	36.2	94.71
liquor store	125	50.29	64.12	92.82	180.66	277.67	831.41
		7.54	9.88	14.8	29.42	45.38	135.69
bookstore	126	46.29	57.12	80.66	152.26	221.03	650.29
		7.63	9.92	14.83	29.55	43.41	128.76
library	141	58.54	72.38	102.61	194.44	275.47	783.86
		8.67	11.02	16.19	31.38	44.88	128.72
night club	149	61.27	72.56	96.27	172	266.14	644.26
		8.84	10.9	15.35	29.59	46.25	115.82
clothing store	169	72.09	86.95	120.06	235.17	320.04	920.34
		11.14	13.99	20.53	42.34	58.63	171.79
car rental	196	91.37	107.25	142.95	252.14	352.26	889.84
		13.67	16.89	23.97	44.91	63.83	165.54
parking	281	136.63	160.78	202.45	363.43	504.01	1248.92
		19.55	23.91	33.26	62.34	87.48	220.6
atm	297	131.66	148.88	190.53	339.13	491.26	1382.03
		18.62	21.75	29.72	57.46	85.47	250.42
gas station	347	153.38	169.56	210.34	383.49	565.08	1580.96
		23.12	26.32	34.82	69.25	105.49	308.41
pharmacy	369	173.49	195.14	247.32	446.25	649.94	1846.01
		24.45	28.08	36.97	70.33	104.13	303.26
cafe	608	305.48	328.5	385.3	613.32	805.09	2097.42
		44.18	49.64	61.73	107.47	146.33	407.17
bakery	834	444.79	457.99	525.32	803.75	1078.03	2776.04
		61.7	66.73	80.89	137.3	193.21	539.39

40×40 coarse grid. The average across all POIs we experimented with is around 100ms.

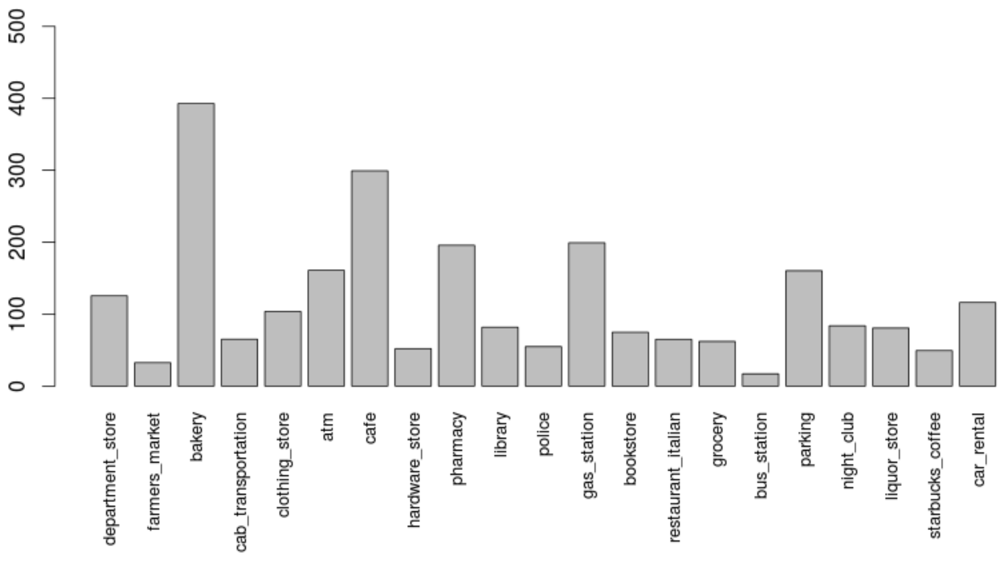

Figure 6.3: Average run times (milliseconds) on actual device (for 40x40)

So, even combined with communication overhead, most mobile users should see sub-second response times.

6.5.3 Expected privacy and overhead

We consider three different forms for the adversary's prior probability distribution – (i) no knowledge–*uniform-global*: equal probability throughout the 320×320 cells, (ii) locality knowledge–*uniform-local*: equal probability in a circle of 25 cells radius, zero everywhere else, and (iii) precise knowledge–*gaussian*: normally distributed probabilities; mean cell at the center and variance of 50 cells. Figure 6.4 depicts the uniform-local and the gaussian knowledge distributions. We assume that the attacker's background knowledge is always correct, i.e. the user can never be at a cell where the attacker's prior probability is zero.

Figure 6.5 shows the expected privacy achieved for different coarse grid sizes. The data points in each line correspond to $\hat{Z} = 80, 40, 20, 10, 8$ and 5, from left to right. We choose

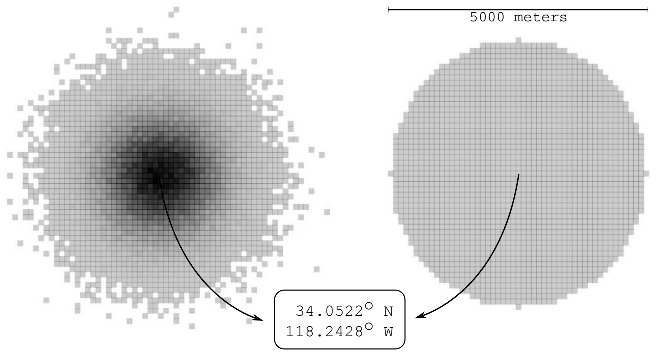

Figure 6.4: Uniform-local (right) and gaussian (left) background knowledge. Darker cells imply higher probability.

three different keywords—starbucks coffee (92 POIs), gas station (347 POIs) and bakery (834 POIs)—to evaluate the quantities in the case of low, medium and high density POIs.

Based on empirical data, it is reasonable to say that the expected exact privacy for all three POI densities is much above levels of concern, greater than 90% in this case. This implies that it will be difficult for the adversary to accurately make a random "guess" about the user's location using the posterior distribution, even if precise information (Gaussian knowledge adversary) on the whereabouts of the user is available to the adversary.

The expected privacy under inexact localization depends primarily on the extent of background knowledge. As expected, the uncertainty about the user's location is significantly less when the adversary has more precise knowledge. Larger values of $\hat{Z}$ help improve the expected privacy to some extent. Note that, for lower values of $\hat{Z}$ (larger sub-grids), the privacy level we observe (high or low) is primarily due to the prior knowledge of the adversary. Larger sub-grids will encompass most of the locality where the adversary's prior knowledge is concentrated. Since the convergence requirement is enforced, the expected privacy value from the posterior distribution will be the same as that from the prior distribution.

The expected interest set size shows some variations across different knowledge forms and POI densities. In general, smaller values of $\hat{Z}$ results in more cells in a region; therefore, more number of top-K sets are merged to create the interest set. The denser the POI, the higher is the number of unique top-K sets. The set sizes are larger for the uniform-local

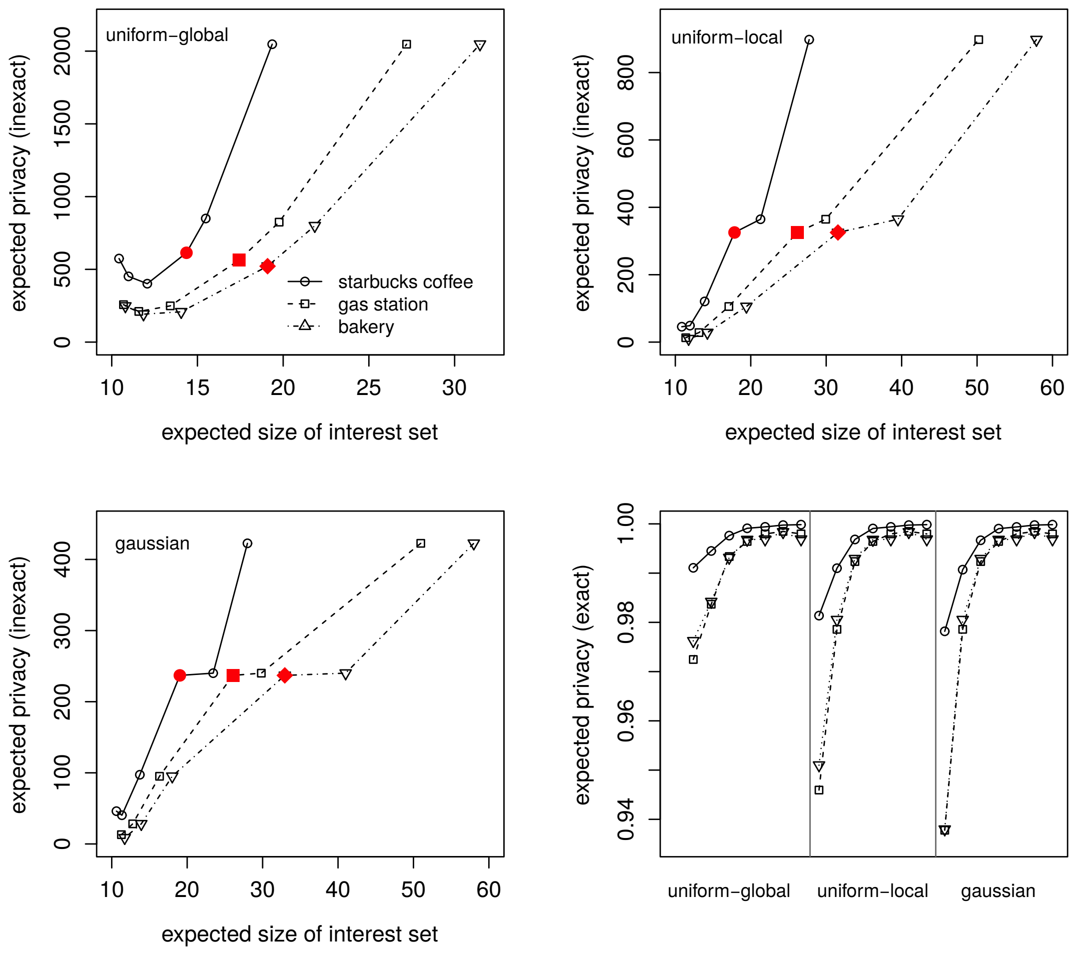

Figure 6.5: Expected privacy and expected interest set size trade-off. Data points in each line correspond to $\hat{Z} = 80, 40, 20, 10, 8$ and 5, from left to right.

and gaussian knowledge adversaries; since the user is highly likely to be located in central downtown, the variations in the top-K POIs are also expected to be the most (due to the higher concentration of POIs).

The solid data points in the first three plots signify the case of $\hat{Z} = 10$ (output regions of the $\mathcal{R}$ function are 32×32 cells). Irrespective of the general trends, use of this value results in expected privacy levels of *at least* 2 km^2 (200 cells) and interest sets of around 30. An area of 2 km^2 is equivalent to around 1000 homes with $22,000$ ft^2 lots, which we consider to be a significantly large area for a privacy conscious user. The expected interest set size is larger than what is necessary, but may prove to be useful if the user does not find an acceptable choice in the top-10 results. Retrieval of detailed feature data for 30 POIs is also not expensive considering that most current applications already retrieve more than that (Google Places allows retrieval of data on up to 60 POIs in a query).

6.6 Summary

In this chapter, we proposed our first algorithm that fits into the two-roundtrip architecture. We used the realistic ranking method that considers the prominence of the POIs in addition to the distance from the query point. We brought together several techniques to ensure that the LPPM is efficient enough for a client side implementation. We implement these algorithms on realistic simulators and actual mobile devices to ensure that the cost of quality of service drop is minor.

Chapter 7

Multiple Query Scenario

Pursuing our model from the previous chapter, the user is located in box B_u which consists of $b \times b$ cells and the interest set I_u is the union of the top-K POIs of each cell in B_u. As long as multiple queries by the user happen when the user is in the same box, the attacker's knowledge of the user's location will not be enhanced. The coarseness of the attacker's estimation of user's location remains $b \times b$ cells. Consider the case where the user moves form one box to another between two consecutive queries and the time interval between these two queries is larger than the time needed by the user to reach the farthest cell in A_R from the current cell. In this case, the attacker is still not able to enhance his knowledge about the user's location. This is because, there is enough time for the user to move to any cell in the grid $\mathcal{G}$. The work in this chapter is based on our outcome in [58,60].

Now we consider the converse scenario, where the time interval between the two queries is less than the time needed by the user to go from the current cell to the farthest possible cell in grid $\mathcal{G}$. In this case, the attacker may be able to narrow down the user's location to an area less than $b \times b$ cells. This is illustrated in Figure 7.1. Let T be the time period needed by the user to move by one cell, assumed to be constant. It shows two adjacent boxes A and B, where $b = 4$. Assume that the time interval between two queries, t, is less than or equal to the time required to move by one cell ($0 < t \leq T$). Let us further assume that the user was in one of the cells in box A that borders with box B. The user moves by one cell into box B and then issues her second query. This clearly allows the attacker to narrow down the user's location to the boundary cells (shaded) of the box B because he sees the first query's interest set matches with box A and the second query's interest set matches with box B, and the user had only enough time to move by one cell. The attacker is able to narrow down the user's location to an area much smaller than $b \times b$, thus clearly breaching the user's privacy requirement. This shows that obfuscation is not guaranteed in the case of multiple queries happening across boxes: this is the main problem this chapter addresses. The techniques proposed for single query scenario need to be enhanced to preserve the privacy of the user to the expected $b \times b$ level in the case of multiple queries.

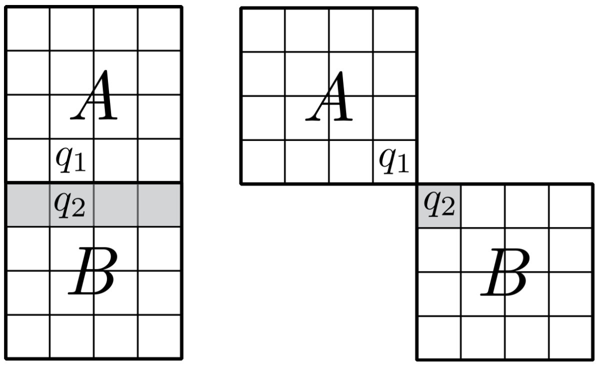

Figure 7.1: Location inference during multiple queries.

7.1 Extended Attacker Model

For the multiple query scenario, in addition to the capabilities mentioned in Section 4.7, we assume that the attacker knows the unit time period, T, needed by the user to move by one cell. If the attacker observes two consecutive queries, based on the time elapsed between the two queries, the attacker can estimate the maximum number of cells, n, the user can move between the two queries. For the multiple query scenario, we continue utilizing the notations introduced so far, but we modify it by using a subscript to indicate the query number, e.g. B_k represents the box selected for interest set generation during the k^{th}query q_k. By definition, B_k contains the user's location at that time instance and C_k is the set of cells in B_k. Correspondingly, I_k is the generated interest set, and Φ_k represents the attackers estimated probability distribution at the end of the k^{th} query. The distribution Φ_1 is the attacker's estimation after the first query is made, as given by Equation 4.3.

The attacker's goal is to narrow down the user's location to a specific cell. Short of that, the attacker tries to determine the likelihood of existence of the user in a particular cell, by calculating a probability distribution of the user's existence in each cell. Within the selected area, the attacker can pre-determine the possible $b \times b$ sized boxes that could be selected by the algorithm. He computes the interest set for each of these boxes. Once he observes the interest set I_k, for any query, he looks up the boxes whose interest set match I_k and determines the possible set of $b \times b$ boxes the user could be in.

7.2 Algorithm for Multiple Query Scenario

The reason for privacy loss during multiple queries with time interval constraints is due to the fixed pre-partitioning. Fixed pre-partitioning is suitable for the single query scenario or the first query, but not for the subsequent queries in the multiple query scenario. In the case of multiple queries, to prevent this privacy loss during a subsequent query, instead of keeping the initial fixed partitioning, we first create a new area, hereafter called the *selection area*, by expanding the box generated at the previous query to its neighboring cells. If n is the number of T time periods elapsed between two subsequent queries, then a *neighboring cell* is any cell that is no more than n rows or columns away from the current box. Formally, $n = \left\lceil \frac{t_k - t_{k-1}}{T} \right\rceil$, where t_{k-1} and t_k are the time of issuing queries $k-1$ and k, respectively. Next, the box for the new query is determined by selecting a *random* box of size $b \times b$ from within the selection area that also includes the user's cell.

7.2.1 Selection area

The selection area, S_k, represents all possible boxes the user could be in for query, q_k, given as

$$\begin{aligned} S_k &= \left\{ b \times b \, \text{boxes in} \cup_{c \in B_{k-1}} nbr(c,n) \right\} \\ nbr(c,n) &= \left\{ c' | c' \, \text{can be reached from} \, c \, \text{in} \, n \, \text{steps} \right\}. \end{aligned} \tag{7.1}$$

If the user does not hit the border of the grid $\mathcal{G}$ while moving n steps from any cell in box B_{k-1}, then the selection area S_k for the query q_k forms a square of size $(b+2n)\times(b+2n)$. If the border of $\mathcal{G}$ is reached before the n steps, S_k can be a rectangle. However, if Z is large enough, the chance of having a rectangular S_k is slim. Figures 7.2a and 7.2b show S_k where $n = 1$ and $n = 2$, respectively. The numbers inside each cell c_i signify the number of $b \times b$ boxes inside the selection area that contain the cell, i.e., the number of possible $b \times b$ boxes from which the algorithm could choose for the next query if the user is located in c_i. We call this number the *weight* w_i of a cell. For instance, in Figure 7.2b the algorithm can

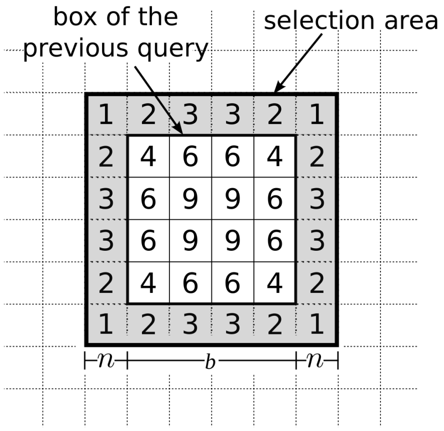

(a) $n = 1$.

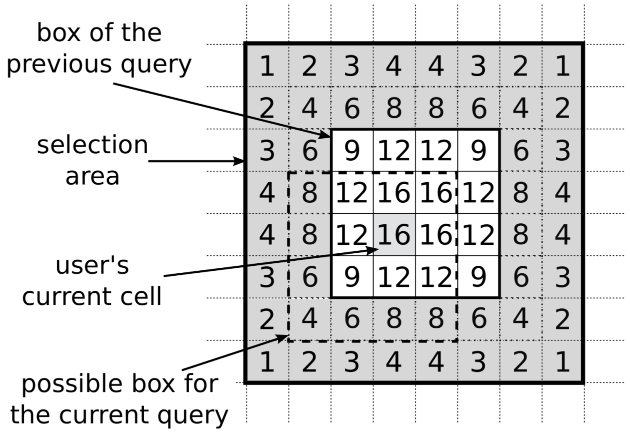

(b) $n = 2$.

Figure 7.2: Selection area for a $(4 \times 4$ size) box.

choose one out of sixteen possible boxes.

Let the cells of S_k be numbered $c_1, c_2, c_3...c_{(b+2n)^2}$ starting at the top left corner, continuing row by row. As we advance by one cell to the right along the horizontal direction, the number of possible boxes that could be created from the cell c_2 increase by one as well. If $2n \geq b$, this increment continues until the cell c_b is reached. This is illustrated in Figure 7.2b, where $b = 4$ and $n = 2$. When $2n < b$, the increment of the number of possible boxes stops at the cell c_{2n+1} as shown in Figure 7.2a, where $b = 4$ and $n = 1$. The number of possible boxes for the rest of the cells in the first row continue to be b until we reach the cell occurring b cells before the top right corner if $2n \geq b$. If $2n < b$, then it will continue to be $2n + 1$ until we reach the cell that occurs $2n + 1$ cells before the top right corner.

Thereafter, the number of possible boxes decrease till it becomes one again at the cell on the top right corner. Coming to the second row, one can easily deduce that the first cell on the second row has two possible boxes, one from the cell above and one at the current cell. Similarly, the next cell can generate four possible boxes, two boxes created at the cell above and two created at the current cell, and so on. The number of possible boxes for rest of the cells can be determined following the same process. One has to note that the same logic applies for a traversal along the vertical direction. A weights matrix with the number of possible boxes for each cell can be formulated as follows. Create a row vector $\bar{x}$ of the weights of the first row and a column vector $\bar{y}$ of the weights of the first column. The multiplication $\bar{y} \times \bar{x}$ gives the weights matrix for the entire S_k.

7.2.2 Choosing a box

Our algorithm makes the selection of the $b \times b$ box (for interest set generation) based on whether the issued query is the first one, or one of the subsequent ones. Algorithm 7.1 uses pseudo functions whose objectives are discussed next. For the first query, as described

Algorithm 7.1 Box selection for interest set generation.

Global Initialization: Time of previous query $t_p = 0$; Previous box $B_p = \textbf{\textit{null}}$
Input: Current time t; Box size b; User cell c_u
Output: Box B

```
 1: function BoxForCurrentQuery($t$, $b$, $c_u$)
 2:     $\mathcal{G} \leftarrow Z \times Z$ grid                                  ▷ Initial grid.
 3:     if first query then
 4:         $B \leftarrow \mathcal{G}$.FixedBox($b, c_u$)           ▷ ($b \times b$) box from pre-partitoned grid.
 5:     else
 6:         $n \leftarrow \left\lceil \frac{t-t_p}{T} \right\rceil$
 7:         $S \leftarrow \mathcal{G}$.GetSelectionAreaBoxes($B_p, n$)      ▷ ($b \times b$) boxes in selection area.
 8:         $B \leftarrow$ RandomSampling($S, c_u$)          ▷ Random box from $S$ includes $c_u$.
 9:     end if
10:     $t_p \leftarrow t$
11:     $B_p \leftarrow B$
12:     return $B$
13: end function
```

in Section 6.1, the grid $\mathcal{G}$ is pre-partitioned into fixed non-overlapping boxes of size $b \times b$. The algorithm simply chooses the box that contains the user's cell.

Let us assume that the algorithm is trying to generate the interest set for query q_k and n be the maximum number of cells the user could have moved after the previous query. For the second query, and subsequent ones, the algorithm first calculates n based on query timestamps and determines the selection area S_k. The box for the current query B_k is selected by picking a $b \times b$ box uniformly at random from S_k such that it contains the user. The algorithm uses the same techniques presented in the previous chapter for the single query scenario to efficiently generate the interest set I_k.

Since the client can cache earlier results, it only requests details for POIs that are new to this box, i.e. $I_{retrieve} = I_k - \mathbf{I}$, where $\mathbf{I}$ is the cache (set) of all POIs retrieved earlier and $I_{retrieve}$ is the set of POIs to be retrieved by the current query. This will continue till the current user session ends. When the time interval is large enough for the user to reach the farthest cell in $\mathcal{G}$, the algorithm starts a new session with the fixed pre-partitioning step.

7.2.3 Obfuscation

Since the user cannot move any farther in the given number of time units (n), the chance for the user being in a cell outside the selection area is zero. Refer to Figure 7.2 for the cases where $n = 1$ and $n = 2$. Further, each cell in the selection area (any numbered cell in the figure) has a chance (probability > 0) that the user could exist in that cell after n time units. Algorithm 7.1 randomly selects a box from this selection area when issuing query q_k, and because there is non-zero probability of user being in any cell of the box selected for the new query, obfuscation is preserved.

7.3 Specific Scenario

In this scenario, we assume that the selection area S_k is a square and the attacker can infer the exact interest set I_k. Given I_k, the attacker is able to find all boxes of size $b \times b$ corresponding to the set I_k. But we assume here that, there is exactly one $b \times b$ box (the one that was actually used by the algorithm B_k) corresponding to I_k. Further, the user's movement model is assumed to be a simple random walk. So, the user located in any cell

$c_i \in C_{k-1}$, can move n cells in any direction or she could stay in the same cell with *equal* probabilities before issuing query q_k. This gives us a square of side length $n+b+n = 2n+b$, which represents the set of all possible cells, C_k, the user could move to in n time units from current cell c_i. In this case, for any cell $c_j \in C_k$ the *transition probability* $\Pr(c_i \rightarrow c_j)$ is a constant value $\rho = \frac{1}{(b+2n)^2}$; for all other cells, it is zero.

Refer to Figure 7.2. It shows the selection area S_k that is created based on the box B_{k-1}. By following the same logic used for counting the number of possible boxes from a cell c_i in Section 7.2.1, if the user moves n steps or less from the top left corner cell of the selection area, we can reach only the top left corner cell of the box B_{k-1}. Considering the next cell in the first row of S_k , we can reach the first two cells in the box B_{k-1}. This will continue until the cell c_b, if $2n \geq b$, or the cell c_{2n+1}, if $2n < b$. The process is symmetric if started from the right side, vertically down from the top corner, or vertically up from the bottom corner. Thus, the weight w_i also represents the number of cells in B_{k-1} that the user could be in and reach c_i in at most n steps. Note that for cells within B_k, the weight w_i includes the possibility that the user decides to stay in the same cell, c_i. By the time the user performs query q_k, the attacker combines his knowledge of the user's movement model and B_k to compute a new distribution for the user's location as follows.

$$\lambda_k(c_i) = \sum_{c_j \in C} \left(\Pr(c_j|B_{k-1}) \times \Pr(c_i \rightarrow c_j)\right), \tag{7.2}$$

where λ_k represents the probability distribution of the user's location based on the movement model. After observing the new interest set, and a subsequent determination of the box B_k of the current query, the attacker can enhance his knowledge using Bayesian inference

$$\Phi_k(c_i) = \Pr(c_i|B_k) = \frac{\Pr(B_k|c_i) \times \lambda_k(c_i)}{\sum\limits_{c_j \in B_k} \left(\Pr(B_k|c_j) \times \lambda_k(c_j)\right)}. \tag{7.3}$$

Let the previous probability distribution for the attacker Φ_{k-1} be uniform, i.e., $\Phi_{k-1}(c_i) = \frac{1}{b^2}\ \forall c_i \in B_{k-1}$. We have – (i) the number of non zero terms (or $\frac{1}{b^2}$ terms) in $\lambda_k(c_i)$, given by

Equation 7.2, is w_i and $\Pr(c_i \to c_j) = \rho$, $\forall c_j \in B_k$. Hence, $\lambda_k(c_i) = \frac{\rho.w_i}{b^2}$, (ii) the weight w_i of any cell c_i in the selection area also represents the number of boxes that includes c_i, and selection is done uniformly at random, hence $\Pr(B_k|c_i) = \frac{1}{w_i}$. By substituting these values of $\lambda_k(c_i)$ and $\Pr(B_k|c_i)$ into Equation 7.3, the probability distribution in the new box B_k is

$$\Phi_k(c_i) = \frac{\frac{1}{w_i} \times \frac{\rho.w_i}{b^2}}{\sum\limits_{c_j \in B_k} \left(\frac{1}{w_j} \times \frac{\rho w_j}{b^2}\right)} = \frac{1}{b^2}. \tag{7.4}$$

So we conclude that, the probability distribution for the current query Φ_k is uniform if the probability distribution for the previous query was uniform.

7.3.1 Uncertainty of the attacker

To measure the attacker's uncertainty, we use *entropy* (Equation 7.5). Intuitively, a higher entropy value reflects higher uncertainty for the attacker about the user's exact cell [141]. If the attacker's expectation of the user's existence in all cells, $c \in C_k$, is equal, then the entropy is maximum and it is equal to $2 \log b$, where b is the side length of the box. Throughout the following discussion, we will refer to a box that maintains this property as a *balanced* box. A balanced box is a square area of size $b \times b$ where the probabilities of the user's existence in any cell is the same

$$H(\Phi_k) = -\sum_{c \in C_k} \Phi_k(c) \log \Phi_k(c). \tag{7.5}$$

Without any other background knowledge, if the attacker narrows down the user to a $b \times b$ box, he assigns equal probability of $\frac{1}{b^2}$ to each cell in this box, which indicates highest uncertainty for the attacker.

We have just shown that if the box used in the previous query is balanced, then the box used for the current query will also be balanced. Even for the case where the previous query uses a unbalanced box, in most cases, the entropy measure for the next query increases. It eventually converges (not in an ever increasing sequence) to the maximum value (the entropy of a balanced box). We show this phenomenon in action by using four movement simulations: two along pre-defined paths (denoted by P_1 and P_2) for 1000 queries, one along a random path (denoted by P_3) for 5000 queries and a spiral path (denoted by P_4) originating at the top-left corner of a 320×320 cells map, and moving towards the center. The pre-defined paths are generated such that the user is exposed to varying local distributions of the POIs. The privacy parameter b is set to 32, which implies an obfuscation expectation of roughly $10km^2$. We simulate two different scenarios for the attacker's initial knowledge Φ_0.

Gaussian	a two-dimensional Gaussian distribution centered at the user's actual location.
Precise	probabilities distributed between the user's actual location and a few neighboring cells.

Figure 7.3 summarize the entropy values for the four movement simulations in the context of the Gaussian initial knowledge. The quick convergence[1] to a uniform posterior distribution (entropy saturation) is evident in all three simulations under our assumptions for this scenario. It is also evident that once the entropy attains its highest value, changes do not occur. Figure 7.4 depict similar observations for the case of a precise knowledge attacker.

7.4 General Scenario

In the above section, we assume an attacker having high inference capabilities that can infer the exact interest set and relate that to a single box. But we model that attacker with an assumption of a random walk in terms of user's movement behavior. This is done to introduce the concepts that we will discuss with a more realistic attacker in this section.

7.4.1 Movement model

After the first query, the user starts moving along a path and uses the LPPM to retrieve POIs at time $t > 1$. We assume now that a summary of the user's movement patterns is

[1]Entropy in Figure 7.3 looks like a flat line because only for the few first queries the attacker will get values less than the saturation value.

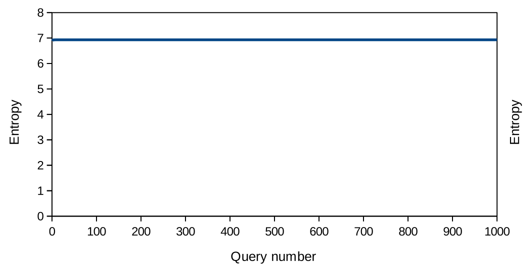

(a) Path P_1.

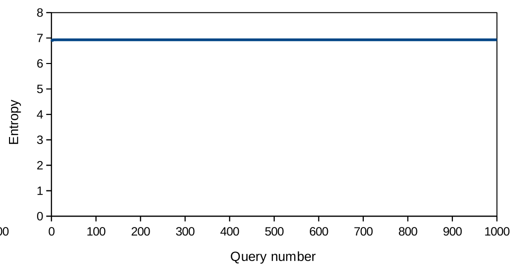

(b) Path P_2.

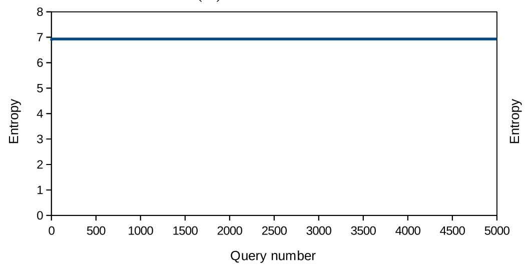

(c) Path P_3.

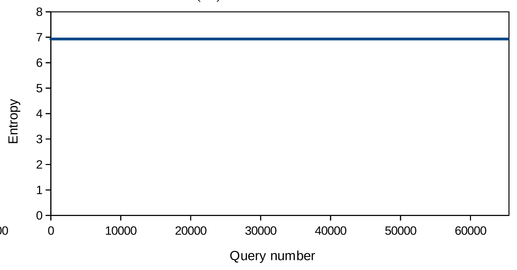

(d) Path P_4.

Figure 7.3: Entropy of the obfuscated area with Gaussian background knowledge for the attacker.

available to the adversary in the form of a *transition matrix*. A transition matrix $\mathcal{T}(A_i, A_j)$ provides the probability of the user moving from one area A_i in $\mathcal{G}$ to another area A_j. For example, the set of cells can be divided into non-overlapping areas of $b \times b$ cells, and the adversary's knowledge of the user transitioning between these areas is encoded in the transition matrix. A transition matrix can be extracted from available traces of a user's movement [141]. We consider the transition probability between individual cells to be directly proportional to the transition probability between the areas to which they belong. If c_i and c_j are two cells in areas A_i and A_j respectively, we compute the cell-wise transition probability matrix as

$$\Pr(c_i \to c_j) = \frac{\Pr(A_i \to A_j)}{b^2 \times b^2} = \frac{\mathcal{T}(A_i, A_j)}{b^4}. \tag{7.6}$$

This computation does assume that all cells in an area are habitable; it is easy to accommodate the case of some cells being inhabitable by modifying the proportionality constant b^4.

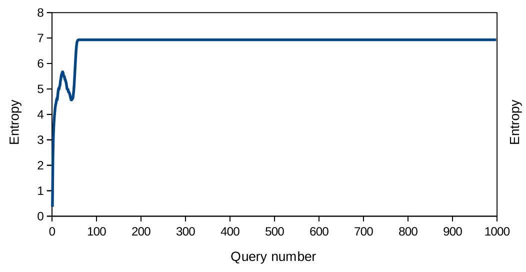

(a) path 1.

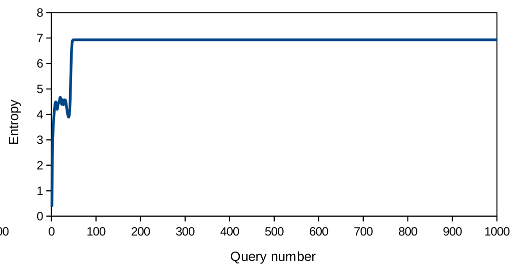

(b) path 2.

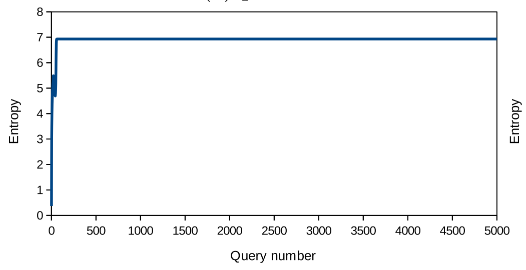

(c) path 3.

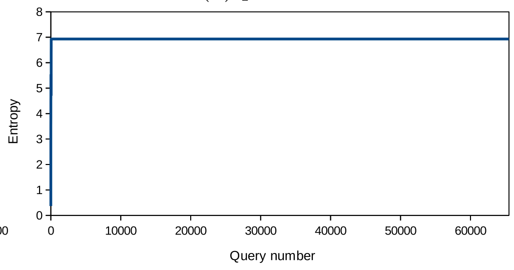

(d) path 4.

Figure 7.4: Entropy of the obfuscated area with precise background knowledge for the attacker.

Let t_{k-1} denote the time step when the user last used the LPPM, and the current time be $t_k = t_{k-1} + Tn$. The LPPM outputs I_k at this time step. Before using this new observation, the adversary refines his location distribution using the known movement model of the user. Starting with the notation $\lambda_0 = \Phi_{k-1}$, the adversary first obtains λ_k by iteratively applying the following expression

$$\lambda_k(c) = \sum_{c' \in C} \left(\lambda_{k-1}(c') \times \Pr(c' \to c)\right). \tag{7.7}$$

This computation updates the adversary's last known distribution with information based only on the movement patterns of the user. This is same as the *forward variable* in a typical forward-backward algorithm. In the absence of any output from the LPPM, $\Phi_k = \lambda_k$. A final update can be performed using the output I_k, similar to as in the first query

$$\Phi_k(c) = \Pr(c|I_k) = \frac{\Pr(I_k|c)\lambda_k(c)}{\sum\limits_{c' \in C} \Pr(I_k|c')\lambda_k(c')}. \tag{7.8}$$

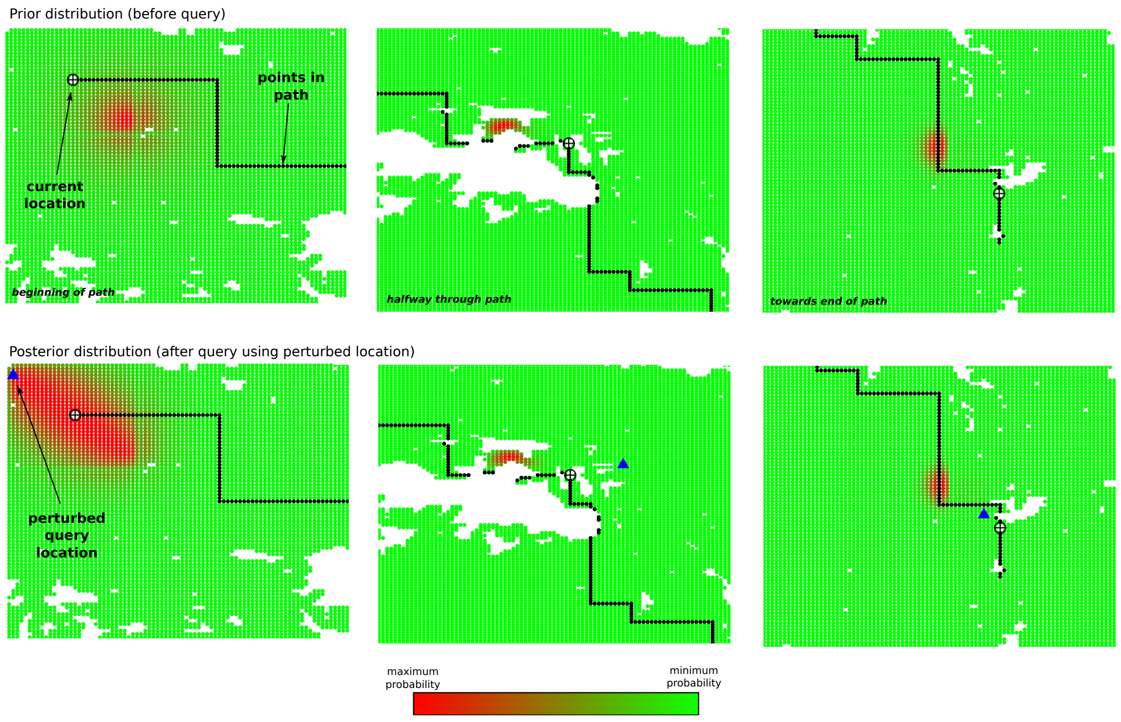

Figure 7.5: Prior and posterior distribution after queries along a path. Darker (red) regions signify higher probability mass.

Figure 7.5 shows snapshots of the inference process of the adversary at different points in time. The user in this case uses an LPPM to generate a perturbed location by adding planar Laplace distributed noise, and makes queries using this location. The figure depicts how the location of the perturbed query point (in addition to knowledge of the perturbation mechanism and the user's transition matrix) helps the adversary refine the prior distribution. As seen in the beginning of the path, the refinement resulted in good approximation of the user's actual location. As the user moves, the distribution becomes more concentrated, and refinements depend on where the perturbed point is generated.

Given all outputs generated by an LPPM along an entire path, the posterior distribution at a time step can be better refined by using knowledge of what output was produced after that point in time (by using a backward variable). We do not perform this refinement in the computation of Φ_k. As such, the accuracy of the adversary's method in estimating intermediate locations of the user (the path) is assumed to be not critical; it is the final destination that we seek to keep private. The presented method aligns with the forward-backward algorithm when executed at the last query point; no observations exist after the last query to compute a backward variable.

7.4.2 Computing $\Pr(I|c)$

Let $I_{retrieve}$ denote the interest set observed by the adversary in the query q_k. Recall that the POIs of interest I_k may only partially be in this set, since some of them may be available in the cache $\mathbf{I}$ of earlier queries. Consider the following two sets.

$$\begin{aligned} \nu_k(c) &= \{B|B \in S_k \text{ and } c \in B\} \\ \eta_k(c) &= \{B|B \in \nu_k(c) \text{ and } I_{retrieve} \subseteq \mathbf{BS}(B) \subseteq \mathbf{I} \cup I_{retrieve}\} \end{aligned} \tag{7.9}$$

$\nu_k(c)$ denotes the set of $b \times b$ boxes in the selection area S_k that contain cell c; $\eta_k(c)$ are boxes in $\nu_k(c)$ such that all newly requested POIs ($I_{retrieve}$) are part of the POIs box set $\mathbf{BS}$ for all boxes $B \in \nu_k$, which itself is fully contained in the union of the cache and the newly requested set. $\Pr(I_{retrieve}|c)$ is then equal to $\frac{|\eta_k(c)|}{|\nu_k(c)|}$.

Computation of $\eta_k(c)$ is straightforward for the adversary once $\nu_k(c)$ is known. However, the adversary does not know S_k since it depends on the previous boxes, B_{k-n}. Nonetheless, the adversary can perform approximations, denoted by $\hat{\nu_k}(c)$ and $\hat{\eta_k}(c)$. As base cases, we have $\hat{\nu_1}(c) = \{B|c \in B\}$ and $\hat{\eta_1}(c) = \{B|c \in B \text{ and } \mathbf{BS}(B) = I_1\}$. To approximate $\hat{\nu_k}(c)$, the adversary can consider the union of all selection areas that can be generated from boxes in $\hat{\eta}_{k-1}(c)$.

$$\begin{aligned} \hat{\nu_k}(c) &= \{B|B' \in \hat{\eta}_{k-1}(c) \text{ and } B \in S' \text{ and } c \in B\} \\ \hat{\eta_k}(c) &= \{B|B \in \hat{\nu_k}(c) \text{ and } I_{retrieve} \subseteq \mathbf{BS}(B) \subseteq \mathbf{I} \cup I_{retrieve}\}, \end{aligned} \tag{7.10}$$

where S' is the selection area generated from the box B'. We use in $\frac{|\hat{\eta_t}(c)|}{|\hat{\nu_t}(c)|}$ as an estimate of $\Pr(I_k|c)$ in Equation 7.8.

7.5 Empirical Evaluation for General Scenario

In this section, we discuss the experiments performed to support the conclusions from several aspects of the proposed algorithm. The first set of experiments compare both privacy and performance of our LPPM against the geo-indistinguishability based LPPM introduced by Andres et al. [6]. The second experiment is performed to show that requesting the details of the additional POIs in incremental fashion will significantly reduce the bandwidth impact. In the third experiment we measure the impact of the box size on the privacy of our LPPM.

Andrés et al. generate perturbed locations for location-based POI search. Geo-indistinguishability provides probabilistic limits on the inferential advantage that an adversary can gain with knowledge of the perturbed location and the perturbation mechanism. Given a user cell c_u and a privacy parameter ϵ, the mechanism adds random noise drawn from a planar Laplace (extension of the Laplace distribution to two dimensions) distribution to the user's location and generates the perturbed location z. Doing so provides the guarantee that

$$\frac{Pr(z|c_1)}{Pr(z|c_2)} \leq e^{\epsilon d(c_1,c_2)}, \tag{7.11}$$

where c_1 and c_2 are any two cells, and d is a distance function. To retrieve POI details, the mechanism then issues a query using z and an A_R around z. All POIs inside the A_R are retrieved from the service provider. Andrés et al. provide confidence bounds on the size of the A_R that also includes a specific area around the actual location of the user called the interest area, denoted by A_I. The user can then choose a POI from the retrieved set depending on how far it is from her location.

7.5.1 Experimental setup

The same experimental setup described in Section 6.5.1 is used here. We further process the grid to identify cells that are not habitable (potentially because of a natural or artificial blockage). We perform this step by collecting the latitude and longitude of the center of each cell, and then using the `snapToRoads` function in Google's Maps Roads API[2] to determine the cells that have a road within 100 meters. This gives us a bitmap signifying if a cell is habitable or not.

Paths and transition matrix

To generate paths along which queries will be made, we consider five regions surrounding Los Angeles–El Segundo, Pasadena, Hollywood, Montebello and the Los Angeles downtown–and use them as sources/destinations that the user mostly travels between. We randomly choose a pair of cells from these five regions as source and destination locations of the user, and then generate a path originating at the source cell and ending at the destination cell. We generate a set of 100 paths using this method. A path is always generated such that it contains habitable cells only.

We encode the 100 paths into multiple transition matrices for use in adversarial inference. Assuming region sizes of 16×16 cells ($2.56km^2$), 32×32 cells ($10.24km^2$), and 64×64 cells ($40.96km^2$), we create three transition matrices. Each transition matrix is obtained by the dividing the 320×320 grid into regions of the corresponding size, and then counting the frequency of transitions happening between regions in the 100 paths. The three different region sizes are used in parametric evaluation of our method. For all other experiments, the 32×32 size is used as the default. A transition matrix is known to the adversary, while the exact paths are unknown. Note that a transition matrix created in this manner implies strong background knowledge since it captures all (and only those) paths on which we will apply an LPPM. It also implies that the adversary's background knowledge is always considered correct, i.e. the user can never be in a region (or cell) where the transition probability is zero.

[2]developers.google.com/maps/documentation/roads/snap

POI retrieval and local cache

We consider that query results must be up-to-date at all points along a path; therefore, the LPPM is invoked at every point along a path. However, we implement the LPPMs with local caching functionality, i.e. results retrieved earlier will not be downloaded again. The geo-indistinguishability approach, as described in the original work, cannot directly make use of the local cache. We assume a modification where the server only returns identifiers of POIs inside A_R; details are then retrieved only for POIs not in the cache. The geo-indistinguishability A_R is also not guaranteed to contain the top-K POIs for the user. For fair comparison, we always set the radius of the A_R to the smallest value such that it contains the user location, as well as all POIs in the top-K set of the user.

7.5.2 Privacy

When multiple queries are performed, the distribution of the POIs along the path has a direct impact on the interest set requested by the user. As such, the nearness and areal privacy metrics (Section 4.8.1) can fluctuate (both increase or decrease) over time. Figure 7.6 depicts the values of these two metrics for one of the paths, with “gas station” as the search keyword, and box length $b = 32$ cells. Since our interest set retrieval mechanism (ISR) issues requests only if the POIs are not in the cache, the number of queries are subsequently lower than the geo-indistinguishability (GI) approach. The GI approach can also makes use of a cache; however, it must issue a query at every time step to determine which POIs in the cache correspond to the result set. When retrievals are made infrequently, the nearness metric can be sustained comparatively higher. More queries enable better approximations for the adversary. It is difficult to make a similar observation on the areal metric from the figure.

In order to understand the overall behavior in multiple paths, we look at the quartiles of the two metrics across all the paths and three POIs with varying density. Figure 7.7 depicts this result. Similar to the observation stated above, nearness in the ISR approach is maintained at a higher level than that in the GI approach. The maximum value of nearness

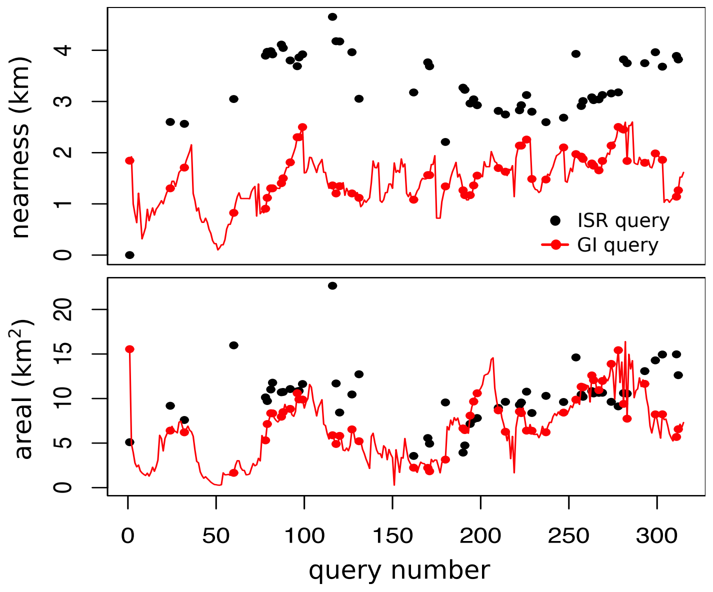

Figure 7.6: Nearness and areal privacy variation along a path. Search keyword = *gas station* and $b = 32$ cells.

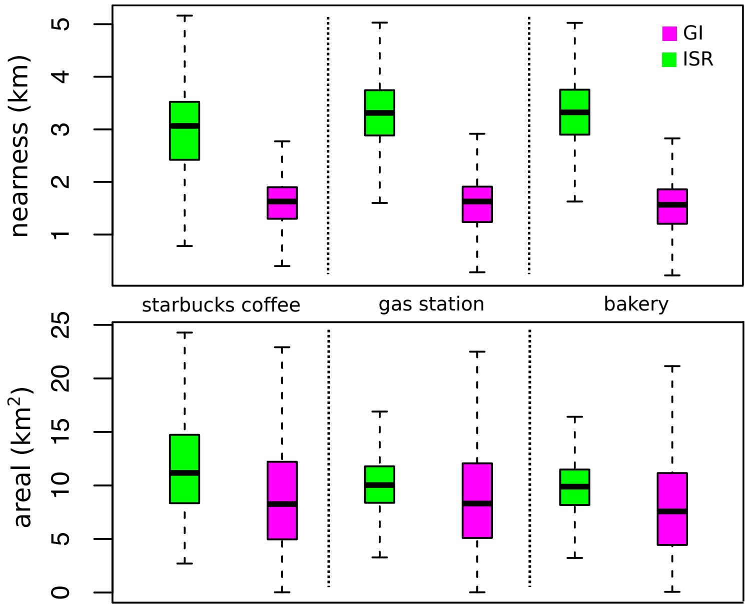

Figure 7.7: Nearness and areal privacy quartiles. $b = 32$ cells.

in the lower quartile (25%) of the ISR data is indeed higher than the upper quartile (75%) of the GI data. The interquartile ranges show no overlap, demonstrating strong evidence that the median nearness value in the two approaches are significantly different.

For areal privacy, we observe that ISR has a higher median value in the three POI types; although, there is no evidence of significant differences. We do observe that for medium and high density POIs ("gas station" and "bakery" respectively), the ISR approach maintains comparatively lower variance in the areal privacy than the GI approach. This is indicative of a stable approach, irrespective of the path taken by the user during the queries. For most parts (upper 75%), the metric is also higher ($\geq 8km^2$) than the theoretical minimum ($5.1km^2$).

We can assess how much information a privacy mechanism has revealed by also focussing strictly on the final destination of a path. Destinations of travel can be argued to be more private than the exact path taken by the user to the destination. Therefore, it is important to analyze what is the state of the adversary's inference when the user has reached the end of a path. Figure 7.8 shows the empirical cumulative distribution function (CDF) of the distance between the last cell of a path and the cell with the highest probability in the adversary's final inferred distribution, i.e. the nearness value. The CDF is generated by collating observations in all the 100 paths and the three POI keywords. Comparatively, about 10% of the cases in the ISR approach has a final nearness value as low ($\approx 1.8km$) as the GI approach; in general, the values are always better. The adversary's inferred location in the ISR approach is significantly distant ($> 5km$) in about 30% of the cases, and more than $2km$ in 95% of the cases.

7.5.3 Bandwidth impact

The interest set retrieval mechanism aims to exploit the fact that top-K sets do not frequently (and significantly) change for nearby query points. We exemplified this in Figure 7.6, which shows gaps between query points. Further, since the approach only retrieves details on pertinent objects, i.e. objects that are part of a top-K set along the path, we

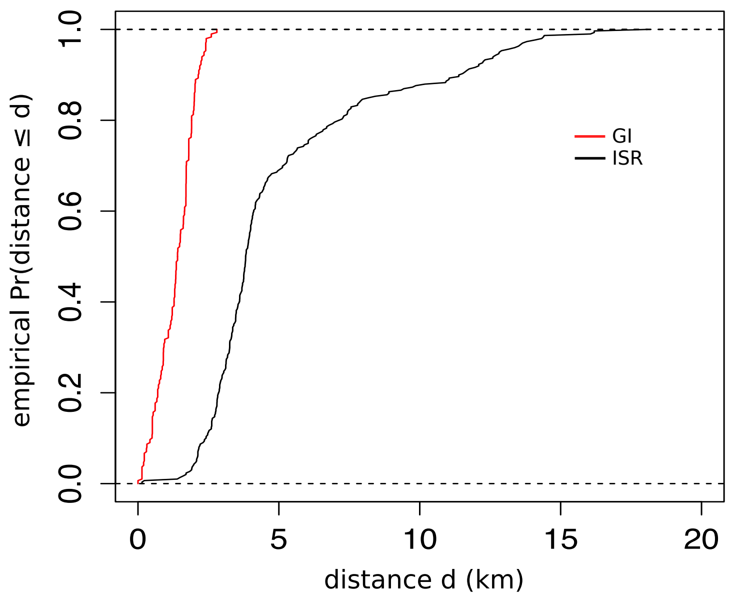

Figure 7.8: Empirical CDF of distance between last cell in a path and the most probable cell in the inferred distribution. $b = 32$ cells.

also expect that download bandwidth is preserved. Figure 7.9 shows the quartiles for the total number of POIs for which details are retrieved by the ISR and GI approaches. The figure also shows the maximum number of POIs inside the large geographical area for each of the three keywords. It can be seen that the GI approach could potentially result in the download of details for all the POIs as a result of using an A_R. To contrast this, the ISR approach downloads details on a median of 12%–30% of the POIs. Although the ISR approach uses a union of various top-K sets to generate the box set, it does not result in too many redundant downloads.

Figure 7.10 displays the frequency distribution of the cardinality of the interest set across all queries (three search keywords and all paths). A total of 264,627 data points are used to generate this distribution. Recall that the interest set is the set for which details are retrieved from the server at a query point. It is empty if the required details are already in the cache (retrieved earlier). We observe that in approximately 90% of the query points, no communication was necessary with the server (empty interest set). This confirms our statement that top-K sets seldom undergo changes between query points. Further, the distribution is heavy tailed, with the frequency dropping significantly as size increases. In

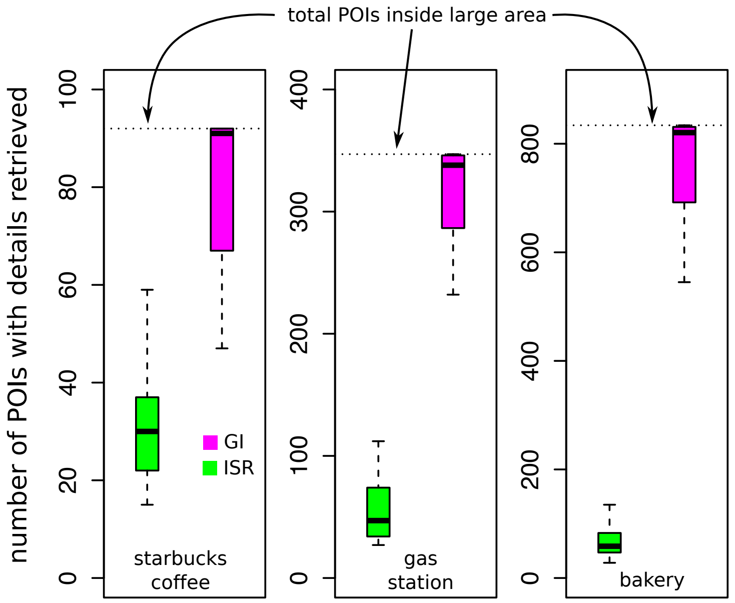

Figure 7.9: Total number of POIs for which details are retrieved during queries along the paths. $b = 32$ cells.

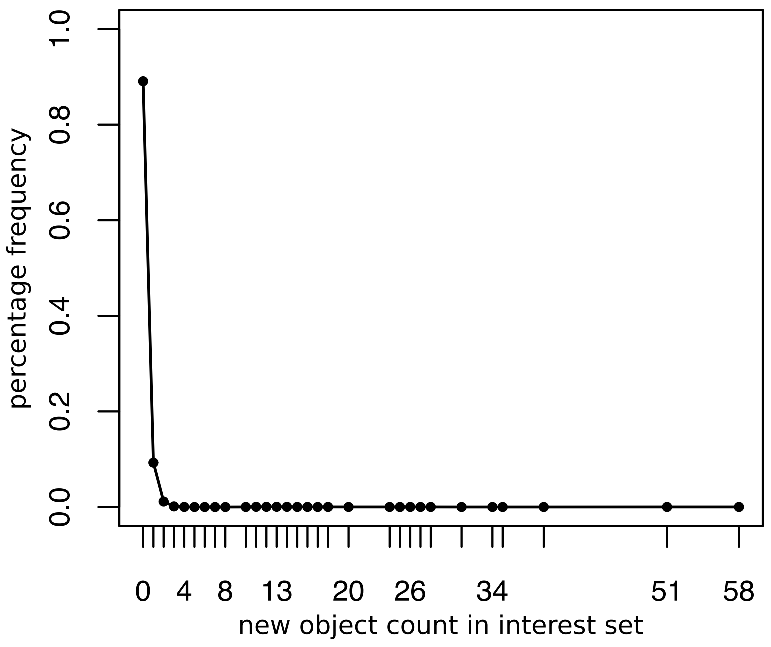

Figure 7.10: Frequency distribution of interest set (POIs for which details are retrieved) sizes. Total potential queries = 264,627.

other words, smaller interest sets are abundant. This is evident of the fact that whenever top-K sets change between successive query points, the changes are often very small (one or two POIs). The top-K set landscape in local search is recurrently plateaued and is slow rising; to the best of our knowledge, this characteristic is rarely exploited by a privacy mechanism.

7.5.4 Impact of box size

Figure 7.11 depicts the nearness and areal privacy for three different choices of the parameter b. Recall that smaller box sizes imply lower expectations of privacy. The trends we observed in the case of 32×32 box size is repeated for other box sizes too, albeit at varying degrees. For example, using a smaller box size leads to lower privacy values, and they increase as larger box sizes are used. A larger box size does imply a larger box set, and can lead to the retrieval of more number of POI details.

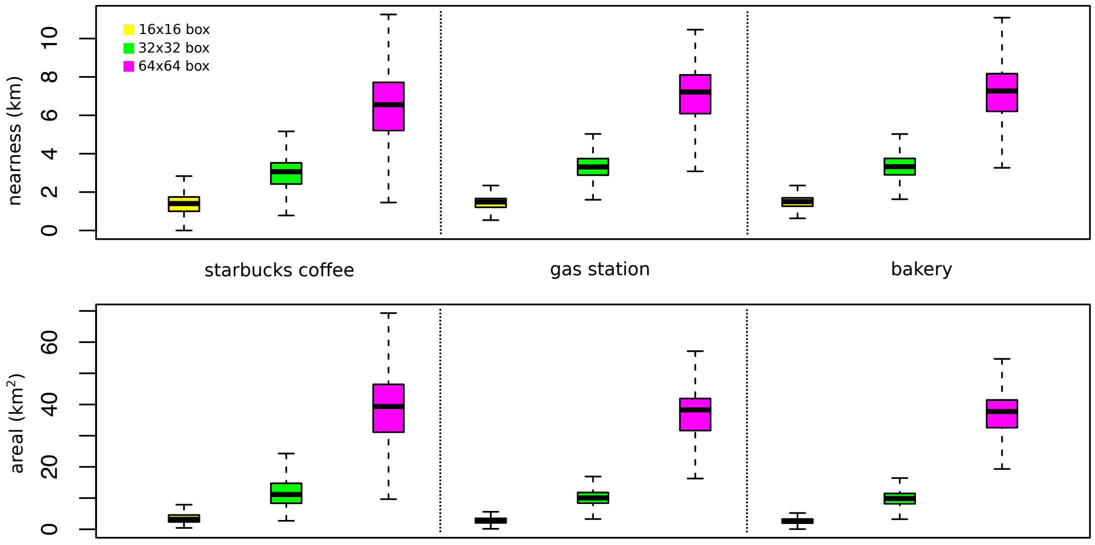

Figure 7.11: Nearness and areal privacy quartiles for different box size b and search keywords.

7.6 Summary

In the previous chapter and this chapter, we have presented two LPPMs that address the single and multiple query scenarios respectively. As discussed in Chapter 4, both LPPMs are proposed within a two round-trip communication architecture. The focus of both chapters has been to propose algorithms that are TTP free, but are practical enough for a mobile device. Much of the client-server programming interfaces necessary to implement the proposed method are readily available today. The interfaces available in the Google Places API can be adopted to implement the protocol. The Google Places API Radar Search Service[3] allows an application developer to search and retrieve information for up to 200 places at once, but with less detail than is typically returned in other forms of search. A request is made using a HTTP URL, and can include the query keyword, a location, and a radius. For the method proposed in this work, the location used may be a popular landmark, or simply the center of a randomly generated large box that includes the user. The maximum allowed radius is $50km$. The result of the request is returned either as a JSON object or an XML document, which includes the matching POIs' *geometry* (latitude and longitude), *place_id* (a unique identifier of the POI) and *rating*, among other metadata. Although the developer can use the place rating as a prominence value, the exact value used by Google is not yet contained in this result. Details of POIs in the interest set can be obtained using a Place Details[4] request. Such a request returns detailed information about a place identified using a *place_id*. The returned JSON object or XML document includes data such as the address of the POI, current events happening there, phone number, opening hours, photos, price level of services offered, user reviews, the POI's rating, and the website of the business, among other things. The availability of programming interfaces such as these makes the proposed privacy preserving POI search architecture feasible in the current market.

We show how both the LPPMs perform well in differing attacker's background knowledge situations. We have shown these LPPMs to be reasonable in terms of performance

[3]developers.google.com/places/web-service/search

[4]developers.google.com/places/web-service/details

using simulation and proved their efficacy using empirical data. We feel the need to extend these concepts such that the privacy offered can be measured more using statistical tools. In the next chapter we address this while maintaining the same communication architecture.

Chapter 8

Differential Privacy Based Solution

Our proposals in chapters 6 and 7 for location privacy centered around the cloaking of the user's location. However, this model failed to provide a formal guarantee on what an adversary can learn by observing the communication between a location privacy preserving mechanism (LPPM) and the application server. More recent proposals such as geo-indistinguishability by Andres et al. [6] address this issue by bounding the degree to which an adversary can distinguish between two locations. A persistent assumption in these proposals (more than a decade worth of research) is that location-based queries (or geo-queries) produce results that are dictated only by the distance of a result object from the query location. However, clearly verifiable in any popular location-based application, geo-query results are ranked based on multiple criteria, distance being just one of them (Section 4.1).

Extending location privacy models to bridge this long present gap is therefore important, and forms the main goal for this chapter. We provide analytical results that characterize the privacy and the quality of service assurances of our extended model. We provide conclusive evidence to support our claims by applying the approach to a nearby POI search in a real-world database. In addition, we develop a prototype Android application to demonstrate how existing third party APIs can be utilized to execute the various steps in the approach, and assess its efficiency and accuracy on a mobile device. The work in this chapter is based on our outcome in [59].

For most part in this chapter, the empirical evaluation is performed using the same experimental settings described in Section 6.5.1. Parametric evaluation is shown on three POI keywords, namely *bookstore, gas station,* and *cafe.* There are 155 bookstores, 347 gas stations and 608 cafes inside the evaluation area, thereby giving us three scenarios corresponding to low, medium, and high occupancy POIs. As before (Section 6.5.1), we assigned values to the POIs from $\{0.95, 0.90, ..., 0.2, 0.25\}$ using a Zipf distribution with exponent 0.8. To further validate our claims, we implement an Android application that can use the on-board GPS device, or a simulated GPS that can provide any desired latitude and longitude to the application. Using this application, we perform experiments covering five different cities (Los Angeles, New York, Paris, Vienna and Beijing), and 15 different keywords chosen from the place types list in the Google Places API. More details on the experiments are provided in their respective sections.

8.1 Architecture

A typical location privacy preserving mechanism (LPPM) for geo-queries may generate an obfuscated location for a query and then retrieve a set of POIs contained within an area centered at the obfuscated location. Execution of these steps is supported, for example, in the `nearbysearch` and `details` endpoints in the Google Places API. The retrieved set is then filtered for the user's actual location and presented to the user. We refer to this architecture as a 1-roundtrip architecture. LLPMs can differ in terms of their privacy guarantees depending on how the obfuscated location is generated. They also differ in terms of their communication overhead depending on the size of the area of retrieval. The local filtering of results can be done strictly on the basis of distance (keep only POIs that are within a certain distance of the user), or on a combination of distance and the prominence value. Note that the former method has received the most attention in the privacy research community, while the latter method is what is deployed in most non-private local search applications. For example, a search for "cafe" in a popular platform such as Google does not always return the nearest cafes, but the top cafes determined by the query location and the prominence value. Therefore, a geo-query search is more accurately a top-K search.

Any LPPM designed along the lines of the above discussion can provide top-K results by modifying the filtering mechanism. Therefore, we do not consider the filtering process to be a significant downside of an LPPM. However, the architecture levies a high communication overhead owing to the retrieval of all POIs in a large area. The data pertaining to a complete POI typically contains details such as name, address, contact numbers, ratings, photos, and multiple reviews. Since most POIs will be filtered out, the bandwidth consumed while retrieving all such details for the POIs inside the area of retrieval is wasted. We therefore consider our 2-roundtrip querying architecture described in Chapter 4 which significantly reduces this communication overhead and allows for the ranking of POIs based on an arbitrary function based on location and prominence.

Recall that in the 2-roundtrip architecture, an LPPM retrieves minimal details about the set of POIs within A_R. It is sufficient to obtain the location and prominence of a POI in this step. Search providers do provide results with such minimal information, for example, a `radarsearch` query in the Google Places API returns the names and locations of POIs within a specified distance of the given location. Prominence values are not yet included in these results, but as shown in Section 4.6, they can be communicated without revealing the underlying computation function. A filtering process is next applied on the POIs and a relevant subset is determined. All details for this subset of POIs are then retrieved from the provider and presented to the user.

8.2 Enforcing Indistinguishability

Consider an LPPM that generates some output set o of POIs and shares it with the service provider as part of the querying process. This output in turn can be used by an adversary to infer potential locations for the user. Under the assumption that the LPPM under use is known to the adversary, along with knowledge of underlying parameters (except the user's location), this inference can be expressed in terms of an odds-ratio with respect to any two locations c and c' , given as

$$\frac{\Pr(c|o)}{\Pr(c'|o)} = \frac{\Pr(o|c)\,\Phi(c)}{\Pr(o|c')\,\Phi(c')}, \tag{8.1}$$

where Φ represents the prior knowledge of the adversary, expressed as a probability distribution over the set of possible locations $\mathcal{C}$. If an LPPM generates o independent of the location, i.e. $\frac{\Pr(o|c)}{\Pr(o|c')} = 1$, we can say that $\Pr(c|o) \propto \Phi(c)$ (convergence), implying that the LPPM did not reveal any information of significance to the adversary. We can then say that any two locations are indistinguishable based on the output of the LPPM. Since the prior knowledge of the adversary can vary, and is outside the control of the LPPM, it is often the output probabilities ($\Pr(c|o)$) that are subjected to analysis. The objective is to maintain a degree of indistinguishability between two locations, i.e. the odds-ratio should remain as close as possible to the ratio of the prior probabilities.

8.2.1 Geo-indistinguishability

The principle of geo-indistinguishability provides a quantifiable degree to which the odds-ratio can deviate from the ratio of the prior probabilities [6]. Consider a 1-roundtrip LPPM that generates an obfuscated location c_z from a discrete set of locations, and then retrieves all POIs within a distance rad_R of c_z.

Definition 8.1 (ϵ-geo-indistinguishability)**.** An LPPM is ϵ-geo-indistinguishable if, for any output c_z produced by the LPPM, and any two locations $c, c' \in C \subseteq \mathcal{C}$ with $d(c, c') \leq r$, we can have

$$\frac{\Pr(c_z|c)}{\Pr(c_z|c')} \leq e^{\epsilon r},$$

where d is a distance function.[1]

For an intuitive understanding, assume that the LPPM is used to query for a user located in Los Angeles downtown. Geo-indistinguishability then ensures that an adversary

[1]Division by zero in $\frac{a}{b} \leq c$ can be resolved by writing the expression as $a \leq bc$.

will be unable to distinguish with high certainty the user's location from other locations in the downtown area; although, the odds-ratio will enable the adversary distinguish between a location in the downtown area versus a location in one of the suburbs (farther away from the user's location). The odds-ratio is always within a factor of $\exp\{\epsilon d(c, c')\}$ of the ratio of prior probabilities. Therefore, the inferential advantage due to the use of the LPPM decreases as the adversary attempts to narrow down the user's location to smaller and smaller areas. Andres et al. proposed this principle for LPPMs along with a mechanism that achieves it. Their mechanism generates c_z using a planar Laplace distribution centered at the user's location. They also discuss how rad_R can be determined such that it contains all POIs within a distance rad_I from the user's actual location.

8.2.2 Indistinguishability for top-K results

We first introduce the notion of a zone. A zone for a given location tells us what other locations generate similar top-K results. We use $top_K(.)$ to denote a function that returns the top-K POIs for a given location.

Definition 8.2 (Zone)**.** For a given location c_0 and $0 \leq m \leq K$, a zone $\mathcal{Z}_m$ is defined as

$$\mathcal{Z}_m(c_0) = \{c | c \in \mathcal{C}, |top_K(c_0) \cap top_K(c)| = K - m\}.$$

Therefore, zone $\mathcal{Z}_m$ contains all locations with exactly m mismatches in the top-K set, relative to the given location c_0.

Figure 8.1 depicts an area of Los Angeles, overlaid with a set of zones. Assume that the user is located in the central zone $\mathcal{Z}_0$. For any pair of locations in $\mathcal{Z}_0$, the top-10 cafe sets are the same (zero mismatch). When expanding into zone $\mathcal{Z}_1$, the top-10 set undergoes a change in one of the POIs (one mismatch). Therefore, for any location $c \in \mathcal{Z}_1$ and $c' \in \mathcal{Z}_0$, we have $|top_{10}(c) \cap top_{10}(c')| = 9$. Similarly, the number of mismatch increases as we move father out from $\mathcal{Z}_0$.

An ϵ-geo-indistinguishable LPPM introduces probabilistic uncertainty based on the distance between two locations. As such, the adversary will gain some inferential advantage

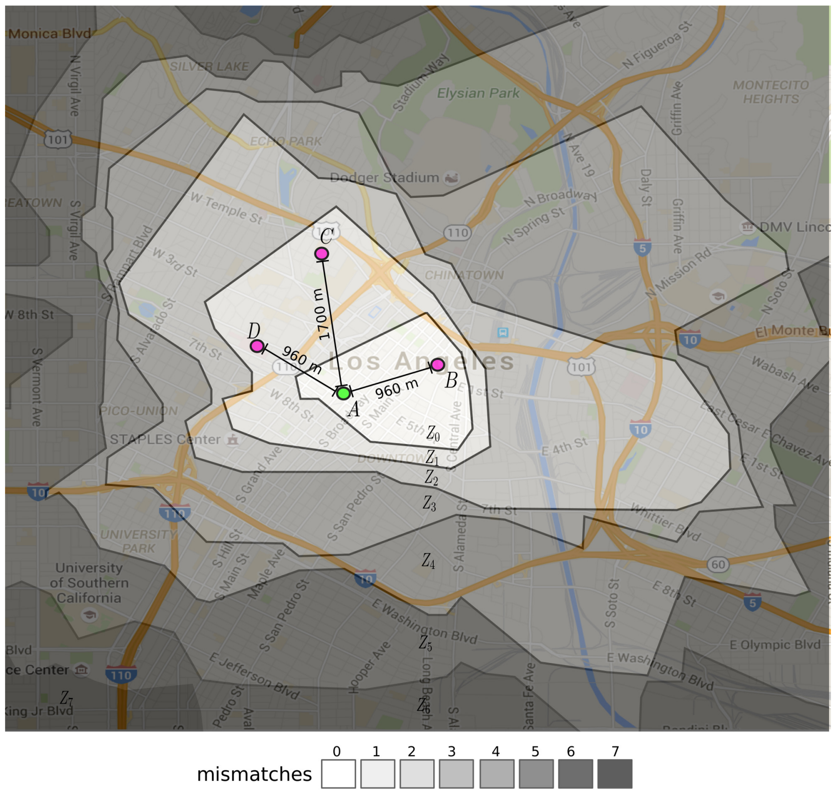

Figure 8.1: Variation in the top-10 cafe set in Los Angeles. Ranking performed with $\alpha = 0.8$.

when distinguishing between the point pairs (A, B) or (C, D) in Figure 8.1. With $\epsilon = \frac{\ln 4}{2000m}$, the prior probability ratio will at most change by a factor of 1.94531 for A and B (or D), and by 3.24901 between A and C. However, from the standpoint of querying from zone $\mathcal{Z}_0$, locations A and B are equivalent since they produce the same result set; similarly C and D are equivalent under the relation of mismatch count. This brings us to the question of whether geo-indistinguishability can be extended to arbitrary functions (instead of only distance) of locations, and if so, under what constraints. More specifically, in the context of ranked geo-queries, we would like an LPPM that provides indistinguishability between two locations based on the similarity of query output from the two locations. In this direction, we extend ϵ-geo-indistinguishability as follows.

Definition 8.3 ((f, ϵ)-geo-indistinguishability)**.** Let $\mathcal{C}$ be a set of locations and O be the discrete set of outputs produced by an LPPM $\mathscr{M}$. Given a function f such that $f : \mathcal{C} \times \mathcal{C} \to [0, 1]$ and a privacy parameter $\epsilon \geq 0$, the mechanism $\mathscr{M}$ is (f, ϵ)-geo-indistinguishability if

$\forall C \subseteq \mathcal{C}$ and $\forall o \in O$, we have

$$\frac{\Pr(o|c)}{\Pr(o|c')} \leq e^{\epsilon\delta},$$

where $f(c \in C, c' \in C) \leq \delta$.

In other words, for any subset of locations where pairwise relations (as measured by the f function) are bounded by some δ, the degree of indistinguishability is also bounded by a function of δ. The principle can also be extended to any subset of O if $\mathscr{M}$ has a continuous range. Since the condition applies to any conceivable subset of locations, we can say that if $f(c, c') = \delta$ for any $c, c' \in C \subseteq \mathcal{C}$, then

$$e^{-\epsilon\delta}\frac{\Phi(c)}{\Phi(c')} \leq \frac{\Pr(c|o)}{\Pr(c'|o)} \leq e^{\epsilon\delta}\frac{\Phi(c)}{\Phi(c')}. \tag{8.2}$$

For example, if f measures the fraction of mismatches, then all locations in $\mathscr{Z}_0$ (Figure 8.1) form a subset where $\delta = 0$. This gives us perfect indistinguishability for locations in $\mathscr{Z}_0$, i.e. $Pr(c|o) \propto \Phi(c)$, $\forall c \in \mathscr{Z}_0$. The boundaries of the zones depicted in Figure 8.1 can expand or shrink depending on the density of the POIs in the area and how ranking is performed. If large central zones do exist for the user, it presents us with an opportunity to provide strong privacy guarantees.

The next question is whether a (f, ϵ)-geo-indistinguishable mechanism exists. Indeed, the general differential privacy mechanism suggested by McSherry and Talwar holds the evidence that a (f, ϵ)-geo-indistinguishable mechanism is possible [114]. This mechanism is driven by a quality function that can associate a real valued score to any $(o \in O, c \in \mathcal{C})$ pair, with higher scores being more desirable.

Theorem 8.1. *Let s be a quality scoring function $s : O \times \mathcal{C} \to \mathbb{R}^+$. Given $c \in \mathcal{C}$ and $\epsilon \geq 0$, the general mechanism $\mathscr{M}_g$ chooses output o with probability* $\Pr(o|c) \propto \exp\{\frac{\epsilon}{2}s(o, c)\}$. *The general mechanism $\mathscr{M}_g$ is $(f, \epsilon\mu)$-geo-indistinguishable, if $\forall C \subseteq \mathcal{C}$, we have*

$$\max_{o' \in O; c,c' \in C} \left(s(o',c) - s(o',c')\right) = \mu\delta,$$

where $\delta = \max_{c,c' \in C} f(c,c')$ *and* μ *is a constant.*

Proof. For some output $o \in O$, and any $c, c' \in C \subseteq \mathcal{C}$ such that $\max_{c,c' \in C} f(c,c') = \delta$ and $\max_{o' \in O; c,c' \in C} = (s(o',c) - s(o',c')) = \mu\delta$, we have

$$\frac{\Pr(o|c)}{\Pr(o|c')} = \exp\left[\frac{\epsilon}{2}\left(s(o,c) - s(o,c')\right)\right] \frac{\sum_{o' \in O} \exp\left[\frac{\epsilon}{2} s(o',c')\right]}{\sum_{o' \in O} \exp\left[\frac{\epsilon}{2} s(o',c)\right]} \leq \exp\left[\frac{\epsilon}{2}\mu\delta\right] \exp\left[\frac{\epsilon}{2}\mu\delta\right] = e^{\epsilon\mu\delta}.$$

□

The general mechanism requires that, in all subsets of locations, the sensitivity of the quality function (maximum difference in scores) is always within a constant factor of the maximum value of the f function in the subset. Therefore, as more and more locations are considered, the sensitivity of the quality function must grow at a rate proportional to the change effectuated in the maximum f value. The proportionality constant μ is important here since it dictates the inferential advantage controlled by the mechanism. Next, we instantiate this mechanism in the context of the 2-roundtrip querying architecture.

8.3 Applying 2-Roundtrip Querying Architecture

The application we consider for a 2-roundtrip querying architecture first retrieves location and prominence data on a set of POIs, computes the top-K sets of a specific set of locations, and then retrieves details on K POIs. More specifically, the application first chooses a location c_z uniformly at random from within a radius rad_z from the user's location c_u. The area created by using this radius is the obfuscation area and denoted by A_Z. Then, the application, retrieves the location and prominence of all POIs matching the search keyword that are within a distance rad_R of c_z(POIs included inside A_R). Thereafter, the top-K set of every location (cell) within a radius of rad_I from c_z is determined. One of these sets is chosen using a (f,ϵ)-geo-indistinguishable mechanism and details are retrieved for POIs in the set. Before discussing the mechanism, we provide some insight into the choice of the various radius values in the application.

8.3.1 rad_z, rad_R and rad_I

A typical `nearbysearch` using the Google Places API requires specification of a similar radius. Consequently, A_R must fully encompass A_Z. This can be achieved by setting $rad_R \geq 2 \cdot rad_z$. A typical `radarsearch` using the Google Places API allows for this value to be up to 50 km. Top-K sets are computed for every location (cell) in A_I, and a choice is made from within these sets. We want the top-K set of the user to be a part of this sampling; since c_z is always within a distance of rad_z from c_u, inclusion of the user's top-K set can be guaranteed by setting $rad_I \geq rad_z$. We do not assume that the three radii values are unknown to the adversary. Therefore, the choice of rad_I reveals a first level approximation of the area of presence of the user. We choose rad_z to control this approximation, and subsequently set $rad_I = rad_z$. Service providers can limit the number of POIs returned from within the area of retrieval (`radarsearch` puts a limit of 200); therefore, we choose rad_R to the minimum value necessary, i.e. $2 \cdot rad_z$. This approach leaves us with making one parametric choice, rad_z , with the other two decided as $rad_R = 2 \cdot rad_z$ and $rad_I = rad_z$.

8.3.2 Choosing a top-K set

We use the computation process discussed in Chapter 6 to determine the top-K sets of all locations in A_I . Let $\mathcal{T} = \{t_1, t_2, \cdots, t_m\}$ represent the collection of these top-K POI sets corresponding to the cells $c_1, c_2, \cdots, c_m \in A_I$, i.e. $top_K(c_i) = t_i$. We consider the following instantiation of the general mechanism $\mathscr{M}_g$.

Definition 8.4 (Mechanism $\mathscr{M}_{fgi}$)**.** Let the quality scoring function $s : \mathcal{T} \times A_I \rightarrow \mathbb{R}^+$ be the fraction of matches between a set $t \in \mathcal{T}$ and the top-K set of location $c \in A_I$, i.e.

$$s(t, c) = \frac{|t \cap top_K(c)|}{K}.$$

Given the user location c_u, mechanism $\mathscr{M}_{fgi}$ outputs a set $t \in \mathcal{T}$ with probability $\Pr(t|c_u) \propto e^{\frac{\epsilon}{2}s(t,c_u)}$.

Details are subsequently retrieved for the POIs included in the output produced by $\mathscr{M}_{fgi}$.

Theorem 8.2. *Mechanism $\mathscr{M}_{fgi}$ is (f, ϵ)-geo-indistinguishable for locations in when*

$$f(c, c') = 1 - \frac{|top_K(c) \cap top_K(c')|}{K}.$$

Proof. The f function here is the fraction of mismatches in the top-K sets of two locations c and c'. If $\max_{c,c' \in C \subseteq \mathcal{C}} f(c, c') = \delta$, i.e. $f(c, c') \leq \delta$, then $|top_K(c) \cap top_K(c')| \geq K(1 - \delta)$.

Consider $|top_K(c) \cap top_K(c')| = K(1 - \delta)$. Therefore, the two top-K sets differ in $K\delta$ elements. The maximum difference in quality is provided by the set t which has the least overlap with one of the sets, and the most overlap with the other while satisfying the condition. If t overlaps in $K\delta + b$ elements in one set, then at least b elements of t will also appear in the other set. Therefore, the maximum difference in quality scores in this case will be $\frac{K\delta+b}{K} - \frac{b}{K} = \delta$.

For cases where $|top_K(c) \cap top_K(c')| > K(1 - \delta)$, the sets will differ in less than $K\delta$ elements; so the maximum difference in quality scores will be less than δ.

Combining both cases, when $|top_K(c) \cap top_K(c')| \geq K(1 - \delta)$, the maximum difference in quality scores will be δ.

$$\max_{o \in O; c,c' \in C \subseteq \mathcal{C} \text{ such that } f(c,c') \leq \delta} \left(s(o, c) - s(o, c')\right) = \delta.$$

Here the constant $\mu = 1$. Therefore, by Theorem 8.1, the mechanism is (f, ϵ)-geo-indistingui-shable. □

(f, ϵ)-geo-indistinguishability implies that, for all pairs of locations in A_I whose top-K sets have at most a fraction of δ mismatch, the probabilities of producing a certain output from either location in the pair will differ at most by a factor of $e^{\epsilon\delta}$ and at least by a factor of $e^{-\epsilon\delta}$ of each other. For location pairs where there are no mismatches ($\delta = 0$), the probabilities will be equal. For location pairs with complete mismatch ($\delta = 1$), the probability ratio is between e^{ϵ} and $e^{-\epsilon}$. This captures the guarantee that any location c (including the user location c_u) will be indistinguishable in zone $\mathcal{Z}_0$ (defined corresponding to $top_K(c)$), and difficult to distinguish from locations in nearby zones. The best case happens when the entire A_I is covered in a single zone, a possibility that can emerge when POIs are sparse, and their ranking involves both distance and prominence.

8.3.3 Characterization

Mechanism M_{fgi} makes locations in zone $\mathcal{Z}_0$ indistinguishable from each other; however, the degree of indistinguishability reduces with respect to locations in other zones. Therefore, we seek to understand how indistinguishability degrades compared to a conventional ϵ-geo-indistinguishable mechanism. The degradation depends on the rate at which the zones change, which for a characteristic set of locations, creates favorable conditions.

Theorem 8.3. *Let o be the output of an ϵ_{gi}-geo-indistinguishable mechanism and $\tilde{o}$ be the output of an (f, ϵ_{fgi})-geo-indistinguishable mechanism when the input (user) location is c_0. Let $C_m = \{c | c \in \mathcal{C}, d(c_0, c) \geq {}^{\epsilon_{fgi} m}/_{\epsilon_{gi} K}\}$ with d as the Euclidean distance function. If $\mathcal{Z}_m(c_0) \subseteq C_m$ for all $m \in \{0, 1, \cdots, K\}$, then $\forall c \in \mathcal{C}$*

$$\frac{\Pr(c|\tilde{o})}{\Pr(c_0|\tilde{o})} \leq \frac{\Pr(c|o)}{\Pr(c_0|o)}.$$

Proof. Figure 8.2 illustrates the relationship between $\mathcal{Z}_m(c_0)$ and C_m. For all $c \in \mathcal{Z} \subseteq \mathcal{Z}_m(c_0) \subseteq C_m$, we have $f(c, c_0) = \frac{m}{K}$. Therefore,

$$\begin{aligned} \max_{c \in \mathcal{Z}} \tfrac{\Pr(\tilde{o}|c)}{\Pr(\tilde{o}|c_0)} &= e^{\epsilon_{fgi} m/K} \\ &\leq e^{\epsilon_{gi} d(c_0, c)}, \forall c \in \mathcal{Z} \quad [\text{since}\, c \in C_m] \\ &\leq \max_{c \in \mathcal{Z}} \tfrac{\Pr(o|c)}{\Pr(o|c_0)}. \end{aligned}$$

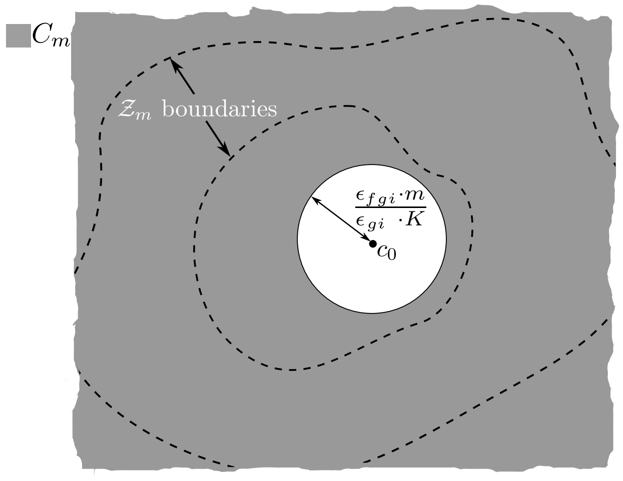

C_m
$\mathcal{Z}_m$ boundaries
$\frac{\epsilon_{fgi} \cdot m}{\epsilon_{gi} \cdot K}$
c_0

Figure 8.2: $\mathcal{Z}_m(c_0)$ and C_m with $\mathcal{Z}_m(c_0) \subset C_m$.

Considering $\mathcal{Z}$ as singleton sets ($\mathcal{Z} = \{c\}$), we obtain $\forall c \in \mathcal{Z}_m(c_0)$

$$\frac{\Pr(\tilde{o}|c)}{\Pr(\tilde{o}|c_0)} \leq \frac{\Pr(o|c)}{\Pr(o|c_0)}.$$

Using the fact that $\mathcal{C} = \bigcup_{m=0}^{K} \mathcal{Z}_m(c_0)$, we have from Equation 8.1, $\forall c \in \mathcal{C}$

$$\frac{\Pr(c|\tilde{o})}{\Pr(c_0|\tilde{o})} \leq \frac{\Pr(c|o)}{\Pr(c_0|o)}.$$

$\square$

The above theorem characterizes when a (f, ϵ)-geo-indistinguishable mechanism is not worse than a conventional geo-indistinguishable mechanism in terms of the discriminatory advantage (the odds-ratio) introduced by the mechanisms. In conventional geo-indistinguishability, relative to any fixed location c_0, indistinguishability as measured by the output probability ratio diminishes continuously with increasing distance from c_0; whereas the changes generate a monotonic step function in $\mathscr{M}_{fgi}$. Theorem 8.3 implies that the step function $\frac{\epsilon_{fgi}}{\epsilon_{gi}} f(c_0, .)$ should preferably grow slower than the distance function $d(c_0, .)$. Therefore, any zone $\mathcal{Z}_m$ should start at a distance of $\frac{\epsilon_{fgi} m}{\epsilon_{gi} K}$ or more from c_0. Figure 8.3 shows this minimum distance in three different scenarios. Each scenario captures the case

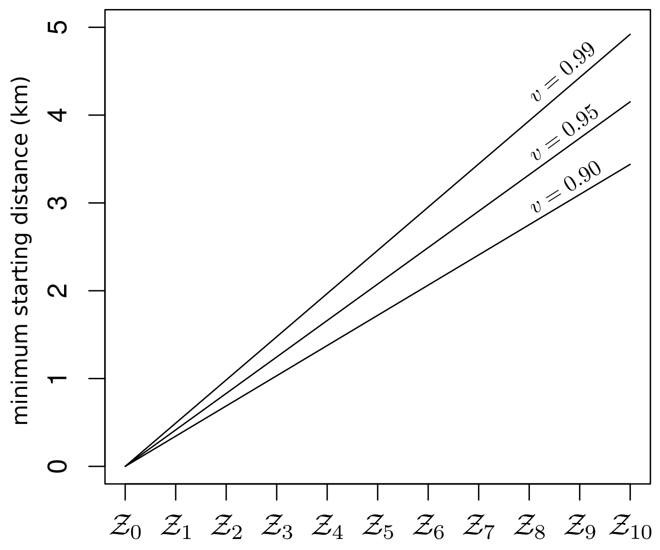

Figure 8.3: Desired minimum starting distance of a zone relative to a location.

when the ϵ values are chosen such that a given level of confidence (v) is always present in the service quality. The parameter ϵ in geo-indistinguishability is chosen so that the area of retrieval contains the obfuscation area ($rad_z = 1km$) with confidence v [6]–the three corresponding ϵ_{gi} values are $\epsilon_{0.99} = 0.00664$, $\epsilon_{0.95} = 0.00474$, and $\epsilon_{0.90} = 0.00389$. Correspondingly, the parameter in (f, ϵ)-geo-indistinguishability is obtained such that at most 8 mismatches can happen with probability v–the three corresponding ϵ_{fgi} values are $\epsilon_{0.99} = 32.67$, $\epsilon_{0.95} = 19.68$, and $\epsilon_{0.90} = 13.38$. We discuss the methodology for this in Section 8.4.3. At a confidence level of 95%, zones are required to have a span of at least 415.19 m, which changes to 492.02 m at 99%. When a zone is wider than this minimum necessary size, it allows subsequent zones to be narrower by an equal amount. Since not all locations in $\mathcal{Z}_0$ are always the required distance away from the closest border of $\mathcal{Z}_0$, it is clear that the inequality does not hold for all query locations c_0. Nonetheless, the inequality may still hold farther out if subsequent zones are wider than necessary. On 1000 random queries in Los Angeles with $\alpha = 0.8$, we observed that the average radius of $\mathcal{Z}_0$ and $\mathcal{Z}_1$ (relative to the centroid of $\mathcal{Z}_0$) is 908 m and 2.086 km respectively for a dense POI such as cafe, while it is 1.212 km and 2.473 km for a sparse POI such as bookstore. In Section 8.7, we empirically compare the privacy guarantee under the expected distance estimation error metric that captures the overall impact of the user possibly querying from central and border locations in $\mathcal{Z}_m$.

8.4 Retrieval Accuracy

The retrieval accuracy in the 2-roundtrip architecture described above is determined by the number of matches in the top-K set chosen by mechanism $\mathscr{M}_{fgi}$ and the top-K set corresponding to the user location. This in turn is influenced by the density of relevant POIs in the neighborhood of the user. For example, the top-10 restaurants relative to a residential location may not be very different, while that relative to a downtown location can change within a short distance of the user location. Similarly, for a more focussed query such as "mediterranean food," the result set may stay the same over a significantly large area. This makes it difficult to analyze the retrieval accuracy without incorporating information from physical POI distributions. Therefore, our approach includes some observations derived from real world POI categories and their densities.

8.4.1 Base match distribution

A top-K ranking function emphasizes both distance and prominence of a POI. As a result, the top-K set corresponding to a location does not undergo abrupt changes in neighboring locations. It can therefore be expected that, irrespective of the use of any privacy mechanism, the top-K set relative to the user's location will have matches with the top-K set of nearby locations. The base match distribution attempts to capture this similarity as a probability mass function.

Definition 8.5 (Base match distribution)**.** The base match distribution $w_{rad,K}$ is the probability distribution corresponding to the discrete random variable $R_{rad,K} : \mathcal{C} \times \mathcal{C} \to \{\Theta, 0, 1, \cdots, K\}$ where

$$R_{rad,K} \begin{cases} \Theta & , if\ d(c,c') > rad \\ |top_K(c) \cap top_K(c')| & , otherwise \end{cases} .$$

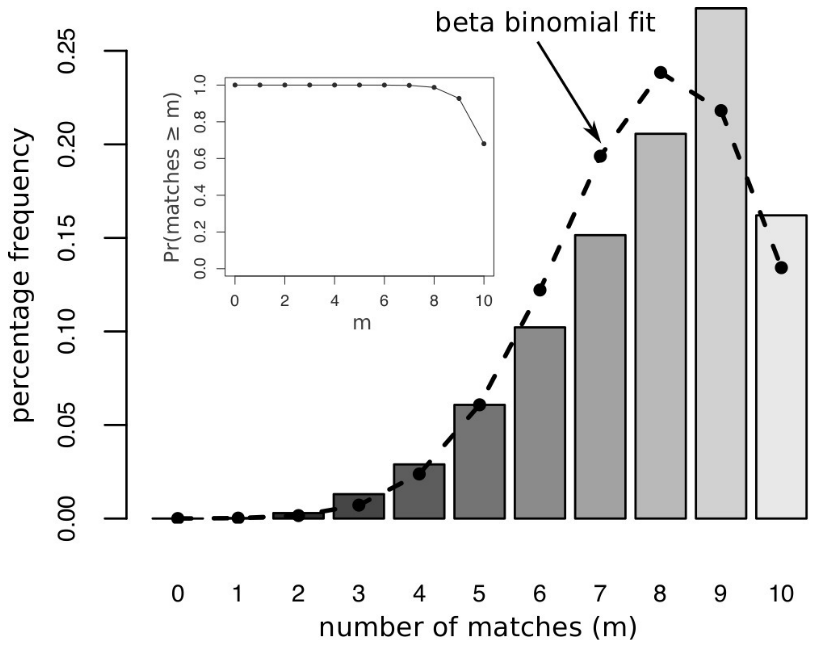

Figure 8.4: Observed and fitted base match distribution ($rad = 2$ km, $K = 10$) for cafes in Los Angeles, CA, USA. Inset figure shows probability of obtaining matches in the set chosen by mechanism $\mathscr{M}_{fgi}$.

The base match distribution $w_{rad,K}(m)$ provides the probability that any two locations within a distance rad of each other will have m matches in their top-K sets. For example, Figure 8.4 shows a histogram of the number of matches (top-10 "cafe" sets) seen in a sample of 10^6 location pairs in Los Angeles, with locations in a pair being at a distance of at most 20 cells (2 km) from each other. We obtain an estimate of the base match distribution $\hat{w}_{20,10}$ by fitting a beta-binomial distribution to this data. This estimate is useful in obtaining an insight into the approximate scale of ϵ that needs to be chosen in $\mathscr{M}_{fgi}$ for the mechanism to generate useful results. It is impractical to estimate a base match distribution for every possible search keyword; therefore, we also validate the comparative effectiveness of using a simple binomial distribution, or even a uniform distribution.

8.4.2 Match probability

When the base match distribution is skewed towards higher matches, a uniform sampling from the different top-K sets can itself lead to a majority of high matches. For example,

$\hat{w}_{20,10}$ implies a match of 8 or more in approximately 60% of the cases. Mechanism $\mathscr{M}_{fgi}$ further scales these probabilities to make the drawing of high match sets significantly more likely.

Proposition 8.1. *Mechanism $\mathscr{M}_{fgi}$ produces an output t for the user cell c_u such that*

$$\Pr\left(|t \cap top_K(c_u)| \geq m\right) = \frac{\sum_{i=m}^{K} w_{rad,K}\left(i\right) \exp\left\{\frac{\epsilon}{2K} i\right\}}{\sum_{j=0}^{K} w_{rad,K}\left(j\right) \exp\left\{\frac{\epsilon}{2K} j\right\}},$$

where $w_{rad,K}$ is the base match distribution for the top-K search.

Proof. For any output choice t that has i matches with $top_K(c_u)$, we have $s(t, c_u) = {}^{i}/_{K}$. Since the expected number of top-K sets with i matches in a radius of rad is $w_{rad,K}\left(i\right)$, we have

$$\Pr\left(|t \cap top_K(c_u)| = i\right) = \frac{w_{rad,K}\left(i\right) \exp\left\{\frac{\epsilon}{2K} i\right\}}{\sum_{j=0}^{K} w_{rad,K}\left(j\right) \exp\left\{\frac{\epsilon}{2K} j\right\}}.$$

Therefore,

$$\begin{aligned} \Pr\left(|t \cap top_K(c_u)| \geq m\right) &= \textstyle\sum_{i=m}^{K} \Pr\left(|t \cap top_K(c_u)| = i\right) \\ &= \frac{\sum_{i=m}^{K} w_{rad,K}(i) \exp\left\{\frac{\epsilon}{2K} i\right\}}{\sum_{j=0}^{K} w_{rad,K}(j) \exp\left\{\frac{\epsilon}{2K} j\right\}}. \end{aligned}$$

□

We can cluster the candidate top-K sets into equivalence classes based on the number of matches they have with $top_K(c_u)$. The base distribution then provides an estimate of the percentage of sets with a given quality score. Mechanism $\mathscr{M}_{fgi}$ exponentially scales the probability of choosing an output with higher quality score. The inset plot in Figure 8.4 shows the impact of this scaling when picking a top-10 cafe set in the example. The scaling increased the probability of obtaining 8 or more matches to 98% with $\epsilon = 30$. Figure 8.5 depicts the match frequencies in three different POI categories, having low, medium and high occupancy across the query area. Mechanism $\mathscr{M}_{fgi}$ is used here with $rad_I = 2$ km, $\epsilon = 30$, and $\alpha = 0.8$ for top-10 ranking. For each category, the data points are generated by performing queries from 1000 randomly chosen locations within the experiment area, with

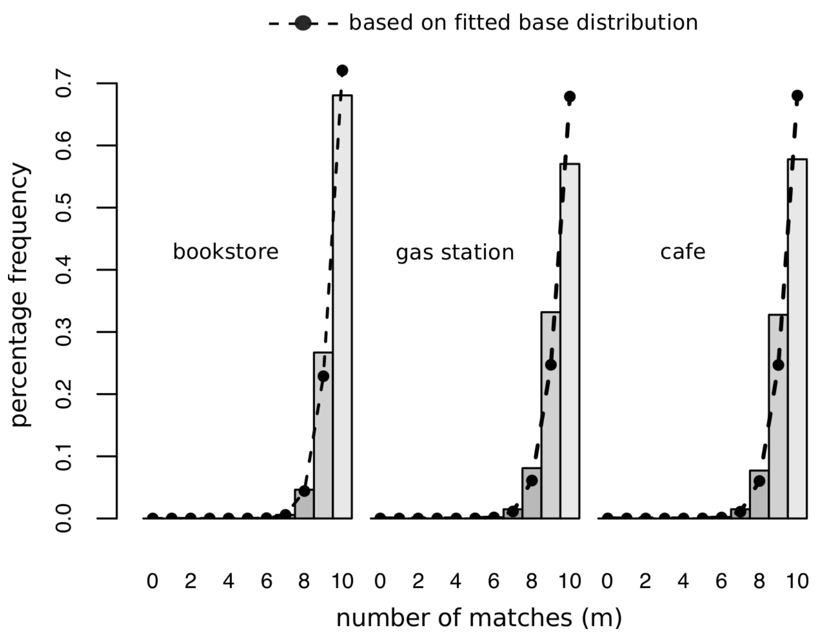

Figure 8.5: Observed match frequencies in three different POI categories. Top-10 sets computed with $\alpha = 0.8$ and $rad_I = 2$ km. $\mathscr{M}_{fgi}$ samples using $\epsilon = 30$.

100 executions of $\mathscr{M}_{fgi}$ at each location. The match probabilities computed from using a fitted base distribution reasonably captures the observed match frequencies. As expected, sparse POIs (bookstore in this case) induce a higher retrieval accuracy.

8.4.3 Choosing ϵ

The choice of ϵ directly influences the output probabilities of the sets, and in turn impacts the retrieval accuracy. We can ensure that $\mathscr{M}_{fgi}$ provides a minimum of m matches with confidence v by solving for ϵ in the following equation derived from Proposition 8.1.

$$v\sum_{i=0}^{m-1} w_{rad,K}(i)\exp\left\{\frac{\epsilon}{2K}i\right\} - (1-v)\sum_{i=m}^{K} w_{rad,K}(i)\exp\left\{\frac{\epsilon}{2K}i\right\} = 0 \tag{8.3}$$

We use a Newton-Raphson iterative solver in `R` to solve for ϵ. Figure 8.6 illustrates the minimum ϵ value necessary to guarantee at least m matches (x-axis) in the chosen set with a confidence of 90%, 95% and 99%. While the use of the base match distribution is preferable in determining ϵ, it is not necessarily practical. The figure also presents the ϵ values obtained by using two other distributions in lieu of the base match distribution–

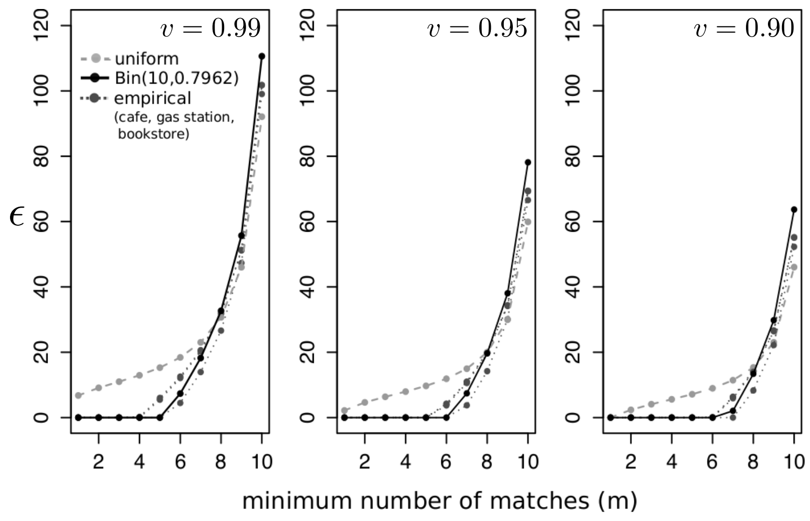

Figure 8.6: Computed ϵ using various base distributions and confidence levels $v = 0.99, 0.95$ and 0.90.

a uniform distribution signifying no knowledge of the base distribution, and a binomial distribution with parameters $n = 10$ and $p = 0.7962$. The parameters of the binomial distribution are chosen such that approximately $\frac{2}{3}$ of the probability mass is concentrated in values greater than 7. This choice is made after analyzing the empirical base distribution of 15 different POI categories, where the total probability mass in $8, 9$ and 10 matches is observed to be between 60-75%. The binomial distribution approximates the trends of the three low, medium, and high occupancy POI categories better than the uniform distribution. It overestimates ϵ when higher match counts are desired. Based on the binomial base distribution, a value of $\epsilon = 32.67$ gives us a 99% probability of obtaining 8 or more matches.

8.5 Parametric Evaluation

The performance of the proposed 2-roundtrip application is determined by a combination of three parameters, namely α : the weight given to distance in the ranking function, rad_z : the obfuscation radius, and ϵ : the privacy parameter in $\mathscr{M}_{fgi}$. We provide comparative results of their impact on the retrieval accuracy for the three example POI categories. The default values are $rad_z = 2$ km and $\epsilon = 30$, with top-10 ranking performed using $\alpha = 0.8$.

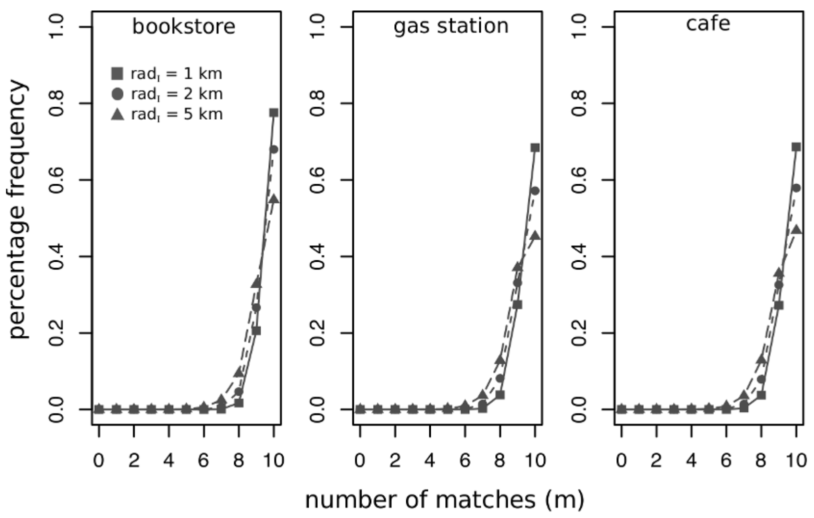

Figure 8.7: Impact of rad_z on retrieval accuracy. $rad_I = rad_z$.

rad_z **impact.** Figure 8.7 depicts the percentage frequency when exactly m matches are obtained between the actual top-K result set and that generated by $\mathscr{M}_{fgi}$. The chances of retrieving the exact set drops as the obfuscation area becomes larger, while that of retrieving a set with one or two mismatches increases. The behavior is not surprising since larger rad_z values, correspondingly a larger rad_I, imply that the potential set of outputs contains a comparatively smaller fraction of samples with $m = 10$. As such, the base distribution has a lower mass at that point. However, increasing rad_z also creates higher chances of covering zones $\mathscr{Z}_1$ and $\mathscr{Z}_2$. The number of potential sets in $\mathscr{Z}_1$ and $\mathscr{Z}_2$ are combinatorially higher than in $\mathscr{Z}_0$ (single top-K set); increasing rad_z creates avenues for inclusion of more of these sets. As long as rad_z is not set so large that other low match sets get included in majority, we can expect to retain the high retrieval accuracy. At $rad_z = 5$ km, we still obtain 8 or more matches with probability greater than 90%, higher in some POI categories.

α **impact.** Figure 8.8 depicts the impact of α on the retrieval accuracy. $\alpha = 0$ signifies ranking based only on prominence, and hence there is a single top-K set corresponding to all locations. $\alpha = 1$ signifies a K-nearest-neighbor ranking; this case presents the least favorable condition for mechanism $\mathscr{M}_{fgi}$. Between these two extreme conditions, differences in the retrieval accuracy is mostly observed for $m = 9$ and $m = 10$. The differences are

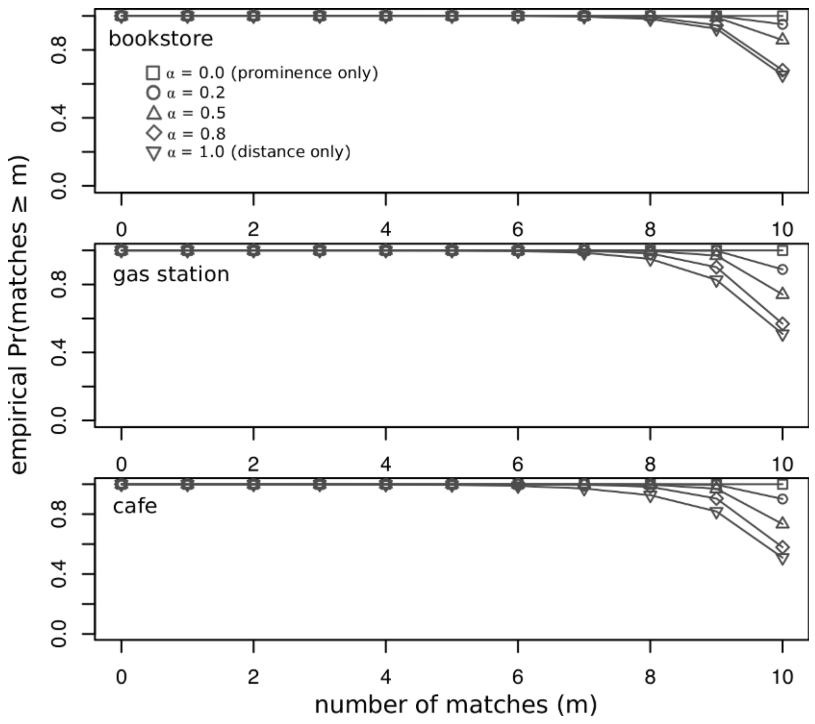

Figure 8.8: Impact of α on retrieval accuracy.

less prominent in the sparsely distributed POI as changes in the top-K set are unlikely for small changes in the user location. With half the weight on the distance value, we obtain a significantly high probability of obtaining 9 or more matches.

ϵ **impact.** Figure 8.9 depicts the impact of ϵ on the retrieval accuracy. Lower values of ϵ reduce the influence of the exponential weights on the base match distribution. At $\epsilon = 0$, the mechanism samples proportional to the base distribution. High matches can be made more likely by increasing its value. Observe that the differences in match probability is more prominent in cases such as $m = 9$ and $m = 10$. Even with a small value such as $\epsilon = 1$, we observe probabilities as high as 80% for 7 or 8 matches. We discussed in Section 8.4.3 how the parameter can be appropriately chosen when a given level of certainty is desired in the number of matches.

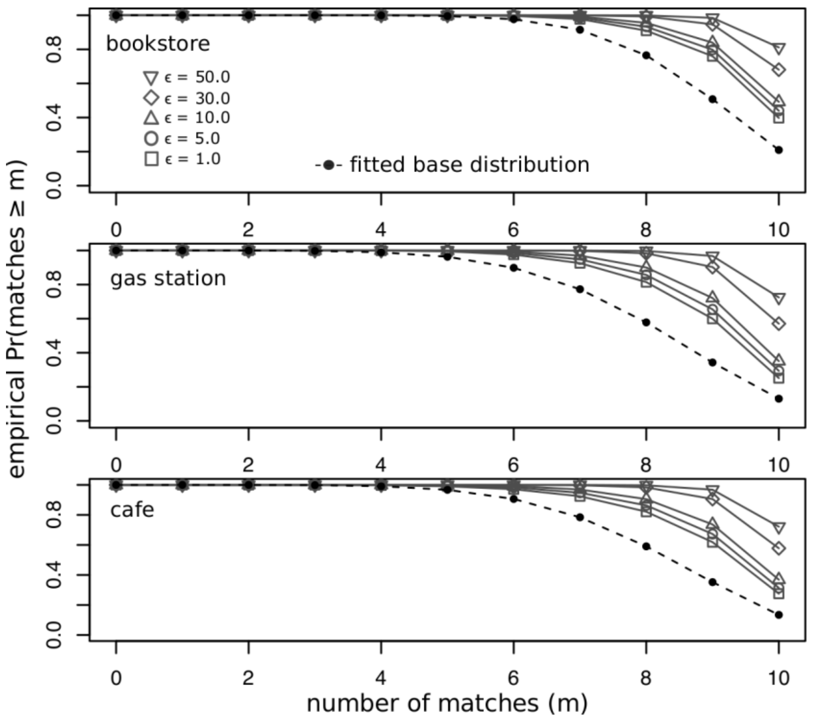

Figure 8.9: Impact of privacy parameter (ϵ) on retrieval accuracy.

8.6 An Android Implementation

We implemented the 2-roundtrip POI search architecture in Android using the Google Places API to perform the queries. The application allows the user to input a search keyword and reads the device GPS (or a simulated GPS) to obtain the user location. It then retrieves POI locations for the search category using a `radarsearch` query. A `radarsearch` query returns locations and unique identifiers for POIs within a specific radius (rad_R) of the query point. The obfuscation area (rad_z) is a configurable parameter which we set to 2 km in the following; correspondingly $rad_R = 2rad_z = 4$ km. 10-nearest-neighbor ranking is performed ($\alpha = 1$), partly because prominence data is not yet available using the Places API, and partly because K-nearest-neighbor search produces the worst case behavior as per the parametric evaluation. Details are then retrieved (using the `details` endpoint and identifiers of the POIs) for 10 POIs decided by the (f, ϵ)-geo-indistinguishable mechanism $\mathscr{M}_{fgi}$ with $\epsilon = 30$. The application is run on a Nexus 5X smartphone over a 4GLTE connection. All networking tasks are performed using a thread-pool with 4 threads.

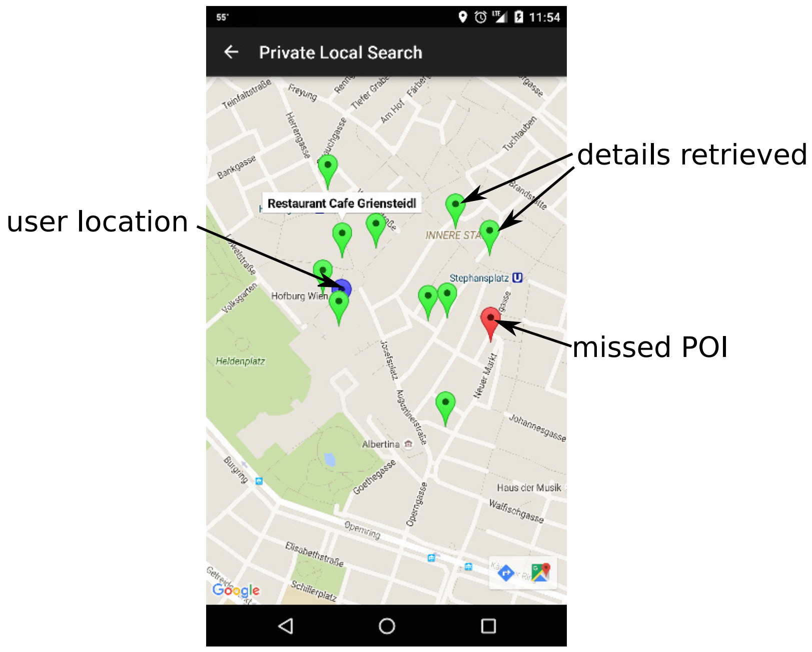

Figure 8.10: Android application screenshot.

We use a desktop application to perform 1000 `radarsearch` queries from random locations for each of the 15 chosen search keywords and in each of five chosen cities (Los Angeles, New York, Paris, Vienna and Beijing), giving a total of 75000 queries. We also run mechanism $\mathscr{M}_{fgi}$ to pick a set for details retrieval. This process allows us to compute retrieval accuracy and analyze the ranks of missed POIs. For a subset of 100 queries (per city per keyword), the Android application is executed on the smartphone and performance results such as timing and bandwidth usage are gathered. We restrict the experiments on the smartphone to a smaller subset since running all 75000 queries from the phone would incur a large cumulative 4G bandwidth (≈ 7.6GB).

Figure 8.10 displays a screenshot of the application where a search for cafes is performed at Hofburg Palace, Vienna, Austria. It shows the 10 POIs chosen by the mechanism, as well as the user's location and the POI that appears in the actual 10 nearest cafes, but missed in the sampling process. The user's location and missed POI are shown here for demonstration only, and should not be communicated to a third party.

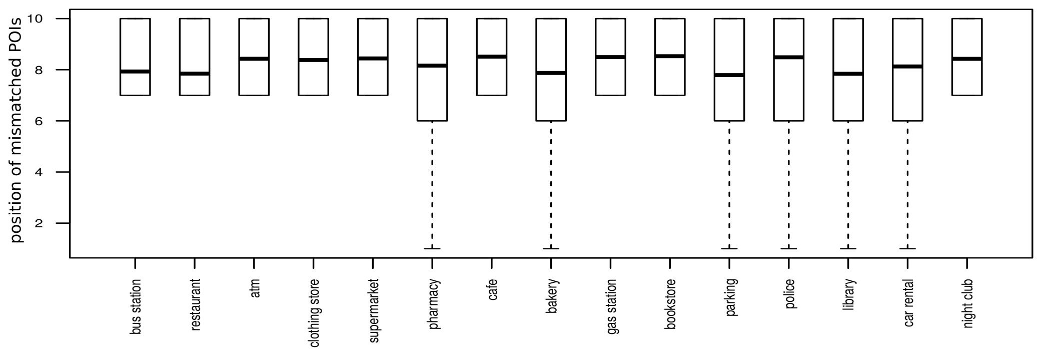

Figure 8.11: Position of POIs in the true top-K set when missed by the application.

Rank of missed POIs. Figure 8.11 shows whisker plots of the position (1 = highest rank, to 10 = lowest rank) of POIs that appear in the actual top-10 set but are missed by the application. Results from the five cities are summarized across different categories. The median position is approximately 8, with POIs in the top 6 positions being retrieved at least 75% of the times. This highlights that changes appearing in the top-10 sets are incremental and often starts in the lower ranked POIs.

Retrieval accuracy. Figure 8.12 summarizes the percentage number of times (empirical probability) when at least a given number of matches are found. The key point we highlight here is that the observations are very similar across the different cities (8.12a) and across different keywords (8.12b). The observations are in accordance with the results seen in the evaluation performed within the Los Angeles area alone.

Performance. Figure 8.13a shows the quartiles of the end-to-end time to execute one complete query in the Android application. The end-to-end time consists of compute and network time. Compute time includes the parsing of network data, computing top-K sets, computing the probability mass function, sampling using the mechanism, and updating the user interface with details of retrieved results. Network time includes connection time to Google servers, issuing requests, and then buffering of responses. As a result of the fast top-K computation algorithm, the compute time is under half a second in all cases. The network communication takes the most time, contributing a median of 2.5 seconds. Note

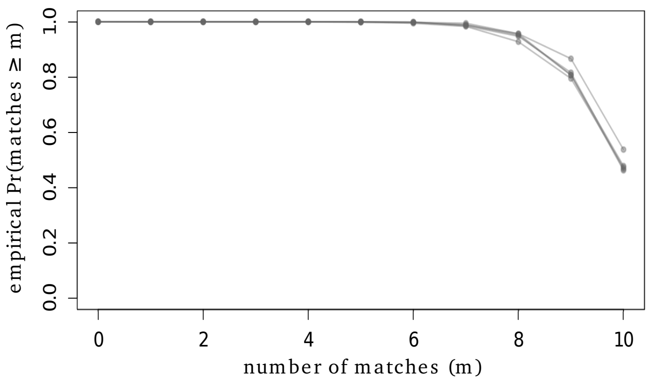

(a) Per keyword for all cities.

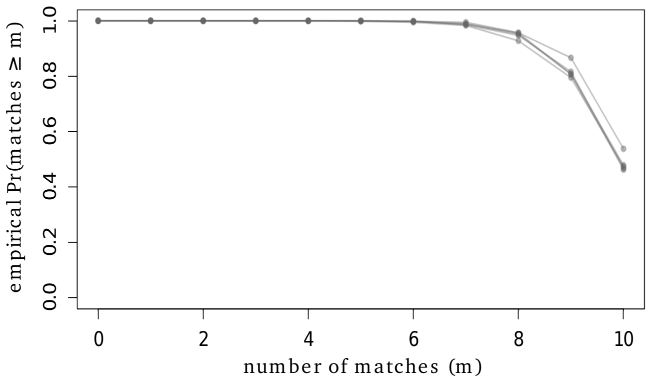

(b) Per city for all keywords

Figure 8.12: Retrieval accuracy.

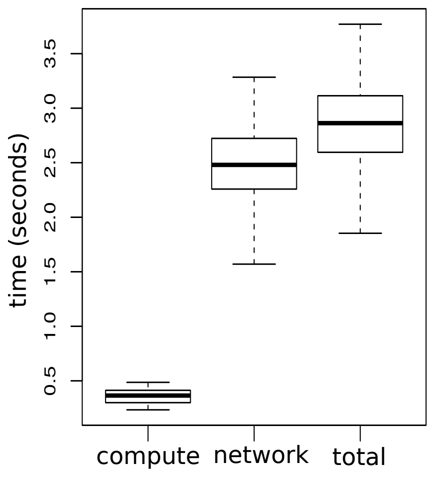

(a) End to end time of one query in the Android application.

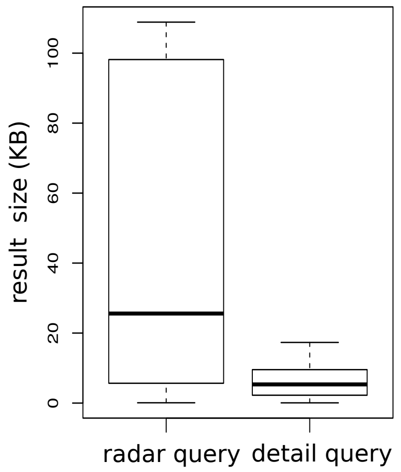

(b) Size (KB) of JSON file retrieved in a **radarsearch** and POI detail query. $rad_R = 4$ km.

Figure 8.13: Overall performance of the 2-roundtrip application.

that the total time to execute a query in a typical search application (e.g. Google Maps search for Android) averages around 2.5 seconds. Therefore, the overhead introduced in the 2-roundtrip application is negligible. Figure 8.13b shows the size of the responses (as JSON files) received from performing a `radarsearch` and a POI detail query. A `radarsearch` query returns an average size of 43.3 KB of data, a median of 26.1 KB, and sizes are between 100 KB to 110 KB in 25% of the queries. Each query to retrieve details about one POI returns an average of 6.3 KB, and a median of 5.4 KB. The 2-roundtrip application performs one `radarsearch` query and retrieves details on $K = 10$ POIs, therefore incurring a median cost of 78.8 KB and an average of 107 KB per query. A 1-roundtrip application will have to retrieve details on all POIs inside the area of retrieval, which amounts to an average size of 1.2 MB per query for 200 POIs found inside the area of retrieval.

8.7 Comparative Performance

For a given prior distribution Φ on locations, the expected estimation error of the adversary measures the average distance between the true location of the user and the location estimated by the adversary (4.8.1). Therefore, this computes the privacy level taking into consideration the likelihood of the user being in locations favorable under Theorem 8.3, as well as those that are not. If o is the output of a mechanism $\mathscr{M}$, then the expected estimation error is computed as

$$experr_M = \sum_{c,c' \in \mathcal{C}; o \in O} \Phi(c)\Pr(o|c)\Pr(c'|o)d(c,c'). \tag{8.4}$$

For a geo-indistinguishable mechanism, $O = \mathcal{C}$. Following the methodology of Andres et al. [6], we compute the minimum required value of ϵ such that the obfuscation area, $rad_Z = 1$ km, is contained within an area of retrieval $rad_R = 2 \cdot rad_z = 2$ km with confidence $v = 0.90$—$\epsilon_{0.90} = 0.00389$.

For mechanism $\mathscr{M}_{fgi}$, $O = \mathcal{T}$ and $\Pr(o|c)$ is computed as

$$\Pr(o|c) = \sum_{c_z \in \mathcal{C}} \Pr(c_z|c)\Pr(o|c_z) \tag{8.5}$$

since the output is generated by first selecting a location (c_z) for retrieval and then choosing an output from one of the top-K sets. Specifically, $\Pr(c_z|c) = 0$ if $d(c, c_z) > rad_z$ and is $\frac{1}{\pi rad_z^2}$ otherwise (c_z is uniformly chosen for POI location retrieval).

Similarly, $\Pr(o|c_z)$ is zero if o is not the top-K set of some location within a distance of rad_z ($rad_I = rad_z$) from c_z. For the prior distribution, we consider a uniform distribution inside an area with 1km radius centered at Los Angeles downtown (34.0522° N, 118.2428° W). We consider the ϵ parameter in $\mathscr{M}_{fgi}$ under two accuracy requirements: 8 or more matches with 95% confidence, and 9 or more matches with 90% confidence. We compute the parameter by solving Equation 8.3 using the empirical base match distribution corresponding to the search keyword and a $\mathsf{Bin}(10, 0.7962)$ distribution as the base match distributions.

For a mechanism that results in uniform probabilities for the terms in Equation 8.4, the expected error in the given scenario is 908 m. Such a mechanism only reveals the area of retrieval, and that the user is most likely somewhere inside it. Figure 8.14 shows the expected error for a top-10 search with the keyword "cafe." The ϵ-geo-indistinguishable mechanism provides an expected error of 691 m; comparatively, the use of mechanism $\mathscr{M}_{fgi}$ results in an expected error of 840 m when using the binomial base distribution (8 matches at 95% confidence level). The difference between the two approaches also appears in the resulting bandwidth usage. There is an average of 117 cafes inside an area of retrieval of radius 2 km. Using the average response sizes reported in Section 8.6, a query using a geo-indistinguishable mechanism would result in the usage of 737.1 KB, compared to approximately 85 KB with the (f, ϵ)-geo-indistinguishable mechanism.

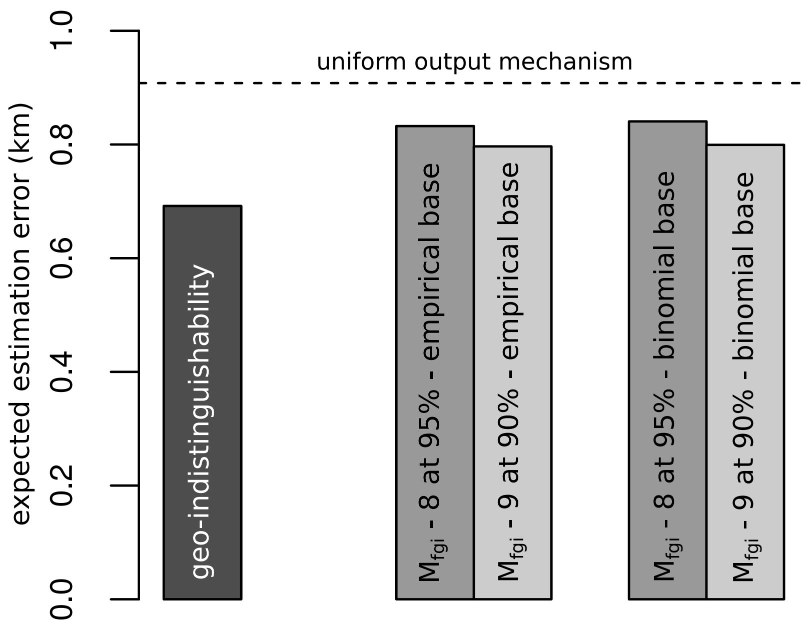

Figure 8.14: Expected estimation error of adversary.

8.8 Adopting Multiple Queries

As with geo-indistinguishability, the privacy assurances in (f, ϵ)-geo-indistinguishability also degrade if used to protect multiple locations. For the scenario where n queries are made in sequence, the effective ϵ value in both mechanisms is $n\epsilon$ at the end of the queries. Clearly, an inherent trade-off can be achieved in the accuracy of query results and the corresponding privacy guarantees. For example, if the value of the parameter is set to $\epsilon = \frac{\epsilon_{end}}{n}$, the privacy level begins at a higher level and degrades to that produced by setting the parameter to $\epsilon = \epsilon_{end}$ in a single query scenario. If n is large, then $\epsilon_{end} \to 0$. This however still provides a bound on the accuracy level, as given by the base match distribution. Note that the empirical privacy evaluation in Section 8.5 indicates that a reasonable level of privacy can be expected with a value such as $\epsilon = 30$. We also observe in the parametric evaluation (Figure 8.9) that the accuracy levels of using $\epsilon = 1$ and $\epsilon = 30$ (or $\epsilon = 50$) are not significantly different. Therefore, it is possible to start with a lower ϵ value, and increase up to to an effective high ϵ value without inducing significant degradation in the utility.

8.9 Summary

In this chapter, we propose a differential privacy based LPPM. Similar to the other LPPMs proposed in this dissertation, this one natively fits our two-roundtrip architecture proposed in Chapter 4. In contrast to the LPPMs proposed in the earlier chapters, the enhanced feature of this LPPM is the rigorous mathematical basis for the privacy guarantee that is proved in this chapter. We introduced a new concept of (f, ϵ)-geo-indistinguishability in which the differential privacy is maintained for any arbitrary function f in contrast to the classical ϵ-geo-indistinguishability in which the differential privacy is maintained with respect to the distance between two locations. Since ϵ-geo-indistinguishability is the state of art, we compare our results against a recent ϵ-geo-indistinguishability LPPM [6] and show that our method can perform better. Finally, we implemented our LPPM as an Android application and tested it. Our method on average adds one second delay compared to the standard GooglMaps application for Android (which does not provide any privacy to the user) thus maintaining the main theme of this dissertation.

Chapter 9

Conclusion

In this chapter, we summarize the dissertation, enlist our contributions to the research in mobile privacy protection, and finally present our thoughts on future direction for this research effort.

Location based services are proving to be very useful to the mobile users as more and more people depend on it. They are of course very attractive to the service providers, as they provide immense opportunities for monetizing knowledge of location of the users. As the utilization of these services increase, so does the concern for user's privacy. There are considerable efforts from the research community to measure, analyze and mitigate this threat. This work makes novel contributions and furthers the research in mobile location privacy.

We started this effort by introducing the concept of location privacy in the context of location searches. We then discuss in detail, how location is considered private by most of the users and the possible problems that could emerge if this privacy is violated. Since having accurate user location information is considered an asset, many service providers give away their service for free, with the intention of monetizing the location data obtained. These service providers have published privacy policies that the user needs to agree to as a condition of utilizing the service. Without technical privacy protection mechanisms, often, the service provider is trusted to adhere to the privacy policy. Here we introduced the concept of a semi-trusted service provider who is curious to know the accurate location of the user.

We then present a brief overview of the effort that already is put in by the computer science research community into location privacy. While doing this, we show an evolution of privacy preserving techniques over several years. Then, we discuss how most of the current techniques fall short of wide adaptation of the requirement of third parties. The introduction of trusted third parties introduce several risks both in terms of privacy and availability. Although some existing LPPMs successfully avoid the TPP requirement, they rank the top-K results of the query based only on the distance from the query point. We discussed this issue in Chapter 4 and showed that real local search applications rank the query results based on both the distance and the prominence value of the retrieved POIs. We justify our approach of TTP less protocol by discussing all these problems in detail, and then clearly stating the problem we address in this research.

We then presented an architecture for a communication protocol that can be used in a TTP less fashion. As part of this, we presented definitions and notation for the different items that make discussions and analysis about our proposed techniques precise. We proposed a two-round-trip architecture. In the first round, the client gets a list of points of interest that pertain to a large region, thus not revealing her location accurately. She then applies an LPPM to the result set to arrive at a narrowed down list of POIs whose detailed information is requested in the second round trip. The LPPM or the encryption applied ensures that the attacker cannot pin point the user's location beyond an acceptable coarse threshold area.

Before proposing our LPPM, we first took a serious look at existing techniques that could be applied as a possible solution to the TTP less LPPM. We explored in detail a mathematical technique called *private information retrieval* and gave it a serious consideration. We not only discussed this technique in detail, but also implemented two algorithms for this technique using standard hardware configurations and readily available open source software libraries. The results we obtained show that they are still far away from practicality to solve our problem. By showing that PIR is still not efficient enough to be practical, we motivate the need to come up with practical LPPMs.

Our solution is to come with LPPMs that eliminate the need for TTP by taking advantage of the processing capabilities available in modern mobile devices. We proposed three LPPMs, and implemented them on representative mobile devices to show that they perform reasonably well, and analyzed them to show that privacy protection characteristics are up to par. In the section below, we summaries the results obtained and discuss those results.

9.1 Results and Discussion

First LPPM we proposed deals with simple scenario where the user issues a single local search and expect the attacker, who can be a semi-trusted service provider, to not be able to place her in a large enough configurable area. Also, the search needs to work with realistic ranking which considers prominence and other attributes of POIs, not just the distance from her current location. We came up with privacy measurements that we use to calculate achieved privacy and performance, and also to make valid comparisons against other LPPMs. Another important result is that we demonstrated the feasibility of these computations by running the algorithm on different sets of real world POI distributions and realistic mobile hardware. Our timing experiments show that the average computation overhead is less than 0.5 seconds which is a reasonable delay in response felt by the user for the privacy achieved.

Next we extend this simple LPPM to accommodate the case of multiple queries scenario, where the user is expected to launch a sequence of queries in succession as she moves around. This scenario adds more challenges to our LPPM since the user now will repeatedly retrieve POI data from a service provider which makes the LPPM more vulnerable to inference analysis under a Bayesian adversary model. We first model this scenario to show how in a multiple query scenario, the single query algorithm fails to achieve the expected privacy. We propose our algorithm along with heuristics to retrieve only needed additional POIs. We show through empirical analysis that our improved LPPM leaks little or no advantageous information to the attacker. The adversarial inferences are limited in a setting with real world POI distributions.

The above approach can efficiently operate in a mobile device, and has minimal impact on the communication bandwidth; empirical comparison of an LPPM implemented under our architecture against other techniques shows that our architecture needs less amount of data exchange between the client and the server. However, this approach does not provide a theoretical guarantee on the privacy level. So in the next step of development, we suggested a differential privacy based LPPM to implement our proposed architecture in order to mathematically justify their privacy level guarantee. In contrast to ϵ-geo-indistinguishability, we introduced the (f, ϵ)-geo-indistinguishability principle that a privacy mechanism can enforce in order to limit the distinguishability between locations. In (f, ϵ)-geo-indistinguishability, locations that are evaluated as being similar under the f function enjoy the same level of privacy under this principle. In the new LPPM, all locations whose top-K result sets have the same number of mismatches relative to the top-K set of a query point become equally indistinguishable. We theoretically characterized the conditions under which the new mechanism provides stronger levels of privacy than a ϵ-geo-indistinguishable mechanism, and provided the framework necessary to tune the mechanism to guarantee a required level of accuracy. The empirical evaluation that we performed drives us to the conclusion that our LPPM can retain high similarity with the sought top-K set, irrespective of how much contribution distance makes to the ranking, the density of the POIs in the search area, or variations in the ϵ parameter. Of course we made sure that the mechanism can execute on a mobile device without generating any noticeable delays or incurring excessive bandwidth cost.

9.2 Further Directions

- We briefly discussed the multiple queries scenario for (f, ϵ)-geo-indistinguishability in Section 8.8. An in-depth exploration of this insight is left for future work.

- The quality scoring function s for the LPPM $\mathscr{M}_{fgi}$ introduced in the Definition 8.4 consider the number of matching POIs between the top-K set result from any location c and the top-K set of the true location of the use, c_u, as the quality of the result set. In Section 8.6 we analyze the rank of missed POIs in the output set produced by the mechanism $\mathscr{M}_{fgi}$. Even though empirical demonstration shows that there is a 75% chance to retrieve POIs in the top 6 positions of the actual set (the set that will result from c_u), further research is needed in this direction. Another LPPM with a different scoring function that takes into account the rank of the top-K POIs can be explored.

- Although there is a good amount of research that went into applying cryptographic techniques for achieving location privacy, they all seem impractical in the real world scenarios, some reasons being; (i) requirement of preprocessing/encryption of data on the service provider, (ii) additional processing on the mobile devices, (iii) major communication overhead, and (iv) lack of precision that comes inherently with transformations such as Hilbert curves. In chapter 5, we took a closer look at one possible cryptography protocol, namely PIR, and we saw that it can offer a high level of privacy protection in both single query and multiple query scenarios. Unfortunately, the current available techniques are not sufficient for the local search problem. Further research and improvements in these techniques can significantly contribute in the design of a LPPM.

- Throughout our discussion in this dissertation we consider the adversary who is interested in finding the last destination of the user. Our privacy metrics focus on that threat model and our proposed LPPMs try to protect the privacy from that perspective. Future research direction is recommended to consider a LPPM(s) under our architecture that protects the user from an attacker that tries to draw traces for the user and infer her movement behavior.

9.3 Summary

Our goal has been to make the privacy enhancing mechanisms useful and practical. We saw a problem where there are several privacy enhancing algorithms, but most confined to laboratories, as their implementation requires huge resources and changes. We noticed the presence and requirement of third parties as the major obstacle to practical implementation. We studied few existing proposals that are already TTP less. We found an opportunity there where we could eliminate a TTP by taking advantage of the considerable power modern mobile devices have. We proposed and implemented three different algorithms that follow the same messaging schema, but achieve configurable location privacy in three different scenarios. We took care to do our simulations using real life data feeds and real mobile devices. To achieve the goal of making the algorithms practical on mobile devices, we implemented several heuristics and ideas borrowed from different fields to ensure that the algorithms perform well enough, i.e., without causing noticeable delay in response times. Some of our proposals have been accepted in peer reviewed platforms, vindicating that this research advances the area of privacy in mobile local search.

References

[1] Pankaj K Agarwal, Mark De Berg, Jirí Matousek, and Otfried Schwarzkopf. Constructing levels in arrangements and higher order Voronoi diagrams. *SIAM Journal on Computing*, 27(3):654–667, 1998.

[2] Rakesh Agrawal, Jerry Kiernan, Ramakrishnan Srikant, and Yirong Xu. Hippocratic databases. In *28th International Conference on Very Large Data Bases*, pages 143–154. VLDB Endowment, 2002.

[3] Carlos Aguilar-Melchor and Philippe Gaborit. A lattice-based computationally-efficient private information retrieval protocol. Technical report, Cryptology ePrint Archive, 2007.

[4] Sheikh I. Ahamed, Chowdhury S. Hasan, Md. M. Haque, and Md. O. Gani. Towards TTP-free lightweight solution for location privacy using location-based anonymity prediction. In *2011 ACM Symposium on Research in Applied Computation*, pages 293–297. ACM, 2011.

[5] Xiangdong An, Dawn Jutla, and Nick Cercone. Reasoning about obfuscated private information: Who have lied and how to lie. In *5th ACM Workshop on Privacy in Electronic Society*, pages 85–88. ACM, 2006.

[6] Miguel E Andrés, Nicolás E Bordenabe, Konstantinos Chatzikokolakis, and Catuscia Palamidessi. Geo-indistinguishability: Differential privacy for location-based systems. In *2013 ACM SIGSAC Conference on Computer & Communications Security*, pages 901–914. ACM, 2013.

[7] Claudio Agostino Ardagna, Marco Cremonini, Ernesto Damiani, De Capitani Di Vimercati, and Pierangela Samarati. Location privacy protection through obfuscation-based techniques. In *21st Annual IFIP WG 11.3 Working Conference on Data and Applications Security*, pages 47–60. Springer, 2007.

[8] Claudio Agostino Ardagna, Marco Cremonini, and Gabriele Gianini. Landscape-aware location-privacy protection in location-based services. *Journal of System Architecture*, 55(4):243–254, 2009.

[9] Daniel Ashbrook and Thad Starner. Using GPS to learn significant locations and predict movement across multiple users. *Personal Ubiquitous Computing*, 7(5):275–286, 2003.

[10] Roland Assam and Thomas Seidl. A model for context-aware location identity preservation using differential privacy. In *12th IEEE International Conference on Trust, Security and Privacy in Computing and Communications*, pages 346–353. IEEE, 2013.

[11] Franz Aurenhammer and Otfried Schwarzkopf. A simple on-line randomized incremental algorithm for computing higher order Voronoi diagrams. *International Journal of Computational Geometry & Applications*, 2(4):363–381, 1998.

[12] Bhuvan Bamba, Ling Liu, Peter Pesti, and Ting Wang. Supporting anonymous location queries in mobile environments with privacygrid. In *17th International Conference on World Wide Web*, pages 237–246. ACM, 2008.

[13] Michael Barbaro, Tom Zeller, and Saul Hansell. A face is exposed for AOL searcher no. 4417749. *New York Times*, 9(2008), 2006.

[14] Jake Bellati, Andrew Brunner, Joseph Lewis, Prasad Annadata, Wisam Eltarjaman, Rinku Dewri, and Ramakrishna Thurimella. Driving habits data: Location privacy implications and solutions. In *IEEE Security and Privacy.* to appear.

[15] Alastair R. Beresford and Frank Stajano. Location privacy in pervasive computing. *IEEE Pervasive Computing*, 2(1):46–55, 2003.

[16] Claudio Bettini, X Sean Wang, and Sushil Jajodia. Protecting privacy against location-based personal identification. In *2nd VLDB Workshop on Secure Data Management*, pages 185–199. Springer, 2005.

[17] Jingguo Bi, Mingjie Liu, and Xiaoyun Wang. Cryptanalysis of a homomorphic encryption scheme from ISIT 2008. In *2012 IEEE International Symposium on Information Theory Proceedings*, pages 2152–2156. IEEE, 2012.

[18] Nicolás E Bordenabe, Konstantinos Chatzikokolakis, and Catuscia Palamidessi. Optimal geo-indistinguishable mechanisms for location privacy. In *2014 ACM SIGSAC Conference on Computer and Communications Security*, pages 251–262. ACM, 2014.

[19] Jan Lauren Boyles, Aaron Smith, and Mary Madden. Privacy and data management on mobile devices. *Pew Internet & American Life Project*, 4, 2012.

[20] Zvika Brakerski, Craig Gentry, and Vinod Vaikuntanathan. (Leveled) fully homomorphic encryption without bootstrapping. In *3rd Innovations in Theoretical Computer Science Conference*, pages 309–325. ACM, 2012.

[21] Joe P Buhler, Hendrik W Lenstra Jr, and Carl Pomerance. Factoring integers with the number field sieve. In *The Development of the Number Field Sieve*, pages 50–94. Springer, 1993.

[22] Ji-Won Byun and Ninghui Li. Purpose based access control for privacy protection in relational database systems. *The VLDB Journal*, 17(4):603–619, 2008.

[23] Christian Cachin, Silvio Micali, and Markus Stadler. Computationally private information retrieval with polylogarithmic communication. In *1999 International Conference on the Theory and Applications of Cryptographic Techniques*, pages 402–414. Springer, 1999.

[24] Patrik Cerwall. Ericsson mobility report, June 2015. `http://www.ericsson.com/res/docs/2015/ericsson-mobility-report-june-2015.pdf`.

[25] Konstantinos Chatzikokolakis, Miguel E Andrés, Nicolás Emilio Bordenabe, and Catuscia Palamidessi. Broadening the scope of differential privacy using metrics. In *13th International Symposium on Privacy Enhancing Technologies Symposium*, pages 82–102. Springer, 2013.

[26] Konstantinos Chatzikokolakis, Catuscia Palamidessi, and Marco Stronati. Location privacy via geo-indistinguishability. *ACM SIGLOG News*, 2(3):46–69, 2015.

[27] YeowMeng Chee, Tao Feng, San Ling, Huaxiong Wang, and LiangFeng Zhang. Query-efficient locally decodable codes of subexponential length. *Computational Complexity*, 22(1):159–189, 2013.

[28] Ruizhi Chen and Robert Guinness. *Geospatial computing in mobile devices.* Artech House, 2014.

[29] Reynold Cheng, Yu Zhang, Elisa Bertino, and Sunil Prabhakar. Preserving user location privacy in mobile data management infrastructures. In *6th International Workshop on Privacy Enhancing Technologies*, pages 393–412. Springer, 2006.

[30] Yohan Chon, Nicholas D. Lane, Fan Li, Hojung Cha, and Feng Zhao. Automatically characterizing places with opportunistic crowdsensing using smartphones. In *2012 ACM Conference on Ubiquitous Computing*, pages 481–490. ACM, 2012.

[31] Yohan Chon, Hyojeong Shin, Elmurod Talipov, and Hojung Cha. Evaluating mobility models for temporal prediction with high-granularity mobility data. In *2012 IEEE International Conference on Pervasive Computing and Communications*, pages 206–212. IEEE, 2012.

[32] Benny Chor, Eyal Kushilevitz, Oded Goldreich, and Madhu Sudan. Private information retrieval. *Journal of the ACM*, 45(6):965–981, 1998.

[33] Chi-Yin Chow and Mohamed F Mokbel. Enabling private continuous queries for revealed user locations. In *10th International Conference on Advances in Spatial and Temporal Databases*, pages 258–273. Springer, 2007.

[34] Chi-Yin Chow, Mohamed F Mokbel, and Xuan Liu. A peer-to-peer spatial cloaking algorithm for anonymous location-based service. In *14th Annual ACM International Symposium on Advances in Geographic Information Systems*, pages 171–178. ACM, 2006.

[35] Chi-Yin Chow, Mohamed F Mokbel, and Xuan Liu. Spatial cloaking for anonymous location-based services in mobile peer-to-peer environments. *Geoinformatica*, 15(2):351–380, 2011.

[36] Henri Cohen. *A course in computational algebraic number theory.* Springer Science & Business Media, 2013.

[37] Maria Luisa Damiani, Elisa Bertino, and Claudio Silvestri. Protecting location privacy against spatial inferences: The probe approach. In *2nd ACM SIGSPATIAL International Workshop on Security and Privacy in GIS and LBS*, pages 32–41. ACM, 2009.

[38] Maria Luisa Damiani, Elisa Bertino, and Claudio Silvestri. The PROBE framework for the personalized cloaking of private locations. *Transactions on Data Privacy*, 3(2):123–148, 2010.

[39] Manlio De Domenico, Antonio Lima, and Mirco Musolesi. Interdependence and predictability of human mobility and social interactions. *Pervasive and Mobile Computing*, 7(6):798–807, 2013.

[40] Yves-Alexandre de Montjoye, César A Hidalgo, Michel Verleysen, and Vincent D Blondel. Unique in the crowd: The privacy bounds of human mobility. *Scientific Reports*, 3(1376):1–5, 2013.

[41] Casey Devet, Ian Goldberg, and Nadia Heninger. Optimally robust private information retrieval. In *21st USENIX Conference on Security Symposium*, pages 269–283, 2012.

[42] Rinku Dewri. Local differential perturbations: Location privacy under approximate knowledge attackers. *IEEE Transactions on Mobile Computing*, 12(12):2360–2372, 2013.

[43] Rinku Dewri, Prasad Annadata, Wisam Eltarjaman, and Ramakrishna Thurimella. Inferring trip destinations from driving habits data. In *12th ACM Workshop on Privacy in the Electronic Society*, pages 267–272. ACM, 2013.

[44] Rinku Dewri, Wisam Eltarjaman, Prasad Annadata, and Ramakrishna Thurimella. Beyond the thin client model for location privacy. In *2013 International Conference on Privacy and Security in Mobile Systems*, pages 1–8. IEEE, 2013.

[45] Rinku Dewri, Indrakshi Ray, and David Whitley. Query m-invariance: Preventing query disclosures in continuous location-based services. In *11th International Conference on Mobile Data Management*, pages 95–104. IEEE, 2010.

[46] Rinku Dewri and Ramakrisha Thurimella. Exploiting service similarity for privacy in location-based search queries. *IEEE Transactions on Parallel and Distributed Systems*, 25(2):374–383, 2014.

[47] Changyu Dong and Liqun Chen. A fast single server private information retrieval protocol with low communication cost. In *19th European Symposium on Research in Computer Security*, pages 380–399. Springer, 2014.

[48] Matt Duckham and Lars Kulik. A formal model of obfuscation and negotiation for location privacy. In *3td International Conference on Pervasive Computing*, pages 152–170. Springer, 2005.

[49] Matt Duckham and Lars Kulik. Simulation of obfuscation and negotiation for location privacy. In *2005 International Conference on Spatial Information Theory*, pages 31–48. Springer, 2005.

[50] Matt Duckham, Lars Kulik, and Athol Birtley. A spatiotemporal model of strategies and counter strategies for location privacy protection. In *4th International Conference on Geographic Information Science*, pages 47–64. Springer, 2006.

[51] Cynthia Dwork. Differential privacy: A survey of results. In *5th International Conference on Theory and Applications of Models of Computation*, pages 1–19. Springer, 2008.

[52] Cynthia Dwork. Differential privacy. In *Encyclopedia of Cryptography and Security*, pages 338–340. Springer, 2011.

[53] Cynthia Dwork and Jing Lei. Differential privacy and robust statistics. In *41st Annual ACM Symposium on Theory of Computing*, pages 371–380. ACM, 2009.

[54] Cynthia Dwork and Aaron Roth. The algorithmic foundations of differential privacy. *Foundations and Trends in Theoretical Computer Science*, 9(3-4):211–407, 2014.

[55] Klim Efremenko. 3-queryy locally decodable codes of subexponential length. *SIAM Journal on Computing*, 41(6):1694–1703, 2012.

[56] Electronic Privacy Information Center. Locational privacy, Mar 2016. `https://epic.org/privacy/location_privacy/`.

[57] Wisam Eltarjaman and Prasad Annadata. Comparative study of private information retrieval protocols. In *6th International Multi-Conference on Complexity, Informatics and Cybernetics*. IMCIC, 2016.

[58] Wisam Eltarjaman, Prasad Annadata, Rinku Dewri, and Ramakrishna Thurimella. Leveraging smartphone advances for continuous location privacy. In *16th IEEE International Conference on Mobile Data Management*, pages 197–202. IEEE, 2015.

[59] Wisam Eltarjaman, Rinku Dewri, and Ramakrishna Thurimella. Indistinguishability of ranked geo-query results. Under review.

[60] Wisam Eltarjaman, Rinku Dewri, and Ramakrishna Thurimella. Private retrieval of POI details in top-Kqueries. Under review.

[61] Srivatsava Ranjit Ganta, Shiva Prasad Kasiviswanathan, and Adam Smith. Composition attacks and auxiliary information in data privacy. In *14th ACM International Conference on Knowledge Discovery and Data Mining*, pages 265–273. ACM, 2008.

[62] Michael R. Garey and David S. Johnson. *Computers and intractability: a guide to the theory of NP-completeness*. W. H. Freeman & Co., 1990.

[63] B. Gedik and Ling Liu. Location privacy in mobile systems: A personalized anonymization model. In *25th IEEE International Conference on Distributed Computing Systems*, pages 620–629. IEEE, 2005.

[64] Buğra Gedik and Ling Liu. Protecting location privacy with personalized k-anonymity: Architecture and algorithms. *IEEE Transactions on Mobile Computing*, 7(1):1–18, 2008.

[65] Quan Geng and Pramod Viswanath. Optimal noise adding mechanisms for approximate differential privacy. *IEEE Transactions on Information Theory*, 62(2):952–969, 2013.

[66] Craig Gentry and Zulfikar Ramzan. Single-database private information retrieval with constant communication rate. In *32nd International Colloquium on Automata, Languages, and Programming*, pages 803–815. Springer, 2005.

[67] Gabriel Ghinita, Maria Luisa Damiani, Claudio Silvestri, and Elisa Bertino. Preventing velocity-based linkage attacks in location-aware applications. In *17th ACM International Conference on Advances in Geographic Information Systems*, pages 246–255. ACM, 2009.

[68] Gabriel Ghinita, Panos Kalnis, Ali Khoshgozaran, Cyrus Shahabi, and Kian-Lee Tan. Private queries in location based services: Anonymizers are not necessary. In *2008*

ACM SIGMOD International Conference on Management of Data, pages 121–132. ACM, 2008.

[69] Gabriel Ghinita, Panos Kalnis, and Spiros Skiadopoulos. PRIVE: anonymous location-based queries in distributed mobile systems. In *16th International Conference on World Wide Web*, pages 371–380. ACM, 2007.

[70] Gabriel Ghinita, Keliang Zhao, Dimitris Papadias, and Panos Kalnis. A reciprocal framework for spatial k-anonymity. *Information Systems*, 35(3):299–314, 2010.

[71] Ian Goldberg. Improving the robustness of private information retrieval. In *2007 IEEE Symposium on Security and Privacy*, pages 131–148. IEEE, 2007.

[72] Shafi Goldwasser, Silvio Micali, and Charles Rackoff. The knowledge complexity of interactive proof-systems. *SIAM Journal on computing*, 18(1):186–208, 1989.

[73] Philippe Golle. Revisiting the uniqueness of simple demographics in the us population. In *5th ACM workshop on Privacy in electronic society*, pages 77–80. ACM, 2006.

[74] Philippe Golle and Kurt Partridge. On the anonymity of home/work location pairs. In *7th International Conference on Pervasive Computing*, pages 390–397. Springer, 2009.

[75] Marco Gruteser and Dirk Grunwald. Anonymous usage of location-based services through spatial and temporal cloaking. In *1st International Conference on Mobile Systems, Applications and Services*, pages 31–42. ACM, 2003.

[76] Marco Gruteser and Baik Hoh. On the anonymity of periodic location samples. In *2nd International Conference on Security in Pervasive Computing*, pages 179–192. Springer, 2005.

[77] Venkatesan Guruswami and Madhu Sudan. Improved decoding of reed-solomon and algebraic-geometric codes. In *39th Annual Symposium on Foundations of Computer Science*, pages 28–37. IEEE, 1998.

[78] Andreas Gutscher. Coordinate transformation - a solution for the privacy problem of location based services. In *20th IEEE International Parallel & Distributed Processing Symposium*, pages 7–13. IEEE, 2006.

[79] Ramaswamy Hariharan and Kentaro Toyama. Project lachesis: Parsing and modeling location histories. In *3rd International Conference on Geographic Information Science*, pages 106–124. Springer, 2004.

[80] Tanzima Hashem and Lars Kulik. Safeguarding location privacy in wireless ad-hoc networks. In *9th International Conference on Ubiquitous Computing*, pages 372–390. Springer, 2007.

[81] Tanzima Hashem and Lars Kulik. "don't trust anyone": privacy protection for location-based services. *Pervasive Mobile Computing*, 7(1):44–59, 2011.

[82] Tanzima Hashem, Lars Kulik, and Rui Zhang. Privacy preserving group nearest neighbor queries. In *13th International Conference on Extending Database Technology*, pages 489–500. ACM, 2010.

[83] Ryan Henry, Yizhou Huang, and Ian Goldberg. One (block) size fits all: Pir and spir with variable-length records via multi-block queries. In *20th Annual Network and Distributed Systems Security Symposium*, 2013.

[84] Jeffrey Hightower and Gaetano Borriello. Location systems for ubiquitous computing. *Computer*, 34(8):57–66, 2001.

[85] Jeffrey Hightower, Sunny Consolvo, Anthony LaMarca, Ian Smith, and Jeff Hughes. Learning and recognizing the places we go. In *7th International Conference on Ubiquitous Computing*, pages 159–176. Springer, 2005.

[86] Baik Hoh, Marco Gruteser, Hui Xiong, and Ansaf Alrabady. Enhancing security and privacy in traffic-monitoring systems. *IEEE Pervasive Computing*, 5(4):38–46, 2006.

[87] Baik Hoh, Marco Gruteser, Hui Xiong, and Ansaf Alrabady. Preserving privacy in GPS traces via uncertainty-aware path cloaking. In *14th ACM Conference on Computer and Communications Security*, pages 161–171. ACM, 2007.

[88] Baik Hoh, Marco Gruteser, Hui Xiong, and Ansaf Alrabady. Achieving guaranteed anonymity in GPS traces via uncertainty-aware path cloaking. *IEEE Transactions on Mobile Computing*, 9(8):1089–1107, 2010.

[89] Lalana Kagal and Hal Abelson. Access control is an inadequate framework for privacy protection. In *W3C Privacy Workshop*, pages 1–6, 2010.

[90] Panos Kalnis, Gabriel Ghinita, Kyriakos Mouratidis, and Dimitris Papadias. Preventing location-based identity inference in anonymous spatial queries. *IEEE Transactions on Knowledge and Data Engineering*, 19(12):1719–1733, 2007.

[91] Jong Hee Kang, William Welbourne, Benjamin Stewart, and Gaetano Borriello. Extracting places from traces of locations. *ACM SIGMOBILE Mobile Computing and Communications Review*, 9(3):58–68, 2005.

[92] Ali Khoshgozaran and Cyrus Shahabi. Blind evaluation of nearest neighbor queries using space transformation to preserve location privacy. In *10th International Conference on Advances in Spatial and Temporal Databases*, pages 239–257. Springer, 2007.

[93] Ali Khoshgozaran, Cyrus Shahabi, and Houtan Shirani-Mehr. Location privacy: going beyond k-anonymity, cloaking and anonymizers. *Knowledge and Information Systems*, 26(3):435–465, 2011.

[94] Hidetoshi Kido, Yutaka Yanagisawa, and Tetsuji Satoh. An anonymous communication technique using dummies for location-based services. In *2005 International Conference on Pervasive Services*, pages 88–97. IEEE, 2005.

[95] Hyoungshick Kim. A spatial cloaking framework based on range search for nearest neighbor search. In *4th International Workshop on Data Privacy Management*, pages 93–105. Springer, 2010.

[96] Swastik Kopparty, Shubhangi Saraf, and Sergey Yekhanin. High-rate codes with sublinear-time decoding. *Journal of the ACM*, 61(5):28:1–28:20, 2014.

[97] John Krumm. Inference attacks on location tracks. In *5th International Conference on Pervasive Computing*, pages 127–143. Springer, 2007.

[98] John Krumm. Realistic driving trips for location privacy. In *7th International Conference on Pervasive Computing*, pages 25–41. Springer, 2009.

[99] John Krumm and AJ Bernheim Brush. Learning time-based presence probabilities. In *9th International Conference on Pervasive Computing*, pages 79–96. Springer, 2011.

[100] Eyal Kushilevitz and Rafail Ostrovsky. Replication is not needed: single database, computationally-private information retrieval. In *38th Annual Symposium on Foundations of Computer Science*, pages 364–373. IEEE, 1997.

[101] Der-Tsai Lee. On k-nearest neighbor Voronoi diagrams in the plane. *IEEE Transactions on Computers*, 31(6):478–487, 1982.

[102] Jae-Gil Lee, Jiawei Han, and Kyu-Young Whang. Trajectory clustering: A partition-and-group framework. In *2007 ACM SIGMOD International Conference on Management of Data*, pages 593–604. ACM, 2007.

[103] Ken C.K. Lee, Wang-Chien Lee, Hong Va Leong, and Baihua Zheng. Navigational path privacy protection. In *18th ACM Conference on Information and Knowledge Management*, pages 691–700. ACM, 2009.

[104] Po-Ruey Lei, Wen-Chih Peng, Ing-Jiunn Su, and Chien-Ping Chang. Dummy-based schemes for protecting movement trajectories. *Journal of Information Science and Engineering*, 28(2):335–350, 2012.

[105] Ninghui Li, Tiancheng Li, and Suresh Venkatasubramanian. t-closeness: privacy beyond k-anonymity and l-diversity. In *In 21st IEEE International Conference on Data Engineering*, pages 106–115. IEEE, 2007.

[106] Fuyu Liu, Kien A Hua, and Ying Cai. Query l-diversity in location-based services. In *10th International Conference on Mobile Data Management*, pages 436–442. IEEE, 2009.

[107] Ashwin Machanavajjhala, Daniel Kifer, John Abowd, Johannes Gehrke, and Lars Vilhuber. Privacy: theory meets practice on the map. In *IEEE 24th International Conference on Data Engineering*, pages 277–286. IEEE, 2008.

[108] Ashwin Machanavajjhala, Daniel Kifer, Johannes Gehrke, and Muthuramakrishnan Venkitasubramaniam. l-diversity: privacy beyond k-anonymity. *ACM Transactions on Knowledge Discovery from Data*, 1(1):1–52, 2007.

[109] Luciana Marconi, Roberto Di Pietro, Bruno Crispo, and Mauro Conti. Time warp: how time affects privacy in LBSs. In *12th International Conference on Information and Communications Security*, pages 325–339. Springer, 2010.

[110] Giannis F Marias, Constantinos Delakouridis, Leonidas Kazatzopoulos, and Panagiotis Georgiadis. Location privacy through secret sharing techniques. In *6th IEEE International Symposium on a World of Wireless Mobile and Multimedia Networks*, pages 614–620. IEEE, 2005.

[111] Natalia Marmasse and Chris Schmandt. Location-aware information delivery with commotion. In *2nd International Symposium on Handheld and Ubiquitous Computing*, pages 157–171. Springer, 2000.

[112] Sergio Mascetti and Claudio Bettini. A comparison of spatial generalization algorithms for LBS privacy preservation. In *2007 International Conference on Mobile Data Management*, pages 258–262. IEEE, 2007.

[113] Sergio Mascetti, Dario Freni, Claudio Bettini, X.Sean Wang, and Sushil Jajodia. Privacy in geo-social networks: proximity notification with untrusted service providers and curious buddies. *The International Journal on Very Large Data Bases*, 20(4):541–566, 2011.

[114] Frank McSherry and Kunal Talwar. Mechanism design via differential privacy. In *48th Annual IEEE Symposium on Foundations of Computer Science*, pages 94–103. IEEE, 2007.

[115] Mohamed F Mokbel, Chi-Yin Chow, and Walid G. Aref. The new casper: query processing for location services without compromising privacy. In *32nd International Conference on Very Large Data Bases*, pages 763–774. VLDB Endowment, 2006.

[116] Mehrab Monjur and Sheikh I. Ahamed. Towards a landmark influence framework to protect location privacy. In *2009 ACM Symposium on Applied Computing*, pages 219–220. ACM, 2009.

[117] Raul Montoliu and Daniel Gatica-Perez. Discovering human places of interest from multimodal mobile phone data. In *9th International Conference on Mobile and Ubiquitous Multimedia*, pages 12:1–12:10. ACM, 2010.

[118] Arvind Narayanan and Vitaly Shmatikov. Robust de-anonymization of large sparse datasets. In *2008 IEEE Symposium on Security and Privacy*, pages 111–125. IEEE, 2008.

[119] Arvind Narayanan and Vitaly Shmatikov. De-anonymizing social networks. In *30th IEEE Symposium on Security and Privacy*, pages 173–187. IEEE, 2009.

[120] Arvind Narayanan and Vitaly Shmatikov. Myths and fallacies of personally identifiable information. *Communications of the ACM*, 53(6):24–26, 2010.

[121] Hoa Ngo and Jong Kim. Location privacy via differential private perturbation of cloaking area. In *IEEE 28th Computer Security Foundations Symposium*, pages 63–74. IEEE, 2015.

[122] Ben Niu, Qinghua Li, Xiaoyan Zhu, Guohong Cao, and Hui Li. Achieving k-anonymity in privacy-aware location-based services. In *2014 IEEE Conference on Computer Communications (INFOCOM)*, pages 754–762. IEEE, 2014.

[123] Ben Niu, Qinghua Li, Xiaoyan Zhu, Guohong Cao, and Hui Li. Enhancing privacy through caching in location-based services. In *2015 IEEE Conference on Computer Communications (INFOCOM)*, pages 1017–1025. IEEE, 2015.

[124] Brian O'clair, Daniel Egnor, and Lawrence E Greenfield. Scoring local search results based on location prominence, 2011. `http://www.google.com/patents/US8046371`.

[125] Femi Olumofin and Ian Goldberg. Revisiting the computational practicality of private information retrieval. In *15th International Conference on Financial Cryptography and Data Security*, pages 158–172. Springer, 2011.

[126] Balaji Palanisamy and Ling Liu. MobiMix: protecting location privacy with mix-zones over road networks. In *IEEE 27th International Conference on Data Engineering*, pages 494–505. IEEE, 2011.

[127] Balaji Palanisamy and Ling Liu. Effective mix-zone anonymization techniques for mobile travelers. *GeoInformatica*, 18(1):135–164, 2014.

[128] Balaji Palanisamy, Ling Liu, Kisung Lee, Shicong Meng, Yuzhe Tang, and Yang Zhou. Anonymizing continuous queries with delay-tolerant mix-zones over road networks. *Distributed and Parallel Databases*, 32(1):91–118, 2014.

[129] Xiao Pan, Xiaofeng Meng, and Jianliang Xu. Distortion-based anonymity for continuous queries in location-based mobile services. In *17th ACM SIGSPATIAL International Conference on Advances in Geographic Information Systems*, pages 256–265. ACM, 2009.

[130] Stavros Papadopoulos, Spiridon Bakiras, and Dimitris Papadias. Nearest neighbor search with strong location privacy. *VLDB Endowment*, 3(1-2):619–629, 2010.

[131] Iain Parris and Tristan Henderson. The impact of location privacy on opportunistic networks. In *2011 IEEE International Symposium on a World of Wireless, Mobile and Multimedia Networks*, pages 1–6. IEEE, 2011.

[132] Donald Reid. An algorithm for tracking multiple targets. *IEEE Transactions on Automatic Control*, 24(6):843–854, 1979.

[133] Daniele Riboni, Linda Pareschi, Claudio Bettini, and Sushil Jajodia. Preserving anonymity of recurrent location-based queries. In *2009 International Symposium on Temporal Representation and Reasoning*, pages 62–69. IEEE, 2009.

[134] Pierangela Samarati. Protecting respondents identities in microdata release. *IEEE Transactions on Knowledge and Data Engineering*, 13(6):1010–1027, 2001.

[135] Pierangela Samarati and Latanya Sweeney. Protecting privacy when disclosing information: k-anonymity and its enforcement through generalization and suppression. Technical report, SRI Computer Science Laboratory, 1998.

[136] Ravi Sandhu. Role hierarchies and constraints for lattice-based access controls. In *4th European Symposium on Research in Computer Security*, pages 65–79. Springer, 1996.

[137] Ravi Sandhu, David Ferraiolo, and Richard Kuhn. The NIST model for role-based access control: Towards a unified standard. In *5th ACM Workshop on Role-based Access Control*, pages 47–63. ACM, 2000.

[138] Salvatore Scellato, Mirco Musolesi, Cecilia Mascolo, Vito Latora, and Andrew T Campbell. NextPlace: a spatio-temporal prediction framework for pervasive systems. In *9th International Conference on Pervasive Computing*, pages 152–169. Springer, 2011.

[139] Adi Shamir. How to share a secret. *Communications of the ACM*, 22(11):612–613, 1979.

[140] Heechang Shin, Jaideep Vaidya, and Vijayalakshmi Atluri. A profile anonymization model for location-based services. *Journal of Computer Security*, 19(5):795–833, 2011.

[141] Reza Shokri, George Theodorakopoulos, Jean-Yves Le Boudec, and Jean-Pierre Hubaux. Quantifying location privacy. In *2011 IEEE Symposium on Security and Privacy*, pages 247–262. IEEE, 2011.

[142] Reza Shokri, George Theodorakopoulos, Panos Papadimitratos, Ehsan Kazemi, and Jean-Pierre Hubaux. Hiding in the mobile crowd: Locationprivacy through collaboration. *IEEE Transactions on Dependable and Secure Computing*, 11(3):266–279, 2014.

[143] Reza Shokri, George Theodorakopoulos, Carmela Troncoso, Jean-Pierre Hubaux, and Jean-Yves Le Boudec. Protecting location privacy: optimal strategy against localization attacks. In *2012 ACM Conference on Computer and Communications Security*, pages 617–627. ACM, 2012.

[144] Reza Shokri, Carmela Troncoso, Claudia Diaz, Julien Freudiger, and Jean-Pierre Hubaux. Unraveling an old cloak: k-anonymity for location privacy. In *9th Annual ACM Workshop on Privacy in the Electronic Society*, pages 115–118. ACM, 2010.

[145] Victor Shoup. NTL - Version 9.4.0, a C++ library for number theory computation. `http://www.shoup.net/ntl/`.

[146] Victor Shoup. *A computational introduction to number theory and algebra*. Cambridge University Press, 2005.

[147] Radu Sion and Bogdan Carbunar. On the computational practicality of private information retrieval. In *Network and Distributed Systems Security Symposium*, 2007.

[148] Mark Sullivan. 3g and 4g wireless speed showdown: which networks are fastest? *PC World*, 2012. `www.pcworld.com/article/253808/3g_and_4g_wireless_speed_showdown_which_networks_are_fastest_.html`.

[149] Latanya Sweeney. Weaving technology and policy together to maintain confidentiality. *The Journal of Law, Medicine & Ethics*, 25(2-3):98–110, 1997.

[150] Latanya Sweeney. K-anonymity: a model for protecting privacy. *International Journal of Uncertainty, Fuzziness and Knowledge-Based Systems*, 10(5):557–570, 2002.

[151] Jameson L. Toole, Yves-Alexandre Montjoye, Marta C González, and Alex Sandy Pentland. Modeling and understanding intrinsic characteristics of human mobility. In *Social Phenomena: From Data Analysis to Models*, pages 15–35. Springer, 2015.

[152] Georg Treu, Axel Kupper, and Ruppel Peter. Anonymization in proactive location based community services. In *Adjunct Proceedings of 3rd International Conference on Pervasive Computing*, 2005.

[153] Praveen Kumar Tripathi, Madhuri Debnath, and Ramez Elmasri. Extracting dense regions from hurricane trajectory data. In *2007 Workshop on Managing and Mining Enriched Geo-Spatial Data*, pages 5:1–5:6. ACM, 2007.

[154] Marten Van Dijk, Craig Gentry, Shai Halevi, and Vinod Vaikuntanathan. Fully homomorphic encryption over the integers. In *29th Annual International Conference on the Theory and Applications of Cryptographic Techniques*, pages 24–43. Springer, 2010.

[155] Lloyd R Welch and Elwyn R Berlekamp. Error correction for algebraic block codes, 1986. US Patent 4,633,470.

[156] Raymond Chi-Wing Wong, Jiuyong Li, Ada Wai-Chee Fu, and Ke Wang. (α, k)-anonymity: An enhanced k-anonymity model for privacy preserving data publishing. In *12th ACM SIGKDD International Conference on Knowledge Discovery and Data Mining*, pages 754–759. ACM, 2006.

[157] Xiaokui Xiao, Guozhang Wang, and Johannes Gehrke. Differential privacy via wavelet transforms. *IEEE Transactions on Knowledge and Data Engineering*, 23(8):1200–1214, 2011.

[158] Yonghui Xiao and Li Xiong. Protecting locations with differential privacy under temporal correlations. In *22nd ACM SIGSAC Conference on Computer and Communications Security*, pages 1298–1309. ACM, 2015.

[159] Min Xie. EDS: a segment-based distance measure for sub-trajectory similarity search. In *2014 ACM SIGMOD International Conference on Management of Data*, pages 1609–1610. ACM, 2014.

[160] Jianliang Xu, Xueyan Tang, Haibo Hu, and Du Jing. Privacy-conscious location-based queries in mobile environments. *IEEE Transactions on Parallel and Distributed Systems*, 21(3):313–326, 2010.

[161] Toby Xu and Ying Cai. Feeling-based location privacy protection for location-based services. In *16th ACM Conference on Computer and Communications Security*, pages 348–357. ACM, 2009.

[162] Sergey Yekhanin. *Locally decodable codes and private information retrieval schemes.* Springer Science & Business Media, 2010.

[163] Xun Yi, Mohammed Golam Kaosar, Russell Paulet, and Elisa Bertino. Single-database private information retrieval from fully homomorphic encryption. *IEEE Transactions on Knowledge and Data Engineering*, 25(15):1125–1134, 2013.

[164] Man Lung Yiu, Christian S Jensen, Xuegang Huang, and Hua Lu. Spacetwist: Managing the trade-offs among location privacy, query performance, and query accuracy in mobile services. In *IEEE 24th International Conference on Data Engineering*, pages 366–375. IEEE, 2008.

[165] Man Lung Yiu, Christian S. Jensen, Jesper Møller, and Hua Lu. Design and analysis of a ranking approach to private location-based services. *ACM Transactions on Database Systems*, 36(2):10:1–10:42, 2011.

[166] Hui Zang and Jean Bolot. Anonymization of location data does not work: a large-scale measurement study. In *17th Annual International Conference on Mobile Computing and Networking*, pages 145–156. ACM, 2011.

[167] Chengyang Zhang and Yan Huang. Cloaking locations for anonymous location based services: a hybrid approach. *GeoInformatica*, 13(2):159–182, 2009.